

**THE ROLE OF POTASSIUM CONDUCTANCES IN REGULATING  
THE EXCITABILITY OF MYELINATED AXONS**

by

**Michael Owen Poulter, Bachelor of Science**

**Department of Pharmacology and Therapeutics**

**A thesis submitted to the Faculty of Graduate Studies and Research,**

**McGill University, Montreal**

**March, 1990 in partial fulfillment of the requirements**

**for the degree of Doctor of Philosophy**

**(c) Michael Owen Poulter**

This thesis is dedicated to:  
the memory of my late father:  
Captain Ronald Poulter

and to my:

mother, Eleanor, Patricia

brother, John, Barry

sister, Janice, Elizabeth

Thanks for patience, love and support  
throughout my university years.

## *ABSTRACT*

Previous results indicate that the functional properties of myelinated axons are considerably more complex than previously believed. The purpose of this study was to further examine the functional properties of potassium conductances in dorsal and ventral root (DRA; VRA) frog myelinated axons by intracellular microelectrode recording. The voltage responses to hyperpolarizing current injection demonstrated: 1) a nonlinear voltage current ( $V/I$ ) relationship in the region just below resting membrane potential; 2) a linear peak and steady state  $V/I$  relationship below  $\approx -95$  mV; 3) a large effective capacitance of the internodal membrane; and 4) an attenuation of the voltage response reflecting the activation of a voltage dependent anomalous rectifying conductance ( $G_{AR}$ ).  $G_{AR}$  is dependent on the presence of sodium and potassium ions in the external medium and is blocked by cesium but not barium ions. 5) An afterhyperpolarizing potential (AHP) after a train of action potentials was accounted for by the presence of a sodium dependent potassium conductance ( $G_{K(Na)}$ ). The functional role of the voltage dependent potassium conductances and  $G_{K(Na)}$  was examined.  $G_{AR}$  appears to regulate the length of a post tetanic AHP. Early accommodation (EAcc) is regulated by  $G_{Kf1}$  in DRA and VRA. Late accommodation (LAcc) and adaptation (Adp) is regulated by  $G_{Ks}$  in both DRA and VRA.  $G_{Kf2}$  may also contribute to EAcc and Adp. Action potential repolarization in DRA and VRA is governed by  $G_{Kf2}$  and  $G_{Kf1}$  respectively.  $G_{K(Na)}$  may also contribute to LAcc and Adp. An evaluation of our experimental results using a computer model based Hodgkin-Huxley type equations suggests that the gating of the sodium conductance plays only a minor role in accommodation and adaptation. These results indicate that potassium conductances play a pivotal role in regulating the excitability of myelinated axons.

## RÉSUMÉ

Les résultats préalable obtenus indiquent une complexité imprévue des propriétés fonctionnelles de ces axones. Le but de cette étude était d'évaluer, au moyen d'enregistrements à partir de microélectrodes intracellulaires, les propriétés fonctionnelles des conductances potassiques des axones myélinisés des racines dorsale et ventrale (ARV; ARD) de grenouille. L'effet d'une injection de courant hyperpolarisant sur le voltage a démontré: 1) une relation voltage-courant ( $V/I$ ) non linéaire à un potentiel membranaire tout juste inférieur à celui au repos; 2) des relations  $V/I$  maximale et à l'équilibre qui semblent linéaires à moins de  $\approx -95$  mV; 3) une membrane internodale à capacitance effective de longue durée; 4) une atténuation du voltage reflétant l'activation d'une conductance rectificatrice anormale dépendante du voltage ( $G_{AR}$ ).  $G_{AR}$  dépend de la présence des ions  $Na^+$  et  $K^+$  dans le milieu extracellulaire tandis qu'elle est bloquée par les ions  $Cs^+$  mais non par les ions  $Ba^{2+}$ . Suite à une salve de potentiels d'action, la post-hyperpolarisation (PP) est due à la présence d'une conductance potassium dépendante du sodium ( $G_{K(Na)}$ ). La fonction des conductances potassiums dépendantes du voltage et de  $G_{K(Na)}$  a été étudiée.  $G_{AR}$  semble régler la durée du PP post-tétanique. L'accommodation rapid (RAcc) est réglée par  $G_{Kf1}$  dans les ARD et ARV. L'accommodation et l'adaptation lente (LAcc; Adp) sont réglées par  $G_{Ks}$  à la fois dans la ARD et la ARV.  $G_{Kf2}$  peut aussi influencer RAcc et Adp. La repolarisation des potentiels d'action dans les ARD et ARV est dictée par  $G_{Kf2}$  et  $G_{Kf1}$  respectivement.  $G_{K(Na)}$  peut aussi influencer TAcc et Adp. Un modèle mathématique utilisant des équations dérivées de Hodgkin-Huxley indiqua que les conductances sodiques jouent un rôle mineur dans l'accommodation et l'adaptation. Au contraire, les conductances potassiums jouent un rôle primordial dans la régulation de l'excitabilité des axones myélinisés.



***ACKNOWLEDGEMENTS:***

Doctor Ante L. Padjen, my supervisor, who provided an excellent learning environment. I never found a time when I did not look forward to nor felt unchallenged by the day to day life in his laboratory.

Doctor A.C. Cuello, chairman of The Department of Pharmacology, and all those on the Graduate committee who provided the opportunity for myself to study and learn in their department.

Doctor E. Puil, my mentor, from the Department of Pharmacology and Experimental Therapeutics, The University of British Columbia Vancouver, British Columbia, Canada who was instrumental in my coming to McGill.

Doctor B. Robaire, my advisor, thanks for the helpful discussions and advice through the years.

Doctor D.M.J. Quastel, for my first opportunity to work in a real research environment in his laboratory at U.B.C.. (Summer 1984 & 85)

Sherry Kennedy, still a dear friend, without whose help I would not have made it through my undergraduate years at U.B.C.

Doctor B. Collier, for beers and more importantly helpful advice throughout my stay.

All the technical and administrative help, Mike Massella, Alan Forster, Roy Raymond and the ladies in the office, Administrative Assistant, Debbie Mercer, Mara Solari, Diane Legget, Clair O'Neil, Fotini Spirikakis and Rosemary Greco.

Christian Band and Julie Ducharme thanks for expert translation of the abstract into French.

Finally, thanks to the Hell's Fish, Bill Bromely B.A., Ken Robbers B.App.Sci., David Noseworthy B.A., Pat Martinet B.A., John Heney, Benoit Tifou B.Sc. M.Sc., Serge Mykita Ph.D, and Don McQuaig, the toughest canoe gang in the world, my time spent in the wilderness provided the breaks in the serious world which gave me the perspective and focus that was necessary to complete this thesis.

## PREFACE

### Note on the Format of this Thesis

In accordance with the Faculty of Graduate Studies and Research the candidate has the option of including as part of his thesis the text of original paper already published by learned journals, and original papers submitted or suitable for submission to learned journals. The text relating to this option is as follows:

The Candidate has the option, subject to the approval of the Department, of including as part of the thesis the text of an original paper, or papers, suitable for submission to learned journals for publication. In this case the thesis must still conform to all other requirements explained in this document, and additional material (e.g. experimental data, details of equipment and experimental design) may need to be provided. In any case, abstract, full introduction and conclusion must be included, and where more than one manuscript appears, connecting texts and common abstract, introduction and conclusions are required. A mere collection of manuscripts is not acceptable; nor can reprints of published papers be accepted.

While the inclusion of manuscripts co-authored by the Candidate and others is not prohibited for a test period, the Candidate is warned to make an explicit statement on who contributed to such work and to what extent. Copyright clearance from the co-author or co-authors must be included when the thesis is submitted. Supervisors and others will have to bear witness to the accuracy of such claims before the Oral Committee. It should be noted that the task of the External Examiner is much more difficult in such cases.

### Chapter 2:

Poulter, M.O., Hashiguchi, T. and Padjen, A.L. A study of frog myelinated axons by intracellular microelectrode recording. Submitted to *J. Neurophysiol.*, June, 1989.

### Chapter 3:

Poulter, M.O. and Padjen, A.L. A study of anomalous (inward) rectification in frog sensory myelinated axon. Submitted to *J. Neurophysiol.*, June, 1989.

Chapter 4:

Poulter, M.O., Hashiguchi, T. and Padjen, A.L. Dendrotoxin blocks accommodation in frog myelinated axons. *J. Neurophysiol.* 62:174-184, 1989.

Chapter 5:

Poulter, M.O. and Padjen, A.L. Voltage dependent potassium conductances regulate action potential repolarization and excitability in frog myelinated axon. Submitted to *Pflügers Arch*, March, 1990.

Chapter 6:

Poulter, M.O. and Padjen, A.L. Evidence for a sodium dependent potassium conductance in frog myelinated axon. Submitted to *Pflügers Arch.*, March, 1990.

## STATEMENT OF ORIGINALITY

All data, observations and conclusions presented in thesis are original except where noted by reference and following exceptions.

### CHAPTER 2

1. The original observation that the V/I curve is nonlinear below resting membrane was made by A. Padjen. Recordings made by T.Hashiguchi were included in the statistics which described average  $R_p$ , Table 2 and the incidence of the V/I nonlinearity.

2. The computer model was originally written by T.H. based on the model reported by Dodge (1963). Refinement of the model regarding constants and presentation were done by myself.

The results presented in chapter 1 provide evidence that the slow potassium conductance is responsible for nonlinearity below resting membrane potential. The unusually long charging time of the electrotonic potential is the combined contribution of the deactivation of  $G_{Ks}$  and the charging of the internodal capacitance. This study is primarily a description of some of the electrophysiological properties of intact frog myelinated axons which has not been looked at closely in previous studies.

### CHAPTER 3

The results presented in Chapter 3 characterize a previously unreported presence of anomalous rectification in frog myelinated axons. The model presented is a further refinement of the model presented in Chapter 2.

Equations used were developed by myself based on the formulations of the h-gate equations reported in Dodge (1963).

#### CHAPTER 4-5

The results reported in these two chapters are an account of the examination of the function of three voltage dependent potassium conductances  $G_{Kf1}$ ,  $G_{Kf2}$ , and  $G_{Ks}$ . The fast conductances,  $G_{Kf1}$  and  $G_{Kf2}$ , appear to regulate spike repolarization in ventral root and dorsal root fibres (v.r.f. and d.r.f.), respectively. In addition, both conductances play a role in early accommodation. Evidence that the conductance  $G_{Ks}$  regulates late accommodation and spike frequency adaptation is first provided by a computer model in chapter 4 and then confirmed by pharmacological means in chapter 5. The equations for  $G_{Kf1}$  and  $G_{Kf2}$  were written by myself.

#### CHAPTER 6

Evidence of a previously unreported sodium dependent potassium conductance is presented in Chapter 6.

#### GENERAL STATEMENT ON ORIGINALITY

This thesis provides evidence that frog myelinated axons are not passive propagators of action potentials due to the presence of potassium conductances. This thesis also asserts that the potassium channels in myelinated axons fit into well defined categories of potassium conductances existing in other neurons. Therefore, the behaviour and regulation of myelinated axon excitability is similar to regulation of excitability in other neurones.

*Three scientists are approached by GOD with a problem. GOD, in a loud a booming Deity-like voice, (as one would expect of God) tells the three scientists the following "In a tree there is animal which has feathers, sings and uh.... oh yes it has silver scales. What do you make of it?" The scientists are quite excited by this data and like most scientists presented with exciting mental cannon fodder they organize a symposium in a far off land to try to decide what this creature is. At the symposium after much discussion the brightest scientist of all stands at the microphone in the great hall of the symposium and expounds "What is important are first observations: it sings, has feathers and it is in a tree. The silver scales," he reasons, "are an anomalous observation. Therefore it must be a bird" All the scientists cheered and soon afterward the three scientists then reported to GOD "It is a bird." GOD quite calmly tells the scientists that, in fact, it is a herring. The scientists, some what chagrined, protested saying that the information provided was misleading and unfair. GOD simply replied "Who said I have to make it obvious?"*

## **TABLE OF CONTENTS**



## Table of Contents

<b>TITLE PAGE</b>	i
<b>DEDICATION</b>	ii
<b>ABSTRACT</b>	iii
<b>RESUME</b>	iv
<b>ACKNOWLEDGEMENTS</b>	v
<b>PREFACE</b>	vii
<b>TABLE OF CONTENTS</b>	xii
<b>INDEX OF FIGURES</b>	xix
<b>CHAPTER 1 INTRODUCTION</b>	
<i>WHAT IS A VOLTAGE GATED ION CHANNEL ?</i>	1-2
<i>PART I-WHAT DOES PHARMACOLOGY TELL ABOUT VOLTAGE DEPENDENT IONIC CONDUCTANCES AND ION CHANNELS?</i>	
<i>SODIUM CHANNELS</i>	1-5
<i>Competitive sodium channel blockers</i>	1-6
<i>Use- or Frequency-dependent sodium channel blockers</i>	1-7
<i>Gate modifiers</i>	1-9
<i>What does the pharmacology of sodium channels     tell us about sodium channels?</i>	1-10
<i>POTASSIUM CHANNELS</i>	1-11
<i>Physiological classification of potassium channels</i>	1-11
<i>Pharmacology of tetraethylammonium</i>	1-14
<i>Pharmacology of 4-aminopyridine</i>	1-16
<i>Pharmacology of neurotoxins which affect potassium channels</i>	1-18
<i>Toxins which block <math>I_K</math></i>	1-18
<i>Toxins which block fast activating potassium channels</i>	1-18
<i>Pharmacology of calcium dependent potassium channels</i>	1-19

## Table of Contents

<i>What does the pharmacology of potassium channels tell us potassium channels?</i>	1-20
<b>CALCIUM CHANNELS</b>	1-24
<i>T-type calcium channels</i>	1-24
<i>N and L-type calcium channels</i>	1-25
<i>What do pharmacologically distinct calcium channels do?</i>	1-26
 <b>NEW APPROACHES TO OLD QUESTIONS: MOLECULAR BIOLOGY OF VOLTAGE GATED ION CHANNELS</b>	 1-27
<i>Structure and function of sodium channels</i>	1-27
<i>Structure and function of potassium channels</i>	1-29
<i>Structure and function of calcium channels</i>	1-31
 <b>PART II: FUNCTIONAL ATTRIBUTES OF MYELINATED AXONS</b>	
<i>Function of myelin and sodium current flow in myelinated axon</i>	1-34
<i>Function of potassium conductances in myelinated axon</i>	1-41
<i>Electrical properties of myelinated axon</i>	1-45
 <b>STATEMENT OF PROBLEM</b>	 1-48
 <b>CHAPTER 2</b>	
<b>A STUDY OF FROG MYELINATED AXONS BY INTRACELLULAR MICROELECTRODE RECORDING</b>	 2-1
<b>SUMMARY AND CONCLUSIONS</b>	2-2
<b>INTRODUCTION</b>	2-4
<b>METHODS</b>	
<i>General experimental methods</i>	2-5

## Table of Contents

<i>Identification of fibres</i>	2-5
<i>Microelectrode technique</i>	2-6
<i>Analysis of results</i>	2-7
<b>TABLE 2.1</b> Parameters used in models.	2-8
<b>RESULTS</b>	
<b>I. Experimental Results</b>	
<i>Resting and action potentials of primary afferent axons</i>	2-9
<b>TABLE 2.2</b>	2-9
<i>Charging time constants of electrotonic potentials</i>	2-10
<i>Voltage-current relationship</i>	2-12
<i>Voltage-current relationship of motoneuron axons</i>	2-17
<b>II. Results of computer modeling</b>	2-18
<i>Modeling of electrotonic potentials</i>	2-19
<i>Modeling of the V/I relationship</i>	2-20
<b>DISCUSSION</b>	2-22
 <b>CHAPTER 3</b>	
<b>A STUDY OF ANOMALOUS (INWARD) RECTIFICATION IN FROG</b>	
<b>SENSORY MYELINATED AXON</b>	3-1
<b>SUMMARY AND CONCLUSIONS</b>	3-2
<b>INTRODUCTION</b>	3-4
<b>METHODS</b>	
<i>Experimental</i>	3-6
<i>Computer Simulations</i>	3-7
<i>Gating Equations for anomalous rectifier conductance</i>	3-7
<b>TABLE 3.1</b> Parameters used in model	3-8
<b>RESULTS</b>	

## Table of Contents

<i>Effect of extracellular cesium and barium ions</i>	3-10
<i>Ionic dependence of anomalous rectification</i>	3-12
<i>Functional aspects of <math>G_{AR}</math></i>	3-15
<b>DISCUSSION</b>	3-20
<i>Physiological role of <math>G_{AR}</math></i>	3-25
<b>CHAPTER 4</b>	
<b>DENDROTOXIN BLOCKS ACCOMMODATION IN FROG MYELINATED AXONS</b>	4-1
<b>SUMMARY AND CONCLUSIONS</b>	4-2
<b>INTRODUCTION</b>	4-4
<b>METHODS</b>	
<i>Experimental procedure</i>	4-6
<b>RESULTS</b>	4-8
<i>Effect of DTX on repetitive activity.</i>	4-9
<i>Effect of DTX on action potentials</i>	4-12
<i>Effect of DTX on voltage-current (<math>V/I</math>) relationship</i>	4-16
<b>DISCUSSION</b>	4-19
<b>APPENDIX</b>	4-27
<i>Computer Model</i>	4-29
<i>Na channel equations</i>	4-29
<i>K channel equations</i>	4-31
<i>Constants</i>	4-32
<i>Conditions for repetitive activity.</i>	4-32

## Table of Contents

### CHAPTER 5

#### VOLTAGE DEPENDENT POTASSIUM CONDUCTANCES REGULATE ACTION POTENTIAL REPOLARIZATION AND EXCITABILITY IN FROG MYELINATED AXON

5-1

*ABSTRACT* 5-2

*INTRODUCTION* 5-3

*METHODS* 5-5

*Computer Model* 5-6

#### *RESULTS*

5-7

*Computer Modeling* 5-14

*DISCUSSION* 5-18

### CHAPTER 6

#### EVIDENCE FOR A SODIUM DEPENDENT POTASSIUM CONDUCTANCE IN FROG MYELINATED AXON.

6-1

*ABSTRACT* 6-2

*INTRODUCTION* 6-3

*METHODS* 6-5

*RESULTS* 6-6

*DISCUSSION* 6-15

### CHAPTER 7 DISCUSSION

*INTRODUCTION* 7-2

TABLE 7-1 7-3

*FAST ACTIVATING POTASSIUM CONDUCTANCES* 7-4

$G_{Kf1}$  7-4

## Table of Contents

$G_{Kf2}$	7-5
<i>SLOWLY ACTIVATING POTASSIUM CONDUCTANCES</i>	7-6
$G_{Ks}$	7-6
$G_{AR}$	7-7
$G_{K(Na)}$	7-8
<i>OTHER FUNCTIONAL ROLES OF POTASSIUM</i>	
<i>CONDUCTANCES IN MYELINATED AXONS</i>	7-9
<i>Conduction velocity</i>	7-9
<i>Leak conductance: Action potential repolarization</i>	
<i>and resting membrane potential</i>	7-11
<i>Excitability and neural coding</i>	7-12
<i>SUMMARY AND CONCLUSION</i>	7-14

## **INDEX OF FIGURES**

## CHAPTER 2

- FIGURE 2.1* A diagram of the experimental preparation. 2-6
- FIGURE 2.2* Voltage-current relationship recorded in a large myelinated primary afferent axon. 2-11
- FIGURE 2.3* Hyperpolarizing voltage response from the linear region of  $V/I$  plotted in semilogarithmic coordinates. 2-13
- FIGURE 2.4* Example of typical voltage-current relationship below resting membrane potential 2-14
- FIGURE 2.5* Effect of TEA on the voltage/current relationship below resting membrane potential. 2-16
- FIGURE 2.6* Effect of barium on voltage/current relationship. 2-17
- FIGURE 2.7* Computer modeling of the ETP. 2-18
- FIGURE 2.8* Computer modeling of the current voltage relationship. 2-21

## CHAPTER 3

- FIGURE 3.1* Voltage responses to hyperpolarizing current pulses are attenuated by activation of inward or anomalous rectifying conductance. 3-10
- FIGURE 3.2* Effect of external cesium ion on anomalous rectification 3-11
- FIGURE 3.3* Effect of cesium on the DAP. 3-12
- FIGURE 3.4* Effect of externally applied barium ion on  $G_{AR}$ . 3-13
- FIGURE 3.5* Effect of sodium ion replacement. 3-14
- FIGURE 3.6* Effect of reducing the external potassium ion concentration. 3-16
- FIGURE 3.7* Effect of raising the external potassium ion concentration on electrotonic potentials. 3-17



**FIGURE 3.8** Effect of cesium on the post tetanic afterhyperpolarizing potential. 3-18

**FIGURE 3.9** Partial blockade of anomalous rectification is accompanied by partial blockade of the fast component of the post tetanic afterhyperpolarization. 3-19

**FIGURE 3.10** Comparison of single and double time constant activation of anomalous rectification in computer model 3-24

#### CHAPTER 4

**FIGURE 4.1** Spontaneous convulsive discharges after DTX treatment. 4-7

**FIGURE 4.2** Effect of DTX on accommodation of sensory (DR) and motor (VR) fibers. 4-10

**FIGURE 4.3** The effect of increasing stimulus strength on DTX treated motor axons. 4-12

**FIGURE 4.4** Effect of DTX on duration of an action potential recorded motor axon 4-13

**FIGURE 4.5** Sample of DRF conducting spike with  $dV/dt$  before and after DTX treatment 4-15

**FIGURE 4.6** Sample of voltage/current (V/I) responses of a single DRF before and after DTX application in the presence of  $0.25 \mu\text{M}$  tetrodotoxin. 4-18

**FIGURE 4.7** Computer generated simulations of voltage responses from axonal membrane. 4-20

**FIGURE 4.8** Computer generated simulation of responses to a current step using model of axonal membrane without  $G_{Kf1}$ . 4-24

<i>FIGURE 4.9</i> Computed effect of $G_{Kf1}$ on action potential in motor axons (VRF).	4-25
---	------

<i>FIGURE 4.10</i> Voltage dependence of fast potassium currents used in the computer model.	4-32
---	------

## CHAPTER 5

<i>FIGURE 5.1</i> Intracellular application of 4-AP blocks outward rectification.	5-9
<i>FIGURE 5.2</i> Effect of 4-AP/TEA on action potential repolarization.	5-10
<i>FIGURE 5.3</i> Effect of 4-AP and TEA on action potential generation.	5-12
<i>FIGURE 5.4</i> Effects of 4-AP and 4-AP/TEA on adaptation.	5-13
<i>FIGURE 5.5</i> Computer simulation of 4-AP and TEA pharmacology.	5-15

## CHAPTER 6

<i>FIGURE 6.1</i> Effect of action potential number and TTX blockade on AHP amplitude.	6-7
<i>FIGURE 6.2</i> Effect of increasing action potential number on AHP generation.	6-8
<i>FIGURE 6.3</i> Effect of action potential prolongation on the AHP.	6-9
<i>FIGURE 6.4</i> Effect of 8-Acetyl-strophanthidin on the AHP.	6-10
<i>FIGURE 6.5</i> Effect of an alteration in membrane potential and raising the external potassium concentration on the AHP.	6-11
<i>FIGURE 6.6</i> Effect of calcium channel blockers on AHP.	6-12
<i>FIGURE 6.7</i> Effect of reducing the sodium ion concentration in the external media on the AHP.	6-14

***FIGURE 6.8*** Effect of lithium ion on AHP.

6-14

## **INTRODUCTION**

### *WHAT IS A VOLTAGE DEPENDENT ION CHANNEL ?*

Current flow across excitable membranes is carried by ions flowing through what is best described as hydrophilic pores which span the membrane, i.e. ion channels. In recent years, molecular biological techniques have shown that, in general, ion channels are multi-subunit protein macromolecules (Catterall 1989). Voltage dependent channels are "gated" (opened and closed) by the transmembrane potential or voltage. This phenomena implies that a conformational change, triggered by the dipole elements of the macromolecule sensitive to potential field, alters the permeability of the channel. The voltage gated regulation of current flow was first described in detail by Hodgkin and Huxley in 1952 (Hodgkin and Huxley, 1952b). They demonstrated, using voltage clamp technique, that the inward current, identified to be carried by sodium ions (Hodgkin and Katz 1949), increased as they made the membrane potential less negative. Thus a gate (the m-gate in their terminology) opened to allow a current carried by sodium ions to flow. After several milliseconds the permeability decreased and a second gate, the h-gate, was hypothesized to exist, which closes to reduce permeability. While this specific description of sodium ion permeability does not hold for all types of voltage dependent ion channels, nevertheless, all voltage gated ion channels can be considered to be membrane spanning macromolecules having gates that open and close in response to changes in membrane potential.

One of the important characteristics of voltage dependent ion channels is their ion selectivity; there are ion channels primarily permeant to sodium, potassium and calcium ions. Voltage dependent conductances act in concert

with other conductance changes in a neurone to define its state of excitability. For example, an ionic conductance activated by a neurotransmitter stimulates the generation of action potentials by activation of voltage dependent sodium channels. Other cellular functions could also be modified by ion fluxes; eg. a change in cell metabolism as a result of calcium influx.

How voltage gated ion channels function to accomplish these tasks has been the subject of great deal of research over the past 40-50 years. These investigations have been carried out by biophysicists, physiologists and pharmacologists who have used a number of different approaches to understand how voltage dependent ion channels modulate the activity of neurones. While it is true that several approaches to this task exist, the use of various pharmacological agents has been one of the most helpful in studying what role voltage gated ion channels play in neurones. Pharmacological agents have been invaluable in a) examining and identifying the various subtypes of ion channels; b) identifying how ion channels\conductances regulate the physiology of the neuron; and c) for the purification and isolation of the channel proteins for analysis by biochemical techniques. The purpose of this introduction is to illuminate some of these approaches as applicable to the main objectives of the present studies, i.e. understanding the role of voltage dependent conductances in the function of myelinated axons.

The first part is a survey of the pharmacology of voltage gated ion channels, followed by a look at the molecular biology of ion channels and the new direction this field is taking the study of ion channels. The second part describes the classical and current view of our understanding of how myelinated axons work. Finally, the pharmacology of potassium conductances in myelinated

axons is reviewed to point out how this approach has elucidated some of the roles of potassium conductances in myelinated axons.

*PART 1: WHAT DOES PHARMACOLOGY TELL ABOUT VOLTAGE  
DEPENDENT IONIC CONDUCTANCES AND ION CHANNELS?*

*SODIUM CHANNELS*

Hodgkin and Huxley (1952b) were the first investigators to directly measure and quantitatively describe current flow associated with the voltage upstroke of an action potential. Earlier, Curtis and Cole (1938) had demonstrated a decrease in impedance (an increase in permeability) associated with the action potential upstroke. However, it was Hodgkin and Huxley who first recognized that the inward current increased as the voltage across the membrane was made less negative (i.e. the m-gate opened). That is, the activation of the current was voltage dependent. They also showed that when the voltage is held constant the current increased at an exponential rate with respect to time (ie. the process was time dependent). In addition, it was demonstrated that the sodium current inactivated (h-gate closed) after a certain period, and that this process was also voltage and time dependent. These attributes of the gating mechanism result in three possible states of the channel: resting, activated and inactivated. Subsequent studies demonstrated that the sodium dependent currents are responsible for the rising phase of most action potentials in the central nervous system, in particular those responsible for conduction of impulses over a long distance, such as in myelinated axons (Hille 1984).

There is a large family of pharmacological agents affecting sodium channels. These agents can be roughly divided into three categories based on their mechanism of action (Hille 1984): simple blockers, use- or frequency-dependent blockers and modifiers of gating (drugs that act by altering the activation and/or



inactivation processes). Studies using each drug type have yielded information as to how the sodium current behaves, as well as details about the structure of the sodium channel.

### *Competitive sodium channel blockers*

The first class of drugs is composed of the naturally occurring neurotoxins tetrodotoxin (TTX) and saxitoxin (STX) and some simple ions (protons, ammonium ions). These agents act only on the external side of the membrane. The mechanism of action of this type of blocker is the inhibition ion permeability at or near the sodium ion pore, a site classified by Catterall and coworkers as neurotoxin binding site 1 (Catterall 1980). In general, the drugs which bind to this site are water soluble. The binding site appears to be associated with the area on the sodium channel protein which is responsible for ion selectivity of the channel, the "selectivity filter". This conclusion is based on a number of experiments that show altered drug binding when the negative charge of the selectivity filter is increased or decreased. For example, by decreasing the pH of the media and altering the ionic charge on the receptor sites, toxin binding was reduced along with a resultant decrease in sodium ion permeability (Ulbricht and Wagner 1975). In addition, the affinity of the receptor can be reduced by treatment with agents that irreversibly alkylate carboxyl moieties, which presumably are part of the selectivity filter (Shrager and Profera 1973; Baker and Robinson 1975; Reed and Raftery 1976). However, there is little correlation between a reduction in selectivity and toxin binding. Aconitine, a drug which reduces selectivity, does not affect binding of TTX (Catterall 1980). Therefore the drug binding site may not be the selectivity filter site but rather an allosteric

site associated with it.

*Use- or frequency-dependent sodium channel blockers*

Frequency- or use-dependent blockers are those agents which block sodium permeability only after the ion channel has been activated (eg. by an action potential). The effect of use-dependent blockers on sodium channel function is manifested by an increased refractory period of action potential generation (the h-gate opens more slowly) and a shift in the voltage dependence of inactivation to more hyperpolarized potentials (Hille 1984). The mechanism of action of this class of drugs has been explained by two different hypotheses. The first explains use-dependent block as a process that requires the channels to open for the drug to gain access to its site of action by moving into the channel from the internal side of the membrane. This hypothesis accounted for the results first reported by Frazier and coworkers who used the local anesthetic drug QX-314 to block sodium channels. QX-314 has a permanent positive charge and no effect when applied extracellularly (Frazier et al. 1970). However, sodium channel block was produced when QX-314 was allowed to leak from the intracellular recording electrode into the intracellular space. Furthermore, the block only occurred when the sodium channels were activated, implying that the opening of the channel was required to expose the receptor site to the drug. Using another, local anesthetic, lidocaine another phenomenon was observed: once use-dependent block was established, the block would decline if the neurone was not stimulated, ie. the drug would somehow lose its efficacy as the stimulation rate was slowed (Hille 1977a, 1977b). Assuming that the concentration of the drug remains constant at the receptor site, simple access to the binding site did not explain frequency dependent recovery.

Although recovery from block could be explained by proposing that the drug could become uncharged and therefore diffuse away from its binding site into the surrounding lipid bilayer (Hille 1977b), it is more elegantly explained by a second hypothesis which describes use-dependent block, referred to as the "modulated receptor hypothesis" (Courtney 1975; Hondeghem and Katzung 1977; Strichartz 1976). It states that the action of use-dependent sodium channel blockers is due to an increase or decrease in the affinity of the "receptor" for the blocking drug, depending on the state of the channel (resting, activated or inactivated). According to this model, in the resting state of sodium channel (m-gate closed and h-gate open) the receptor for the frequency-dependent blockers is in a low affinity state, but affinity increases when the channel is activated. Affinity remains high in the inactivated state as well. When the channel changes back into the resting state, the affinity of the receptor decreases and the block is removed. Since these blockers promote inactivation, it has also been suggested that the drug binds to physical substrate of the h-gate. The conformational change implied by the h-gate closing correlates with the change in affinity for drug.

Another notable feature of this class of compounds is that they are positively charged depending on the pH of the medium and they must be positively charged to act. Since it is unlikely that a charged molecule will diffuse across the lipid membrane when applied extracellularly, their action will depend on the total amount of uncharged drug available to diffuse across the lipid membrane. For example, lidocaine has no effect if the pH of the external medium is lowered sufficiently below lidocaine's  $pK_a$  so that there is effectively no uncharged

form of the drug available to diffuse across the membrane (Hille 1977a).

### *Gate modifiers*

The third classification of agents which affect sodium channels are the so-called gate modifiers. This class of agents act by altering the kinetics of activation and inactivation. They are a large group of drugs which can be further divided into three subgroups. The first subgroup are those agents which tend to prevent inactivation and promote activation. Examples of drugs in this class are veratridine, aconitine, grayanotoxin and batrachotoxin. They are all lipid soluble, bind at what is classified as neurotoxin binding site 2 (Catterall 1980), and they shift the voltage dependence of activation to more hyperpolarized potentials; once the channels open they prevent inactivation (Catterall 1980). The second subgroup are agents which remove inactivation. This group is comprised of both naturally occurring neurotoxins, such as scorpion and sea anemone toxins, the bacterial enzyme pronase, as well as chemical agents N-bromacetamide (NBA), 2,4,6, trinitrobenzene sulphonic acid (TNBS). The neurotoxins are lipid soluble peptides that act from the outside and bind to what is classified as the neurotoxin binding site 3 (Catterall 1980). The chemical agents do not work from the outside and must be applied intracellularly. They appear to act by denaturing a portion of the ion channel which is the h-gate. Finally, the third subgroup shift the voltage dependence of the sodium channel gating. Katz (1936) noticed that reducing the external concentration of calcium can lower the threshold of action potential generation. Similarly, increasing the external concentration of calcium can raise threshold (Brink 1954). This effect has been shown to be due to a shift in the voltage dependence of the sodium channel activation (Campbell and Hille 1976). Lowering the calcium shifts the

voltage dependence of activation to more hyperpolarized values, whereas raising calcium shifts the voltage dependence to more depolarized values. This effect is most easily explained by the binding of calcium to the negatively charged carboxylic acid or phospholipid moieties on the lipid membrane resulting in a decrease in the negative surface potential ("charge screening"). The channel "sees" less membrane potential resulting in an apparent shift in the voltage dependence. The opposite effect is seen if calcium is reduced in the external medium. Charge screening can be induced not only by calcium ions but by many other ions as well (magnesium, manganese, protons).

*What does the pharmacology of sodium channels tell us about sodium channels?*

Both structural and mechanistic information about channel function has been garnered by these pharmacological studies. We know that the site associated with the selectivity filter is hydrophilic. Externally applied agents which decrease the affinity of simple blockers for the channel also alter ion selectivity. Pharmacological action of local anesthetics and agents such as pronase indicate that the structure involved in inactivation is on the cytosolic surface of the channel. Based on the specificity of the gate modifiers, which alter only activation or inactivation, these processes can be viewed as being gates that open and shut independent of one another. What has not been mentioned is that the pharmacology described above has been done on an extremely wide range of mammalian, amphibian and invertebrate nerve, muscle and heart preparations. What may be surprising is that the pharmacology of sodium channels studied is basically the same in all preparations. This implies that sodium channel structure is relatively similar throughout the animal kingdom and with only minor

variation there is only one type of sodium channel. This conclusion is also supported by studies utilizing an antibody raised to a synthetic peptide with the same amino acid sequence as a section of the sodium channel involved in inactivation. This antibody abolished inactivation of sodium channels from a number of different species indicating that the DNA coding for this region on the channel has been highly conserved during evolutionary development (Gordon et al. 1988; Vassilev et al. 1987).

### *POTASSIUM CHANNELS*

The pharmacological agents affecting potassium channels cannot be easily categorized into groups, which block with different mechanisms or alter gating of potassium channels, like drugs affecting sodium channels. There is a plethora of potassium channels with varying specificity for a large variety of drugs, with only one major mechanism of action, competitive channel blockade. For this reason, the pharmacology of potassium channels is presented by discussing the specificity of these drugs for the subtypes of potassium channels, described in the next section.

#### *Physiological classification of potassium channels*

Potassium channels can be roughly divided into two classes: 1) the relatively simple voltage gated and time dependent potassium channels; and 2) those activated by an internal rise of calcium or sodium ions, which also may be voltage and time dependent. The first class of "simple" potassium channels can be subdivided into three types according to their gating kinetics. Historically, the first voltage and time dependent potassium channel described was the so-

called delayed rectifier in the squid giant axon ( $I_K$ ; Hodgkin and Huxley 1952a).  $I_K$  activates relatively slowly ( $\tau \approx 2-4$  ms; compared to the activation of the sodium conductance) and is very slowly inactivating. However, the speed at which  $I_K$  activates in the squid axon appears to be more the exception than the rule. In other tissues, most currents classified as  $I_K$  activate in 10's of milliseconds (Rudy 1988). The second type of current, the fast transient current termed  $I_A$ , activates and inactivates quickly ( $\tau \approx 3-4$  ms) in a voltage and time dependent manner (analogous to the sodium channel; Connor and Stevens 1971; Daut 1973; Hagiwara et al. 1961; Neher 1971). The third type of channel kinetics appear to be somewhat of a mix of the first two types. It appears to be a distinct type of current since it does not inactivate (like  $I_K$ ), yet it activates as quickly as  $I_A$  (in neurones). Its pharmacology (see below) is clearly different from the  $I_A$  and  $I_K$ . Since this current is selectively blocked by the snake toxin dendrotoxin (DTX), it has been named  $I_{DTX}$  (Feltz and Stansfeld 1988). Finally, there is the anomalous or inward rectifying conductance ( $G_{AR}$ ) which is a voltage and time dependent conductance activated by hyperpolarization. It is either a pure potassium or mixed sodium/potassium current (see Chapter 3).

A more complicated class of potassium channels is activated by a transient increase in an internal ion concentration. The first type is a calcium activated potassium conductance ( $G_{K(Ca)}$ ; Meech 1978) and more recently a new type has been demonstrated which is activated by an internal rise in the sodium ion concentration ( $G_{K(Na)}$ ; Bader 1985; Dryer et al. 1989; Poulter and Padjen 1989; Schwindt et al. 1989). The  $G_{K(Ca)}$  is activated by the influx of calcium ions or by the internal mobilization of calcium ions. There are several subtypes of this current which can be voltage dependent ( $I_C$ ) or independent ( $I_{AHP}$ ).

Single channel recording have shown that  $I_C$  has a large unitary channel conductance (100-250 pS) whereas  $I_{AHP}$  unitary channel conductance is small (6-14 pS; Castle et al. 1989). These channels are often inactivated by intracellular calcium concentration. This is achieved either by the direct interaction between calcium and the channel or through a pathway involving the activation of guanine nucleotide binding proteins, which generate intracellular second messengers (Kaczmarek and Levitan 1987). The sodium dependent potassium channel ( $G_{K(Na)}$ ) is less well characterized but, in a manner analogous to  $G_{K(Ca)}$ , it is activated by intracellular sodium and it appears to be voltage independent (Bader 1986; Dyer et al. 1989; Schwindt et al. 1989).

Single channel recordings from neuronal cells have identified channels which can be classified according to the criteria stated above. For example, single channel recordings of potassium currents in squid axon (Conti and Neher 1980) had similar gating characteristics to the macroscopic potassium current described by Hodgkin and Huxley (1952a). A potassium channel which opens only transiently has been identified in a number of preparations (Cooper and Shrier 1985; Hoshi and Aldrich 1988a; Kasai et al. 1986), as well as a fast activating, slowly inactivating channel (Hoshi and Aldrich 1988a; Jonas 1989; Schweitz et al. 1989). These currents were selectively blocked by DTX (Jonas et al. 1989; Schweitz et al. 1989). Hoshi and Aldrich ( $K_X$ ; 1988a, 1988b) and Jonas et al. ( $I_S$ ; 1989) have provided evidence of a slowly activating component of the total potassium current corresponding to the  $I_K$  in vertebrate neurones. As mentioned above single channel recordings have helped confirm the presence of and classify the subtypes of  $G_{K(Ca)}$ . Finally, single channel recordings have confirmed the presence of  $G_{K(Na)}$  in neuronal membrane patches (Haimann



and Bader 1989; Dryer et al. 1989).

*Pharmacology of tetraethylammonium*

Tetraethylammonium (TEA) has been shown to block most but not all types of potassium channels in a wide range of nervous tissues. Its mechanism of action appears to be invariant, therefore TEA's action will be introduced by discussing its action on  $I_K$  only. Somewhat similar to lidocaine, TEA requires the channel to open when applied from the inside of the cell in order to block. The time course of this blockade, which is intermediate in length (compared to lidocaine), was first demonstrated by Armstrong (1966) who showed, in the presence of internal TEA and using short depolarizing pulses (200  $\mu$ s), that the  $I/V$  relationship of  $I_K$  was normal. However, with longer depolarizing steps  $I_K$  became blocked, indicating that the channels must open for block to be established. It was also revealed that if the reversal potential of potassium was raised to 0 mV, causing an inward flow of potassium rather than the usual outward flow, prolonged activation of  $I_K$  relieved the TEA block. Armstrong explained this phenomenon to result from the inward rushing potassium ions flushing the channel of the blocker, implying that the site of action of the blocker is somewhere inside of the channel pore. This observation supports the generally held view that TEA blocks potassium channels by virtue of its similar size to that of the hydrated potassium ion. The diameter of TEA has been determined to be 0.56 nm by measuring the mobility of the ion in water (which depends on the molecule's frictional resistance to movement in the water and therefore is proportional to its size; Robinson and Stokes 1965). This value is very close to size of the hydrated potassium ion whose diameter has been estimated (assum-

ing it is hydrated with 6 water molecules), as 0.46 nM (Armstrong and Binstock 1965). Hoshi and Aldrich (1988a) demonstrated in single channel recording that external application of TEA blocked all four channel types identified in PC12 cells. Single channel recordings have shown that in contrast to internal application, external application of TEA does not require the channel to open to produce block. TEA reduced channel opening events; a finding inconsistent with use-dependent block. Nevertheless, the manner in which TEA blocks a potassium channel may still be relatively simple. TEA, owing to its size and charge, simply competes with the potassium for entry into the pore. Because it is slightly larger it plugs the channel and block occurs.

Although TEA is able to block  $I_K$  in large variety of tissues, it does so over a wide range of concentrations (100  $\mu$ M - 10 mM), depending on the site of application and the type of tissue. Between species, there is considerable variation in the external TEA concentration which produces 50 % block ( $IC_{50}$ ) of  $I_K$ . In the frog node of Ranvier  $IC_{50}$  of externally applied TEA is 400  $\mu$ M whereas in *Myxicola* axon it is 24 mM (Hille 1967; Wong and Binstock 1980). In squid giant axon even isotonic TEA has no effect on  $I_K$  (Tasaki and Hagiwara 1957). Furthermore, the  $IC_{50}$  can vary in the same tissue depending on whether TEA is applied inside or outside the membrane. In frog skeletal muscle the  $IC_{50}$  is 8 mM (external application) whereas it is 400 $\mu$ M for TEA applied to the inside (Stanfeld 1970). However, in contrast to external application, there is little variation in the  $IC_{50}$  applied intracellularly within and among species (approximately 500  $\mu$ M, Hille 1984).

For some conductances, blockade by TEA can be incomplete. For example,  $I_A$  and the  $G_{K(Na)}$  are incompletely blocked by TEA (Rogawski 1985;

Schwindt et al. 1989). TEA also has little effect on the small conductance  $G_{K(Ca)}$ ,  $I_{AHP}$ . This probably reflects the pore size of the channel, which seems to be too small to accept the TEA ion. In fact, there appears to be a correlation between the magnitude of the single channel conductance and the ability of TEA to block; the smaller the single channel conductance, the less TEA is able to block it.

### *Pharmacology of 4-aminopyridine*

4-AP is a membrane permeant blocker which acts on either side of the membrane. It blocks  $I_K$  and  $I_A$  in variety of tissue. Blockade of  $I_K$  and/or  $I_A$  by 4-AP was shown in early studies not to require the channel to open to produce blockade. These studies also suggested that 4-AP preferentially blocked closed channels since blockade decreased as the cell was depolarized, ie. block was voltage dependent (Meeves and Pichon 1977; Ulbricht and Wagner 1976; Yeh et al. 1976). Recently, Arhem and Johansson (1989) have suggested that 4-AP block can be described by a model in which the binding and block of 4-AP is diphasic (there is a parabolic relationship between the rate of binding and membrane potential). Initially, 4-AP blocks only the open channels; at more positive membrane potentials binding decreases and block is relieved. This conclusion is supported by single channel recordings which indicate that 4-AP attenuated  $I_A$  by reducing the duration of channel openings (Kasai et al. 1988). In contrast, other studies have shown the action of 4-AP to be voltage independent (Dubois 1981; Segal and Barker 1984; Thompson 1977). It is notable that the range of concentrations used for these studies varies great-

ly (from 10  $\mu$ M to 10 mM) and these discrepancies in results may arise from these differences in concentration (i.e., voltage dependent block may be concentration dependent). The results may indicate that 4-AP blocks  $I_A$  and/or  $I_K$  1) at relatively low concentrations ( $< 1$  mM) in a voltage dependent manner (Arhem and Johansson 1989; Meeves and Pichon 1977; Ulbricht and Wagner 1976) and 2) at relatively high concentrations ( $> 1$  mM) voltage dependent unblocking is insignificant or non-existent (Dubois 1981; Meves and Pichon 1977; Segal and Barker 1984; Thompson 1977; Ulbricht and Wagner 1976; Yeh et al. 1976).

In some preparations, 4-AP at low concentrations (30-500  $\mu$ M 4-AP) also appears to be a non-voltage dependent potassium channel blocker of a fast activating slowly inactivating potassium current (Gustafsson et al. 1982; Kenyon and Gibbons 1979; Stansfeld et al. 1986; Stansfeld et al. 1987; Zbicz and Weight 1985). This current has been tentatively named  $I_{DTX}$  (see below) since it is also selectively blocked by the neurotoxin DTX in those preparations where it has been tested (Feltz and Stansfeld 1988; Stansfeld et al. 1986; Stansfeld et al. 1987).

Thus, 4-AP's mechanisms of actions are 1) voltage dependent at low concentrations, but requiring relatively high doses to produce complete block and 2) voltage independent and requiring low concentration to produce a block. These results imply that there may be two distinct channels sensitive to 4-AP.

*Pharmacology of neurotoxins which affect potassium channels*

Naturally occurring toxins have played a great role in identifying properties and structure of biologically important receptors. A number of neurotoxins have been isolated that selectively inhibit all the major classes of potassium channels in a range of concentration (usually nM- $\mu$ M range) substantially lower than chemical agents, such as TEA and 4-AP .

*Toxins which block  $I_K$*

Noxiustoxin, isolated from a scorpion venom of *Centruroides noxius*, has been shown to block the  $I_K$  in the squid giant axon (Carbone et al. 1987; Carbone et al. 1982) at 0.1 to 1.0  $\mu$ M. Other toxins which have been reported to selectively block  $I_K$  are equinotoxin, *Panidus imperator* venom, *Conus striatus* venom and antamanide phalloidin (Narahashi et al. 1972; Pappone and Cahalan 1987; Romey et al. 1975 )

*Toxins which block fast activating potassium channels*

Dendrotoxin (DTX), a fraction isolated from the snake *Dendroapsis augusticeps* and mast cell degranulating peptide (MCDP), isolated from bee venom, both appear to block the fast activating slowly inactivating potassium channels seen in a variety of tissues (cf. Dolly et al. 1987 Stansfeld et al. 1987). In the low nanomolar concentrations, DTX selectively blocks one subtype of potassium channels, characterized by fast activation and slow inactivation, and thus defines a unique current type,  $I_{DTX}$  (Stansfeld and Feltz 1988). At higher concentrations (0.5  $\mu$ M) DTX also blocks  $I_A$  (in CA1 pyramidal cells of the

hippocampus, which do not possess  $I_{\text{DTX}}$ , Halliwell et al. 1986), whereas in tissues which have  $I_{\text{DTX}}$ , it has no effect on  $I_{\text{A}}$  (Stansfeld et al. 1986; Stansfeld et al. 1987). One explanation of these observations is that the potassium channels responsible for  $I_{\text{A}}$  and  $I_{\text{DTX}}$  are derived from the same gene and alternative splicing results in two functionally different channels (see later). There is no toxin yet identified which selectively blocks  $I_{\text{A}}$ .

### *Pharmacology of calcium dependent potassium channels*

The two subtypes of calcium dependent potassium channels are selectively blocked by the two different neurotoxins apamin, from bee venom (*Apis mellifera*; Habberman 1984), and charybdotoxin (CTX), from scorpion *Leiurus quinquestriatus* (Miller et al. 1985). Apamin (at concentrations of 100 nM or less) blocks the slowly activating small conductance channel (10-14 pS),  $I_{\text{AHP}}$ , which is insensitive to TEA blockade, both in neuronal tissue (Borque et al. 1985; Pennefather et al. 1985; Szete et al. 1988) and non-neuronal tissue (Blatz and Magleby 1986; Romey and Lazdunski 1984). Apamin has no effect on the large conductance ( $\approx 200$  pS) fast activating TEA sensitive  $G_{\text{K}(\text{Ca})}$ ,  $I_{\text{C}}$ , in neuronal or non-neuronal tissues. However, CTX (in 10's of nM) has been shown to be a selective blocker of  $I_{\text{C}}$  in a variety of tissue (Castle and Strong 1986; Gallin and McKinney 1986; Guiggino et al. 1987; Lancaster and Nicoll 1987; Miller et al. 1985). Although CTX has no effect on  $I_{\text{AHP}}$ , CTX has been reported to block calcium independent potassium channels in rat brain synaptosomes (Schneider et al. 1989), as well as the DTX sensitive potassium current in cultured rat dorsal root ganglion cells (Schweitz et al. 1989). In conclusion, the pharmacology of these potassium channel blockers indicates that there are two distinct  $G_{\text{K}(\text{Ca})}$ : One ( $I_{\text{AHP}}$ ) sensitive to apamin and insensitive to TEA

and CTX, the other ( $I_C$ ) sensitive to CTX and TEA and insensitive to apamin.

*What does the pharmacology of potassium channels tell us about potassium channels?*

In the absence of blockers that selectively alter gating kinetics, like those affecting the sodium channel, little has been revealed on the structure of the potassium channels. However a good deal of information on the number of different kinds of potassium conductances and their functional role has been obtained from pharmacological studies. This information is based largely upon the use of potassium channel blockers with selective action.

Blockade of potassium conductances by TEA has diverse effects. In frog node of Ranvier, where it blocks all voltage dependent potassium channels (Dubois 1981), both the fast activating conductances and the slowly activating ( $I_K$ -like) conductance, it prolongs a single action potential and increases excitability (Poulter and Padjen 1988b; Chapter 5). In rat myelinated axon, where it selectively blocks only one component of the potassium conductance, it increases excitability without affecting action potential duration (cf. Baker et al. 1987; also see section: *Function of potassium conductances in myelinated axon*). TEA increases both evoked and spontaneous transmitter release recorded from a neuromuscular junction preparation (Collier and Exley 1963; Koketsu 1958), likely by prolonging the presynaptic action potential duration and depolarizing the nerve terminal. Both effects would tend to increase the influx of calcium into the terminal and therefore increase transmitter release. Like TEA, noxious-toxin also slowed action potential repolarization in squid axon (Carbone et al.

1987) and increased transmitter release from brain synaptosomes (Sitges et al. 1986), similar to the effect of TEA at the neuromuscular junction (Collier and Exley 1963; Koketsu 1958). These diverse actions are likely not due to TEA blocking only to one channel type. Often it is the case that there is a lack of consistency in identifying the properties of the potassium current(s) blocked by TEA and conclusions regarding the functional attributes of the current are erroneous (also see Discussion p. 7-6 on function of  $I_K$ ).

While the above may be true, despite its apparent specificity, application of DTX produces a variety of effects as well. Harvey and Anderson (1985) have shown that application of DTX increased the frequency of mini end plate potentials at the neuromuscular junction. In frog spinal cord, it leads to convulsive discharges (Collier et al. 1982; Poulter et al. 1989; Chapter 4). DTX also blocks accommodation<sup>1</sup> in the frog myelinated axon, (Poulter et al. 1989; Chapter 4) nodose ganglia (Stansfeld et al. 1986) and hippocampal CA1 neurones (Halliwell et al. 1986). Therefore, specificity of blockade does not necessarily imply specificity of effect on the function of the neurone. This suggests that channels with similar properties can have a wide range of responsibilities depending on the neuronal type and its distribution within the neurone.

What should also be noted is the apparent gray area that exist when one endeavours to classify potassium channels according to their gating characteristics. For example, there is very little difference in the voltage dependence and

---

1. This and subsequent chapters will refer to accommodation as originally defined by Nernst (taken from Katz 1939), as any process which prevents action potential generation or reduces the efficacy of continuous stimulus. Adaptation refers to any process reducing the frequency at which a neuron fires in response to a constant stimulus; early adaptation refers to the difference in the first two interspike intervals, whereas late adaptation refers to subsequent increases in interspike intervals (Jack et al. 1975, p. 355)



the gating characteristics between  $I_{\text{DTX}}$  in rat nodose ganglia (Stansfeld et al. 1986) and  $I_{\text{K}}$  identified in squid axon. Furthermore, in hippocampus  $I_{\text{K}}$  activates much slower than in squid axon.  $I_{\text{K}}$  in squid axon is insensitive to external TEA block (Tasaki and Hagiwara 1957) however,  $I_{\text{K}}$  in hippocampus is blocked by external TEA (Segal and Barker 1984). Despite these rather profound differences they have been classified (by name) as the same current. Therefore, gating characteristics appear to be a somewhat inconsistent criteria for the classification of  $I_{\text{K}}$ .

The mechanisms of block by 4-AP of  $I_{\text{A}}$  and  $I_{\text{A}}$ -like channels indicate that the physiological classification of  $I_{\text{A}}$  may be inaccurate as well. There is little doubt that classification of the fast activating and inactivating (transient) current,  $I_{\text{A}}$ , is valid. However, the pharmacology of currents with more intermediate rates of inactivation ( $I_{\text{A}}$ -like) is quite different from  $I_{\text{A}}$  ( $I_{\text{A}}$ -like are blocked by low doses of 4-AP in non-voltage dependent manner). It may be possible that this  $I_{\text{A}}$ -like current is  $I_{\text{DTX}}$  described above since  $I_{\text{DTX}}$  is also blocked by low doses of 4-AP. Dolly et al. (1987) has pointed out that there appears to be correlation between the slow rate of inactivation and sensitivity to blockade by 4-AP and DTX. This raises the possibility that some currents classified as  $I_{\text{A}}$ , due to their transient kinetics, may turn out to be better classified as an  $I_{\text{DTX}}$ .

To summarize, the pharmacological data suggests that there are at least three types of voltage dependent potassium currents: 1)  $I_{\text{K}}$ , a TEA and noxiustoxin sensitive channel 2)  $I_{\text{A}}$ , a current which is sensitive to 4-AP blockade in the mM range and sometimes to DTX and 3)  $I_{\text{DTX}}$  a current which is sensitive to 4-AP in the  $\mu\text{M}$  range and dendrotoxin and MCDP in the nM range.

While pharmacological data has allowed us to identify classes of currents, ultimately the classification of the voltage dependent potassium channels is still tentative. An obvious method to clarify this situation would be to classify potassium channels based on their cDNA transcripts. One could then classify channels by correlating the amino acid sequences of the clones with their pharmacology and electrophysiology when they are expressed in their native membranes. Investigations along this line of inquiry have begun and preliminary results indicate that the above classification may hold but further characterization may still be required (see: *NEW APPROACHES TO OLD QUESTIONS*).

Finally, an examination of the effects of potassium blockers has produced some general information about the function of the various pharmacologically distinct potassium currents. Despite the uncertainties mentioned above, the use of potassium channel blockers has revealed that 1) fast opening potassium conductances like  $I_C$  (in rat hippocampus) and  $I_K$  (in squid axon) regulate action potential repolarization (Storm 1987; Tasaki and Hagiwara 1957), 2) channels which turn on more slowly like  $I_{AHP}$  (Madison and Nicoll 1984), or which do not inactivate like  $I_{DTX}$  (Poulter et al. 1989) appear to regulate excitability by altering the spike frequency adaptation and accommodation, and 3)  $I_A$  which turns on only transiently regulates spike frequency adaptation, only after the cell has been hyperpolarized by another stimulus, by virtue of its inactivation voltage dependence (Rogawski 1985).

## *CALCIUM CHANNELS*

In recent years a number of investigations have identified and characterized calcium channels present in a wide variety of tissues. This classification has been accomplished in a manner similar to potassium channels. Both physiological criteria, such as voltage dependence, activation/inactivation kinetics, single channel conductance measurements and pharmacological criteria, such as the selectivity of various agents which modify function, have been employed. Based on these criteria, three types of calcium channels have been identified: one low threshold calcium channel (T-type) and two high threshold channels (L-type and N-type; Nowycky et al. 1985a; Fox et al. 1987a, 1987b).

### *T-type calcium channels*

The identification and characterization of T-channels has been more or less straight forward. With only slight variation from one tissue type to another, they all activate at low threshold (below -60 mV), rapidly inactivate ( $\tau = 5-50$  ms) and have a slowly decaying tail current. Their single channel conductance in 100 mM barium is 5-10 pS and they are equally permeant to calcium and barium (Carbone and Lux 1987; Fox et al. 1987a). They have been identified in a wide range of tissue types, for example: smooth, skeletal and cardiac muscle, as well as, neuronal tissue (Benham et al. 1987; Cota and Stefani 1986; Fox et al. 1987a, 1987b; Nilius et al. 1985). They are potently blocked by nickel, cadmium, and cobalt, but are poorly blocked by dihydropyridines (D-600, nifedipine) or *omega*-conotoxin. The current is unaffected by the calcium channel activator,

Bay K 8644.

*N and L-type calcium channels*

Evidence that there exist two types of high threshold calcium channels (above -20 mV) is based primarily on results from single channel recordings. Fox et al. (1987b) demonstrated two conductance states, one of  $\approx 20$  pS (L-type) and another of intermediate size 13 pS (N-type). Unlike T-channels, there are considerable variations in the activation and inactivation kinetics of N-type and L-type channels in different tissues. However, one consistent difference between these channel types is that L-type channels inactivate very slowly whereas N-type channels inactivate with a time constant of  $\approx 30$  ms (Fox et al. 1987a; Nowycky et al. 1985b). Single channel recordings from non-neuronal cells have indicated that the large channel conductance (L-type channels) is blocked by nifedipine and enhanced by Bay K 8644, while N-type conductance is unaffected by these dihydropyridines (Fox et al. 1987b; Hirning et al. 1988; Nowycky et al. 1985b). However, the action of dihydropyridines on neuronal L-type channels is less well established. At concentrations that completely block L-type currents in smooth and cardiac muscle (Bean et al. 1986; Sanguinetti and Kass 1984; respectively) nifedipine blocked only 50% of the L-type current in chick sensory neurones (Fox et al. 1987a). Nifedipine reduced the L-type current 5-50% in only 28 of 56 chick dorsal root ganglia cells (Kasai et al. 1987). This suggests that neuronal L-type channels may have lower affinity for dihydropyridines than L-type channels found in non-neuronal tissue. In fact, L-type neuronal high threshold calcium channels in general may be different from those found in other tissue since *omega*-conotoxin (another naturally occurring peptide neurotoxin isolated from the carnivorous sea snail *Conus geographus*)

is an effective blocker of neuronal high threshold channels, whereas it has little effect on these channels in other tissue (Kasai et al. 1987; McClesky et al. 1987). There is some controversy whether or not *omega*-conotoxin blocks both high threshold conductances or just N-type. Kasai et al. (1987) report blockade of both types, whereas McClesky et al. (1987) report that only N-type is blocked. The other possibility is that the persistent calcium current (and therefore L-type, since N-type inactivates much more quickly) being blocked may not be "pure" L-type and there may be a component of N-type that does not inactivate which is insensitive block.

*What do pharmacologically distinct calcium channels do?*

Functional studies on the T-channels have not been done in neuronal tissue. However, taking into consideration their attributes (see above) and that they might be primarily located in cell bodies Jahnsen and Llinas (1984) have suggested that they would be well suited for modulation of bursting and pacemaking activity through the activation of potassium channels.

The function of the high threshold calcium channels in light of their pharmacology is still controversial. Transmitter release from synaptosomal preparations is resistant to dihydropyridine treatment (Perney et al. 1986; Hirning et al. 1988) whereas *omega*-conotoxin is effective in blocking transmitter release (Reynolds et al. 1986), implying that the N-type is important for neurotransmitter release. Although *omega*-conotoxin blocks transmitter release in frog neuromuscular junction (Kerr and Yoshikami 1984), it has no effect on transmitter release in the mouse neuromuscular junction (Anderson and Harvey

1987). Therefore, more studies will be needed to resolve these discrepancies.

### *NEW APPROACHES TO OLD QUESTIONS: MOLECULAR BIOLOGY OF VOLTAGE GATED ION CHANNELS*

Until recently the tools for studying the function and pharmacology of voltage dependent ion channels in neurones have essentially rested in the hands of biophysicists. Thus, by using a battery of electrophysiological techniques, we know a good deal about how fast ion channels open and close, what ions they are selective for and how they behave macroscopically and at the single channel level. At the molecular level, the structure of the ion channel was often inferred by the action of drugs on these channels (as in the case of the TTX binding site and the sodium channel). However, over the past number of years many questions concerning the structure and function of ion channels has been wrestled from the hands of electrophysiologists and placed in the care of biochemists. What is the structure and amino acid sequence of the channel? What is the nature of the amino acids lining the pore of the ion channel? What amino acids form the mouth of the ion channel pore which presumably are important for ion selectivity? These are all questions upon which electrophysiologists can only speculate. In the following pages, an overview of the kinds of answers to these questions will illustrate the important new information molecular biology has obtained concerning structure and function of voltage dependent ion channels.

#### *Structure and function of sodium channels*

As mentioned in opening paragraphs, drugs have been used to isolate channels for native membranes. TTX and STX, were used to isolate and purify the

sodium channel protein from the electric organ of electroplax *Electrophorus electricus* (Agnew et al. 1978). A similar strategy was used to isolate the sodium channel protein in rat brain (Hartshorne and Catterall 1981). Both sources of sodium channel contained a 230-260 kD protein which has been termed the  $\alpha$  subunit. The mammalian  $\alpha$  subunit was also found to be associated with two other polypeptides designated the  $\beta_1$  and  $\beta_2$  subunits (36 kD and 33 kD respectively), whereas in electroplax these peptides were absent. Studies which reconstituted the subunits in various combinations demonstrated that the  $\alpha$  subunit is critical for ion channel function (Hartshorne et al. 1985). Removal of the  $\beta_2$  subunit has no effect on channel function, whereas, loss of the  $\beta_1$  subunit reduced the ability of the channel to bind toxins, conduct ions and removed voltage dependence (Messner et al. 1986). However, more recent studies based on expression of the  $\alpha$  subunit (injecting mRNA into *Xenopus* oocytes) have demonstrated that the  $\alpha$  subunit retains its unitary channel conductance and voltage dependence but inactivates at a two to three fold slower rate (Auld et al. 1988). This discrepancy might be explained by the method that was used to separate the  $\beta_1$  subunit from the  $\alpha$  subunit, which may have partially denatured the latter unit (Messner et al. 1986). Despite this uncertainty, it is evident that the  $\beta_1$  subunit does stabilize or somehow modulate the function of the  $\alpha$  subunit.

The structure of the  $\alpha$  subunit was deduced by Noda et al. (1984) by an analysis of the cDNA sequence which codes for the polypeptide. The cDNA was believed to result from the transcription of a single gene which contains 4 internal homology units each containing 6 regions (S1-S6) which are homologous. By plotting the relative hydrophobicity of the amino acid sequences coded

for by the four homologous units it was hypothesized that these sequences span the lipid membrane in a rectangular formation, the centre of which forms the ion channel. Noda et al. (1984) hypothesized that only the S1, S2, S5, and S6 regions of these amino acid units are buried in the lipid however, it is now generally agreed that all regions (S1-S6) span the membrane (Catterall 1989).

### *Structure and Function of Potassium channels*

The first cloned potassium channel protein was isolated by screening the mRNA library of rat kidney. Takumi et al. (1988) assayed for an mRNA which when injected into *Xenopus laevis* oocyte caused the expression of an outward current activated by depolarizing voltage steps. The cDNA cloned from the isolated mRNA codes for a 130 amino acid protein containing only one hydrophobic domain consisting of six hydrophobic regions, S1-S6. Other studies have identified a number of proteins coding for potassium channels proteins (Papazian et al. 1987; Strömmer et al. 1989). A great deal of homology has been found among them, especially in the S4 region of the membrane spanning portion of the protein. In fact, this region has been shown to exist in all voltage sensitive ion channels. Its characteristic feature is a repeating Lys/Arg-X-X sequence occurring 4-8 times (where X is a hydrophobic amino acid). The potassium channel protein isolated from *Drosophila melanogaster* contained hydrophobic regions which are believed to arrange themselves into a structure similar to the individual homologous units of the sodium channel (Papazian et al. 1987; Catterall 1989). The difference is that the potassium channel proteins are about one fourth the size of the sodium channel protein, and a single potassium channel protein does not likely form a single ion channel. By analogy, it has been suggested that individual proteins may assemble as a tetramer, forming a



structure similar to the sodium channel protein (Timpe et al. 1988).

The multitude of different potassium channels proteins is not thought to reflect a multitude of potassium channel genes. (Tempel et al. 1988; Schwarz et al. 1988; Strümher et al. 1989). Evidence suggests that there are two basic mechanisms by which this diversity occurs. The first is through alternative splicing of large primary transcript (*Shaker* gene; Schwarz et al. 1988). Tempel et al. (1988) demonstrated that alternative splicing of a single gene could produce two different potassium channels. Expression of these gene products in oocyte, produced two type of currents: one rapidly activated and inactivated and the other rapidly activated but slowly inactivated. The second mechanism is through the expression of variant genes believed to arise from a common ancestor gene (Stümher et al. 1989). It was demonstrated that a family of homologous proteins, when functionally expressed in oocyte, produced four channels each with different gating characteristics and pharmacology. Two channel types were rapidly activating and slowly inactivating, sensitive to DTX, MCDP and CTX in nM concentrations but had differing TEA sensitivity ( $IC_{50}$  of 0.6 mM vs 129 mM). Another channel type, which rapidly activated and inactivated was sensitive to low millimolar 4-AP concentrations ( $IC_{50} = 1.5$  mM) and relatively insensitive to DTX block. The fourth clone produced a channel with an intermediate inactivation rate and it was blocked only at relatively high concentrations of 4-AP ( $> 10$  mM). Whether or not these proteins are naturally occurring is still a matter for speculation; however, these two mechanisms could account for the diversity of potassium channels observed *in vivo*.

A recent study by Mackinnon and Miller 1989 has demonstrated, that the

binding and blocking efficacy of CTX could be altered by site directed mutagenesis of the *shaker* cDNA sequence. Previous studies have shown that CTX blocks the channel by binding to the mouth of the ion pore (Anderson et al. 1988). By changing the negatively charged glutamate-422 amino acid residue to a glutamine, the binding was reduced 3.5-fold along with a concomitant decrease in blocking efficacy. Substituting a lysine for the glutamate reduced binding by 12.5-fold completely abolishing the blocking activity of CTX. These alterations in binding and blocking efficacy indicated the region of the protein which may make up the mouth of the ion channel. Furthermore, since glutamate-422 was shown to be in or around the mouth of the channel protein it was concluded that the location of the glutamate-422 residue is on the outside of the membrane, thus limiting the possible folding combinations of the hydrophobic regions of the channel protein. From this analysis it follows that this protein has six membrane spanning regions similar to that reported for the homology units of the sodium channel (Catterall 1989).

### *Structure and Function of Calcium channels*

Similar to the strategy used to purify the sodium channel using the high affinity ligands TTX or STX, the voltage dependent calcium channel was isolated by purification of a protein fraction which binds organic calcium channel blockers (dihydropyridines, DHP, eg. nifedipine). This procedure helped isolate the L-type calcium channel protein (Curtis and Catterall 1984; Flockerzi et al. 1986). A large DHP binding protein was obtained (130-170 kD  $\alpha_1$ ) associated with a number of smaller proteins (143 kD  $\alpha_2$ ; 27 kD  $\beta$  and 30 kD gamma subunits; cf. Catterall 1989). Reconstitution of the purified DHP binding protein

demonstrated that it was a calcium channel (Flockerzi et al. 1986). The  $\beta$  subunit of the calcium channel protein is a substrate for phosphorylation by cAMP dependent protein kinases. The probability of channel opening was shown to be positively correlated with the amount of phosphorylation (Flockerzi et al. 1986). The function of the other subunits is not clear at this time.

It is interesting to note that the structure of the  $\alpha_1$  calcium channel protein, determined by a hydrophylic profile of the amino acid sequence coded by cDNA sequence, is the same as that determined for the sodium channel. In fact, calcium channel cDNA sequence shows 55% homology with the sodium channel protein. Like the potassium channel, this protein also showed homology with the sodium channel in the S4 region with the characteristic Lys/Arg-X-X repeating pattern.

In summary, biochemical approaches have revealed a number of structural features common to the three families of voltage gated ion channels. All channel proteins reside in the membrane as "pillars" of amino acids, with lipid membrane, extracellular and intracellular domains, coded for by what is termed as cDNA "homology units". The sodium and calcium channel cDNAs have four internal homology units, which are believed to be the product of a single gene. The potassium channel proteins are different: their genes contain a cDNA sequence coding for only a single membrane spanning amino acid sequence. Within each membrane spanning unit there are "homologous regions" (S1-S6), believed to be buried in the lipid membrane. The S4 region in all three channel types is highly conserved and it is not found in non-voltage dependent ion channels suggesting that this structure constitutes the voltage sensor for these

channels. Conformational changes in this region may generate the small current which flows during channel opening, the gating current (Armstrong 1981). This and other sites hypothesized to be important for ion selectivity, drug binding and allosteric modulation are all candidates for site directed mutagenesis. It is reasonable to expect that these types of studies would eventually generate a full description of ion channels structure and function.

## ***PART II: STRUCTURE AND FUNCTION OF MYELINATED AXONS***

### ***Function of myelin and sodium current flow in myelinated axons***

The structure of myelinated axons in the peripheral and central nervous system (PNS; CNS respectively) is distinguished from that of all other neurons by being encapsulated by a proteolipid spiral, myelin. In the periphery this wrapping, which is essentially an organelle of a type of glial cell (Landon 1982), is provided by the Schwann cell. Schwann cells are segmentally distributed along the axonal membrane such that one cell wraps around 200-2000  $\mu\text{m}$  of axon with 100-200 layers of myelin (Landon 1982). At the ends of individual Schwann cells there are small gaps of unmyelinated axon or nodes, first identified by the anatomist Ranvier (1878). Thus, myelinated axons are segmented into distinct regions: internodes, wrapped in a thick myelin sheath divided by short unmyelinated regions, nodes. Although PNS and CNS myelinated axons have different cells providing their myelin coat (CNS uses oligodendrocytes) both structures share many physiological and functional properties. It has been recognized for some time that the internode and node are functionally distinct. During conduction of action potentials, nodes have considerably more current flowing through them than internodes (Huxley and Stampfli 1949a). Because the current predominantly flows ("jumps") between nodes, this type of conduction has been termed saltatory conduction (from Latin saltare = to dance).

Erlanger and Blair (1934) were the first to suggest and provide evidence that conduction in myelinated axons might be saltatory in nature. They found that block of action potential conduction by current stimulus or by altering the composition of the Ringer solution (increasing the calcium or potassium ion

concentration) could be more easily produced at the node than the internode. They concluded that the node was less well insulated than the internode and perhaps excitation spread from node to node. Their hypothesis was based on observations, made by Lillie (1925), who showed that an analog nerve (an iron wire interrupted by sections of glass insulation) conducted in a saltatory manner. This hypothesis was supported in a number of studies which followed (Erlanger and Blair 1938a; Tasaki 1940; Tasaki and Takeuchi 1941). However, it was not confirmed until Huxley and Stämpfli (1949a) were able to directly measure and demonstrate that the current flow in the node was considerably larger than in the internodal region. This contrasts to conduction in squid axon where conduction proceeds as an even current flow between adjacent membrane regions (Hodgkin 1971).

Until recently, the nature by which myelination was believed to maintain saltatory conduction was through acting as an insulator. Myelin increased the resistance of the internodal membrane, "forcing" current flow through the nodal membrane and thus, excitation spreads from node to node (Huxley and Stämpfli 1949b; Tasaki 1953; Hodgkin 1971). The myelin resistance and capacitance calculated by Huxley and Stämpfli (1949a) supported the assertion that myelin was a low capacitance, high resistance shield to current flow. While it is true that saltatory conduction can occur under some circumstances when the myelin has been interrupted (Rasminsky and Sears 1972), it is recognized that myelination is essential for normal saltatory conduction.

With the advent of voltage clamp technique of the nodal membrane, activa-

tion of inward current flow was shown to be essentially the same as the activation of the voltage dependent current underlying the upstroke of the action potential in squid axon (Dodge 1963; Frankenhaeuser and Huxley 1964). In frog myelinated axon voltage clamp measurements also demonstrated that there was a potassium current in the nodal membrane whose presence was considered to be of little importance with regard to saltatory conduction (Dodge 1963; Hille 1984; Schmidt and Stämpfli 1966). These results, together with the understanding that myelin acts as an insulator, described saltatory conduction in myelinated nerves as the flow of a sodium dependent voltage activated current from node to node.

Recent studies provide two kinds of evidence that requires a modification of this "classical" model of myelinated axon: 1) the internodal membrane may be charged during action potential propagation. 2) myelinated axons are endowed with a multiplicity of potassium channels (see below). These two aspects of the myelinated axon have provided the impetus to reexamine our understanding how myelinated axons function.

Intracellular recording from intact nonmammalian (Barrett and Barrett 1982; Poulter et al. 1989) and mammalian myelinated axons (Blight and Someya 1985) have demonstrated the presence of a depolarizing after potential (DAP) following an action potential. The DAP has an amplitude of up to 10 mV which decays with a time constants of approximately 20, 2 and  $< 1$  ms (Blight and Someya 1985) rat myelinated nerve and approximately 100 ms in lizard myelinated axon (Barrett and Barret 1982). Barrett and Barrett (1982) were the first to suggest that this DAP represents the passive discharge of the internodal membrane capacitance charged by an action potential in the adjacent

node. In addition, the unusually long hyperpolarizing electrotonic potential recorded from intact myelinated axons has also been suggested as evidence of charging of the internodal membrane (Barrett and Barrett 1982; see also Chapter 2). Based on the morphology of myelinated axons (reviewed in Ellisman et al. 1983) three paths for this leak of capacitive current were considered: 1) the periaxonal space (the space between the innermost myelin layer sheath and the internodal membrane); 2) the clefts of Schmidt-Lanterman or the intracellular path through the cytoplasmic belts in the Schwann cell; and finally 3) through the extracellular spaces of the compact myelin sheath. These observations clearly differed from the classical electrical model of myelinated axon since it implied that the internodal membrane was not electrically inert and may therefore participate in the spread of excitation.

Blight (1985) noted that the resistance of combined internodal membrane and myelin layers is not as high as the specific resistance of some nonmyelinated neuronal membranes (Bush 1981; Carpenter 1973; Gorman and Mirolli 1972) and perhaps the importance of the resistance of myelin has been over emphasized. With this in mind, Blight (1985) has argued, with the help of a computer model, that a lower resistance myelin sheath that allows current flow through the internodal membrane could account for the presence of the DAP (supporting explanation 3 above). These calculations do not support the hypothesis that the main function of the myelin wrapping is to act as an insulator. Furthermore, Blight (1985) went on to suggest that the more important function of the multilayered stacking of myelin around the internodal membrane is to reduce the otherwise large effective capacitance of the internodal membrane. So, while it is true that Hodgkin and Stämpfli (1949b) recognized that a low



capacitance is necessary for saltatory conduction, our present understanding implies that the reduction of capacitance of the internodal membrane conferred by myelination may be more important than its insulating qualities.

Even if this interpretation is not completely correct it is evident that the internodal membrane is "actively" involved in the mechanism of saltatory conduction. Thus, it has been suggested that the physiological role of the DAP may be to help bring to threshold subsequent nodes during the spread of excitation (Barrett and Barrett, 1982; Blight, 1985). Charging of the internodal membrane may also account for the 7-20 ms period of superexcitability following the single action potential in frog and mammalian myelinated nerves (Raymond 1978; Blight and Someya 1985).

A low internodal capacitance, as well as other factors (see below), has also been recognized as a necessity for high conduction velocities (Huxley and Stämpfli 1949b; saltatory conduction in itself is not enough to produce high conduction velocities). Numerous studies indicate that demyelination (produced either experimentally or through disease) causes the internodal membrane to have a larger capacitance which accompanies a reduction in conduction velocity (Kocsis and Waxman 1985). The importance of the capacitance versus resistance of the internodal membrane has been compared in another computer model (Moore et al. 1978). Varying the capacitance and conductance independently, it was possible to demonstrate that changes in the myelin sheath conductance had a negligible effect on conduction velocity. However, increasing the specific capacitance of the myelin reduced conduction velocity considerably. This effect could be reversed by adding more wraps of myelin thereby reversing the effect of increasing the specific capacitance.

Two other factors are also recognized to affect conduction velocity 1) internodal length and 2) fibre diameter. Huxley and Stämpfli (1949a) gave analytical arguments that suggested internodal length affects conduction velocity. Increasing the internodal length increases conduction velocity to maximum after which there is broad range at which the conduction velocity is maximal. Internodal lengths beyond this range decrease conduction velocity. Studies have supported these theoretical conclusions (cf. Ritchie 1982a). For example, regenerated nerve fibres having internodal lengths half of normal fibres were found to have near normal conduction velocities (Sanders and Whitteridge 1946; Ritchie 1982b; Shrager 1988). Fibre diameter and conduction velocity have been shown to roughly linearly related, in several early studies on peripheral myelinated axon (Hursh 1939; Tasaki 1953). Rushton (1951) proposed a theory which indicated that myelinated nerves appear to be constructed in manner which maximizes their conduction velocity for a given fibre diameter, such that the ratio of axon diameter to total fibre diameter (which includes myelination) is always close to 0.6. In this way evolution has caused axons of different diameter to optimize their degree of myelination in order to maximize their conduction velocity. To summarize the velocity of saltatory conduction is increased in myelinated fibres by a low internodal capacitance combined with an optimal internodal length and axon/fibre diameter ratio.

In addition to myelin's contribution to the electrical properties of the axon, myelin appears to play a role in regulating the distribution of sodium channels on the axonal membrane (Bray et al. 1981). Ritchie and Rogart (1977) demonstrated (what had been suspected for some time) that the density of sodium

channels (as measured by TTX and STX binding sites) was higher on the nodal membrane than on the internodal membrane. A number of studies which indicate that sodium channel density increases on demyelinated or unmyelinated internodal membrane (Bostock 1982; Bostock and Sears 1976, 1978; Rasminsky 1982; Ritchie 1982b). In frog sciatic nerve fibres, Shrager (1988) showed that Schwann cell proliferation following demyelination resulted in redistribution of sodium channels. Shrager followed the remyelination over a period of up to 5 months and found that in regions which were previously internodal, occasionally two proliferating Schwann cells would meet and form a new node. It was found that at these new nodes the sodium current density was greater than before, when the membrane was internodal. The sodium channels in these new "nodes" were not thought to come from the new synthesis of channels but resulted from the migration of the "old" sodium channels. Thus, it would appear that Schwann cells somehow reorganized the axonal channels. In this study it was also believed that there was no transfer of sodium channels from the Schwann cells to the axon. In similar studies done on mammalian axons it has been suggested that an increase in sodium channel number may be the result of a contribution of sodium channels from the Schwann cells (Chiu and Ritchie 1984). These results led Chiu and Ritchie (1984) to propose that during development, Schwann cells may synthesize sodium channels and transfer them to the axonal membrane. Evidence for transport of protein molecules and sodium channel immuno reactivity in the Schwann and glia cells has been demonstrated in a number of studies (Black et al. 1989; Gainer et al. 1977; Gray and Ritchie 1985; Kreigler et al. 1981).

*Function of potassium conductances in myelinated axons.*

Classical descriptions of myelinated axons concerning potassium currents stated they were non-existent (in the case of mammalian axons; Hille 1971) or that only one type was present (in the case of the frog; Hille 1971). The classical view of the function of myelinated axons did not place any importance on the potassium conductances present in amphibian myelinated axon. In fact, their presence in frog axon was considered to be somewhat of an anomaly. This conclusion fit well with the belief that all axons were "faithful propagators of action potential conduction which neither synthesized or modulated their activity" (Hille 1984). Unlike understanding the function of the sodium conductance in axon, elucidating the role of potassium conductances in myelinated axons has been less straightforward. Recent voltage clamp and pharmacological studies have demonstrated the presence and differential distribution of a number of fast and slowly activating potassium conductances in both mammalian and amphibian myelinated axons (described in subsequent sections; Black et al. 1990; Dubois 1981; Grissmer 1986). This new information points out that potassium conductances in axons may be important modulators of function as well recognized in other neurones.

Voltage clamp studies of *mammalian* intact peripheral myelinated showed that the potassium currents were small or were not present (Brismar 1980; Chui et al. 1979; Horackova et al. 1968). However recordings from voltage clamped rabbit sciatic nerve fibres showed a fast activating potassium conductance ( $\tau = 1-3$  ms) following experimental demyelination suggesting an internodal origin (Chui and Ritchie 1980). Recent pharmacological studies have demonstrated the presence and differential distribution of a slow potassium conductance in mammalian axons. Using extracellular recording and current clamp technique,

TEA has been shown to block a slow component of a depolarizing electrotonic potential (ETP; Baker et al. 1987). It was also demonstrated in the same study that this slow component of the ETP was 30 times greater in magnitude in the node than in the internode. In addition, TEA has been shown to block a slowly developing hyperpolarization elicited by a burst of action potentials in a peripheral myelinated axon (Eng et al. 1988; Kocsis et al. 1987). Sensitivity to TEA in these studies was shown to be independent of the degree of myelination implying that this conductance also originates in the node. In agreement with voltage clamp studies described above, 4-AP has been demonstrated to block a fast activating potassium conductance located in the internode (Bowe et al. 1987; Foster et al. 1982; Ritchie 1982b). This conclusion is based on the observation that action potential repolarization is delayed more by 4-AP in demyelinated fibres than in myelinated fibres, reflecting a differential distribution of fast activating 4-AP sensitive potassium conductances to the internode. Presumably, myelination prevents access of 4-AP to the channels on the internodal membrane. Similar results have been obtained using axons from central nervous system, where sensitivity to 4-AP decreased as myelination of the nerve progressed (Kocsis et al. 1982). In the same study the ability of TEA to block a slowly activating potassium conductance was not affected by the degree of myelination. Thus, both voltage clamp and pharmacological studies have demonstrated a differential distribution of potassium conductances in mammalian myelinated nerve.

The effects of potassium channel blockade have revealed that these conductances are functionally distinct. In rat optic nerve and peripheral nerve blocking, the hyperpolarizing afterpotential with TEA (resulting from activation of the slow potassium conductance) increased the excitability of the fibre,

whereas 4-AP broadened the action potential without altering the excitability (Kocsis et al. 1985; Kocsis et al. 1987). These results also agree with those reported by Baker et al. (1987) who showed that in response to a prolonged depolarizing current pulse, TEA treated fibres generated more action potentials than control fibres. The additional function that these conductances may have is to lower conduction safety, as suggested by Padjen and Hashiguchi (1983). Reduction in the safety factor may contribute to branch point block in the terminal region of primary afferent fibres and therefore may be a mechanism of presynaptic inhibition (cf. Redman, 1979).

However, the functional significance of the differential distribution of two kinetically different conductances is not clear. The location of the fast channels in the internode, which may not be sufficiently activated to turn-on the fast potassium conductance (Barrett and Barrett 1982, Blight 1985), would appear to be inconsistent with their reported function to modify action potential generation. So, while it is relatively easy to rationalize the functional significance of the differential distribution of sodium channels, the significance of the distribution of the various potassium channels remains obscure.

Some aspects of the pathophysiology of demyelinating diseases (such as multiple sclerosis) may be related to the unmasking of potassium channels. Waxman (1989) has suggested that the activity of potassium channels in the exposed internode will tend to hold the demyelinated axon's membrane potential close to the equilibrium potential of potassium, at a value which is further away from threshold of the fibre, and thus would obstruct conduction. However, this is unlikely to be the mechanism by which conduction is impeded by

potassium channel activity. There is no evidence to suggest that 4-AP has any effect on resting membrane potential in demyelinated fibres, implying that these channels are not open at rest. It is more likely that the main effect of increased potassium channel activity will be a decrease in the conduction safety factor. Activation of the internodal potassium channels will shunt the spread of current resulting in a failure to stimulate subsequent nodes. A number of experimental studies have noted that 4-AP treatment restores conduction in demyelinated fibres (Sherret et al. 1980; Targ and Kocsis 1985). These results have prompted the use of 4-AP as a therapy for alleviating some of the symptoms of multiple sclerosis (Jones et al. 1983; Stefoski et al. 1987). However the

In *amphibian* node of Ranvier and internode three voltage dependent potassium conductances have been identified, the fast activating incompletely inactivating  $G_{Kf1}$  and  $G_{Kf2}$  and the slowly activating incompletely inactivating  $G_{KS}$  (Dubois 1981; Grissmer 1986). The presence of three kinetically different components has also been confirmed by patch clamp studies (Jonas 1989). These conductances are also unevenly distributed on the axonal membrane. Grissmer (1986) has calculated the potassium channel density to be 20 times smaller in the internode than in the node. Voltage clamp studies of the isolated node and internode have also shown that these potassium currents are blocked by a variety of agents. TEA blocks all three potassium conductances, whereas 4-AP blocks only the fast activating currents (Dubois 1981; Grissmer 1986). Purified dendrotoxin (toxin 1) from the venom of the green mamba snake *Dendroaspis polyepsis polyepsis* blocks only  $G_{Kf1}$  (Benoit and Dubois 1986) whereas the plant terpene capsaicin blocks  $G_{Kf2}$  (Dubois 1982). Unlike potassium conductances in mammalian axons, few studies have addressed the question of what functional role these conductances play in regulating electrical

properties and the excitability of frog myelinated axons.

*Electrical properties of myelinated axons*

Intracellular recordings from myelinated fibres, in contrast to intracellular recording from many other preparations, has not been extensively used and consequently is not fully characterized. Consequently electric current flow in axon which is modeled on the conduction of a core conducting cable structure, is incompletely described since the properties and elements (potassium conductances etcetera) of this cable are still largely unknown (Blight 1985; Jack et al. 1975, Moore et al. 1978). In the next section considerations are presented that point out that myelinated axon cannot be modeled as a uniform cable. In light of this fact, an example is presented in which, an estimate of the electrotonic spread was calculated and checked by empirical means demonstrating that despite an incomplete description of cable properties of myelinated axon, one can still estimate how the electrotonic potential reflects the charging of a portion of the axonal membrane.

For a uniform cable (e.g. cylindrical unmyelinated axon) the amount of space charged by passing a step current pulse in the cable varies according to the following equation (cf. Rall 1977):

$$\lambda^2 = R_m / (R_e + R_i)$$

where:  $\lambda$  is the space constant (defined below)

$R_m$  is the membrane resistance

$R_e$  is the extracellular resistance



$R_i$  is the resistance of the intracellular space.

If  $R_m$  is constant and the cable is at a steady state, the cable equation relating the space constant and the voltage at some distance  $x$  from the step current source can be expressed as (Rall 1977):

$$\lambda^2 \frac{d^2 V}{dx^2} - V = 0$$

This means that  $V$  (voltage) depends only on  $x$  (the distance from the current source) and not on  $t$  (time). This can be solved to show that at a point where the voltage displacement is  $V_0$  at  $x = 0$  that:

$$V = V_0 \exp(-x/\lambda)$$

Therefore,  $\lambda$  expresses the rate at which the voltage displacement  $V_0$  decays as one moves away from the current source (analogous to the rate of charging reflected by a time constant). During the development of a voltage response (before steady state is reached), not only is the voltage displacement smaller but the rate at which it develops is slower the further one moves away from the current source (Jack et al. 1975). Thus, points close to the current source are at steady state earlier than points more distant. One can calculate the time constant resulting from this effect by plotting the natural log of  $V$  versus time ( $t$ ) which yields a straight line having the slope  $-1/\tau$ . For excitable membranes resistance is nonlinear with respect  $V$  but estimates of  $\lambda$  and  $\tau$  can still be made.  $\lambda$  can be measured at steady state and  $\tau$  estimated small stimulus steps which minimize errors produced by nonlinearity.

By virtue of the fact that myelinated axons have differential distribution of both myelin and voltage dependent ion channels, myelinated axon must be considered as nonlinear *and* non uniform cables structures. In this case the equations used to describe the relationship between  $V$  and  $t$  are more complicated (cf. Rall 1977), but it is still exponential (Hodgkin and Rushton 1946). Although some attempts have been made to do so (Andrietti and Bernardini 1984; Blight 1985) presently there is no cable model which adequately reflects electrotonic potentials recorded from myelinated axon. Consequently, there is no quantitative description the lambda since there is no description of the nonuniform current flow along the axonal membrane. However, lambda has been measured empirically; in myelinated axons these values range from approximately 1-4 mm (Barrett and Barrett 1982; Rall 1977). Barrett and Barrett (1982) estimated that based on a space constant of 4.6 mm approximately 1 cm of axon is being (calculated at steady state; i.e. at 0 Hz frequency). As a means of checking this value they calculated the resistance predicted from this value. Assuming that the specific capacitance of the internodal membrane being charged is  $1 \mu\text{F}/\text{cm}^2$  the effective capacitance will be  $2.2 \times 10^{-9} \text{ F}/\text{cm}$ . A representative time constant ( $\tau_e$ ) for the membrane was shown to be 100 ms. Therefore, using  $\tau_e = R_e C_e$ , the effective resistance ( $R_e$ ) can be calculated to be  $45.5 \text{ M}\Omega$ . They concluded that, since this  $R_e$  was within the range of those experimentally determined, the electrotonic potential reflected the charging of a distance calculated by the empirically determined space constant. Therefore, an electrotonic potential reflects the electrotonic spread of current along the axon involving a distance approximately  $\pm 4$  internodes (and nodes) (assuming an internodal length of 1 mm) from the site of injection.

## *STATEMENT OF THE PROBLEM*

From the above exposé it is clear that our understanding of several important areas of myelinated axon function is incomplete. The purpose of this dissertation was to address some of these questions in two ways:

- 1) to further characterize the electrical properties of myelinated axon with respect to potassium conductances and
- 2) to investigate the possible functional roles of potassium conductances in regulating the excitability of myelinated axon.

These investigations were carried out by combining intracellular micro-electrode recording technique, which has not been extensively utilized to study intact myelinated axons, and the detailed knowledge of the pharmacology of the identified voltage dependent potassium conductances identified by voltage clamp.

Upon my arrival in A.L.P.'s laboratory, the direction of the laboratory was occupied with the study and characterization of primary afferent depolarization (PAD). It was obvious that one of the main obstacles for this investigation was the very large outward rectification present in these axons. It was hoped that the reduction of outward rectification might aid the examination of PAD, or allow the recording of calcium mediated events from the terminals (cf. Barrett et al. 1988). It was also part of larger design to understand how potassium channels affect the rectification and cable properties of myelinated axon. As part of this effort I was given a sample dendrotoxin and I was asked to assay its ability to block the very large outward rectification present in myelinated axons. As

evidenced in Chapter 4 it had a only a small effect on the outward rectification while having a rather specific and unique effect on the accommodating properties of the axon.

Judging by the relatively scant literature at the time (1985) dealing with the function of potassium conductances in myelinated axons, it was apparent that their presence in axons was still considered to be somewhat of an anomaly. Presented with the juxtaposition of clear evidence that potassium conductances do regulate excitability, and a lack of knowledge in this area, my curiosity was piqued and my course was set.

**A STUDY OF FROG MYELINATED AXONS BY INTRACELLULAR  
MICROELECTRODE RECORDING**

by

Michael O. Poulter, Toshio Hashiguchi and Ante L. Padjen

(Submitted to The Journal of Neurophysiology)

## *SUMMARY AND CONCLUSIONS*

1. Intracellular microelectrode technique was used to study the membrane properties of large primary afferent fibres (conduction velocity  $> 10$  m/s) attached to isolated frog spinal cord.
2. The hyperpolarizing electrotonic potentials had a far slower charging phase than those recorded from the isolated node of Ranvier. The longest charging time constant was often greater than 200 ms. Electrotonic potentials could be fitted with two time constants: one in the range of 70 - 210 ms, the other less than 20 ms. However, it was often apparent that the charging was more complex and that ETPs had an indeterminate number of time constants.
3. Steady state voltage-current relationships, obtained by injection of constant current pulses, were nonlinear. There was a pronounced outward rectification above resting membrane potential, as well as a previously unreported outward rectification below resting membrane potential.
4. Application of external tetraethylammonium (10 - 20 mM) depolarized the fibre and decreased the rectification below resting membrane potential. This pharmacological sensitivity indicated that the slow potassium conductance ( $G_{Ks}$ ; Dubois 1981) is responsible for the outward rectification below resting membrane potential. Block of this outward rectification was also accomplished by adding external barium ions (2 - 10 mM) to the perfusing media.
5. Although the deactivation process of the slow potassium conductance can

partly contribute to the slow charging phase of the electrotonic potential, a capacitive component, such as the internodal space (Barrett and Barrett 1982), is more likely responsible for the slow time course of electrotonic potentials in primary afferents. Similar large time constants were found in recordings from peripheral nerves and motor fibres.

6. A standard Hodgkin-Huxley model of the node of Ranvier (Hille 1971), failed to mimic the outward rectification below resting membrane potential. A modified model, which incorporated the slow potassium conductance ( $G_{Ks}$ ; Dubois 1981) simulated outward rectification of primary afferent axons below resting membrane potential.

## INTRODUCTION

Although myelinated nerve axons were one of the first neuronal structures examined by intracellular microelectrodes, very few studies followed the early reports (Tasaki 1953; Woodbury 1952). Thus, our knowledge about the biophysical properties of axons originates primarily from the very successful use of voltage-clamp technique on the nodes of Ranvier (Dubois 1981; Grissmer 1986; Hille 1971) and extracellular recording techniques (Huxley and Stämpfli, 1949a, 1949b). We have used intracellular microelectrode recording from frog large myelinated primary afferent axons to study the mechanism of primary afferent depolarization (Padjen and Hashiguchi, 1983). In the course of these studies it was noticed that some of the electrophysiological properties of axons cannot be explained by previous studies of the node of Ranvier. We have attempted to resolve some of these discrepancies by investigating the properties of relatively intact myelinated fibres. Impalement of primary afferents is most likely to take place in the internodal region and understanding the electrical characteristics of recordings from this region is important for the proper interpretation of the physiology and pharmacology of primary afferent depolarization (Padjen and Hashiguchi 1983).

We are reporting results of our experiments on both primary afferent sensory axons and motoneuron axons, as well as our attempts to model the previously unreported electrical properties using Hodgkin-Huxley equations (Hodgkin and Huxley 1952b), as applied to myelinated axons (Dubois 1981; Hille 1970, 1971) and the biophysical constants reported (Barrett and Barrett 1982; Blight and Someya 1985). Some of the results have been reported in a preliminary form (Hashiguchi and Padjen 1983).



## METHODS

### *General experimental methods*

Experiments were done on hemisected frog spinal cords isolated mostly from *Rana pipiens* and some from *Rana catesbeiana*, placed in a small chamber (0.150 ml) and continuously perfused with frog Ringer's solution at 10°C to 14°C. Normal frog Ringer contained in mM: NaCl, 115; KCl, 2; CaCl<sub>2</sub>, 2; HEPES buffer (pH adjusted to 7.3), 10; dextrose, 11. Ringer solutions containing 0.2  $\mu$ M tetrodotoxin (TTX-R) or 2 mM Mn (Mn-R) were used to block conduction and/or synaptic transmission.

### *Identification of fibres*

Most of the recordings were obtained from dorsal roots at the entrance zone of the 8th - 10th vertebral segment (see *FIGURE 2.1*). In some experiments axons were penetrated in the roots at the sites 10 mm or more distant from the spinal cord. For comparison, several motor axons were also studied. All of the fibres in this study belonged to the group of large myelinated axons, judged by their conduction velocity ( $> 10$  m/s) and their ability to follow trains of high frequency stimulation without delay, evoked via suction or bipolar platinum electrodes on the peripheral ends of the dorsal roots (see *FIGURE 2.1*). In some experiments, histological verification using HRP injection confirmed intraaxonal localization of the microelectrode, but a detailed comparison of the morphology and electrophysiology has not been done.

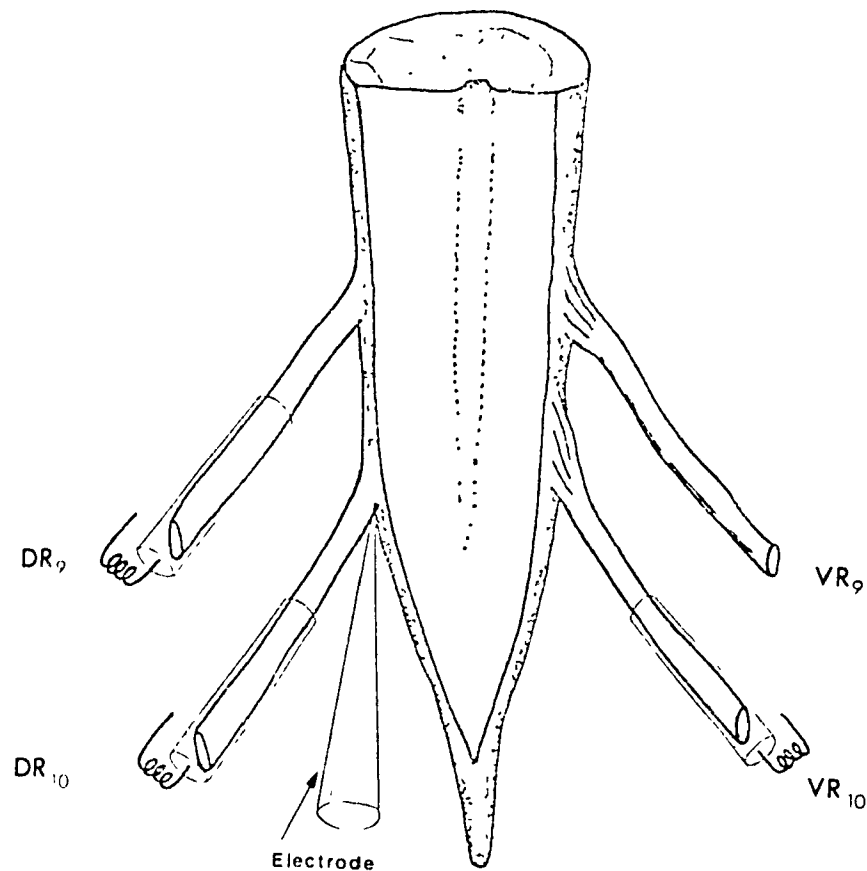


**FIGURE 2.1** A diagram of the experimental preparation. Isolated hemisected cord was placed in a chamber where its ventral or dorsal roots (VR and DR) could be stimulated by platinum wire electrodes in a pool of mineral oil. Microelectrodes were inserted into axons at the entry zone of dorsal roots, as shown.

### *Microelectrode Recording technique*

Glass microelectrodes were filled with KCl (3 M) or K sulfate (0.5 M) and had D.C. resistance of 40 - 100 M $\Omega$ . They were selected for their low noise and ability to pass up to 2 nA of current without rectification. Microelectrodes were connected to an amplifier with a fast rise time (40  $\mu$ s with electrode resistance of 100 M $\Omega$ ) constructed by T.H. and/or made by Dagan Corp. An active bridge

circuit allowed simultaneous current injection and recording through the same electrode ("current-clamp" technique). Results were analyzed from the film records of the oscilloscope traces and/or from the data digitized and stored on video tape using a PCM based A/D converter (at 22 kHz and 16 bit resolution, following a low pass 8 pole Bessel filter set at either 5 or 10 kHz). Off-line analysis was accomplished using a microcomputer based A/D converter (Modular Instruments Incorporated, 12 bit resolution).

### *Analysis of results*

Curve fitting was done using Asystant software package which uses a least squares fit based on Gauss-Newton algorithm. Fits were considered adequate only when  $r^2$  was greater than 0.99 and the squared error was less than  $1.0 \times 10^{-2}$ . All fits were obtained using a minimum of the 250 sample points from the charging phase of an ETP (sampling rate = 1 kHz). Log plots of some ETFs were used to check fitted data for close agreement.

When appropriate, results were calculated as mean  $\pm$  standard deviation.

### *Computer simulations*

Computation of voltage-current relationship and electrotonic potential was obtained by solving standard Hodgkin-Huxley equations (Dodge 1963; Hodgkin and Huxley 1952b ). Computations were made for nodal and internodal membranes under various experimental conditions. Voltage responses were calculated using constants, which were representative of the effective resistances

capacitance for the axonal structure being simulated.

Two models were compared, one using standard nodal parameters (Dodge 1963; Hille 1970, 1971), and a modified model which included parameters for the slow potassium current ( $G_{KS}$ , Dubois 1981) and the internodal region (Barrett and Barrett 1982; Blight and Someya 1985).

Equations for  $G_{KS}$ :

$$\alpha = .028 \exp(E_m/33) \quad (1)$$

$$\beta = .0008 \exp(E_m/33) \quad (2)$$

$E_m$  = membrane potential

TABLE 2.1 Parameters used in models.

Conductance	$E_{rev}(mV)$	$G_o$ (nSiemens)
leak	-75 mV	10
$G_{KS}$	-100 mV	40

Other Constants:

Capacitance: 1.0 nF (internodal)

1.0 pF (nodal)

Temperature = 15°C

Sodium Conductance = 0

## RESULTS

### I. Experimental Results

#### *Resting and action potentials of primary afferent axons*

Results described in this study were obtained from more than 100 stable recordings from primary afferent axons. It usually took more than 15 min for the membrane potential to stabilize subsequent to penetration of axons. Addition of tetrodotoxin ( $0.2 \mu\text{M}$ ) or  $\text{MnCl}_2$  (2.0 mM) to normal Ringer abolished spontaneous activity and hyperpolarized the membrane causing the resting potential to be close to -80 mV (TABLE 2).

TABLE 2.2

Resting Membrane Potential	N	Mean	$\pm$ S.D.
in: normal Ringer	42	-73.8 mV	6.1
TTX Ringer	54	-79.3 mV	4.5
Mn Ringer	14	-77.2 mV	5.1
Peak Resistance			
in: normal Ringer	19	68.9 M $\Omega$	32.1
TTX Ringer	50	65.6 M $\Omega$	21.1
Mn Ringer	15	86.8 M $\Omega$	50.9

All fibres studied generated action potentials in response to peripheral stimulation or intracellular current injection. Their amplitude width and threshold were very similar to action potentials recorded from isolated nodes of Ranvier (Stampfli and Hille 1976). On average, action potentials were  $96.3 \pm 11.0$  mV ( $n = 75$ ) in amplitude and  $1.99 \pm 0.4$  ms ( $n = 63$ ) in duration at half height with a threshold of  $-53.1 \pm 8.0$  mV ( $n = 62$ ). Action potentials generated by short intracellular current injection were often followed by a slow depolarizing afterpotential, similar to that seen in large motor myelinated fibres, and believed to be due to the passive discharge of the internodal membrane (Barrett and Barrett 1982; cf. Poulter et al. 1989).

#### *Charging time constants of electrotonic potentials*

The constant current injection and simultaneous recording of membrane potential displacement (standard "current clamp" technique) was used to generate electrotonic potentials (ETPs). The charging time constant of the hyperpolarizing ETPs was much longer (as evident in *FIGURE 2.2A*) than the 0.5 ms time constant calculated for the node of Ranvier (Hille 1971, 1984) implying that other process(es) are involved. The longest charging time constant was often greater than 200 ms, in agreement with the observations of Barrett and Barrett (1982). Electrotonic potentials recorded in the linear region of the  $V/I$  (see below) could be fitted with two time constants: one in the range of 70 - 210 ms, the other less than 20 ms, or occasionally between 2 - 5 ms. *FIGURE 2.3* shows a log plot of the charging phase of a hyperpolarizing ETP where two time constants are obvious (76 ms and 3 ms) and a third slightly longer time constant may also be present (not calculated). However, it was often apparent that the charging was more complex and our computational methods (see

Methods) were not sufficient to resolve multiple time constants that were less than an order of magnitude different.

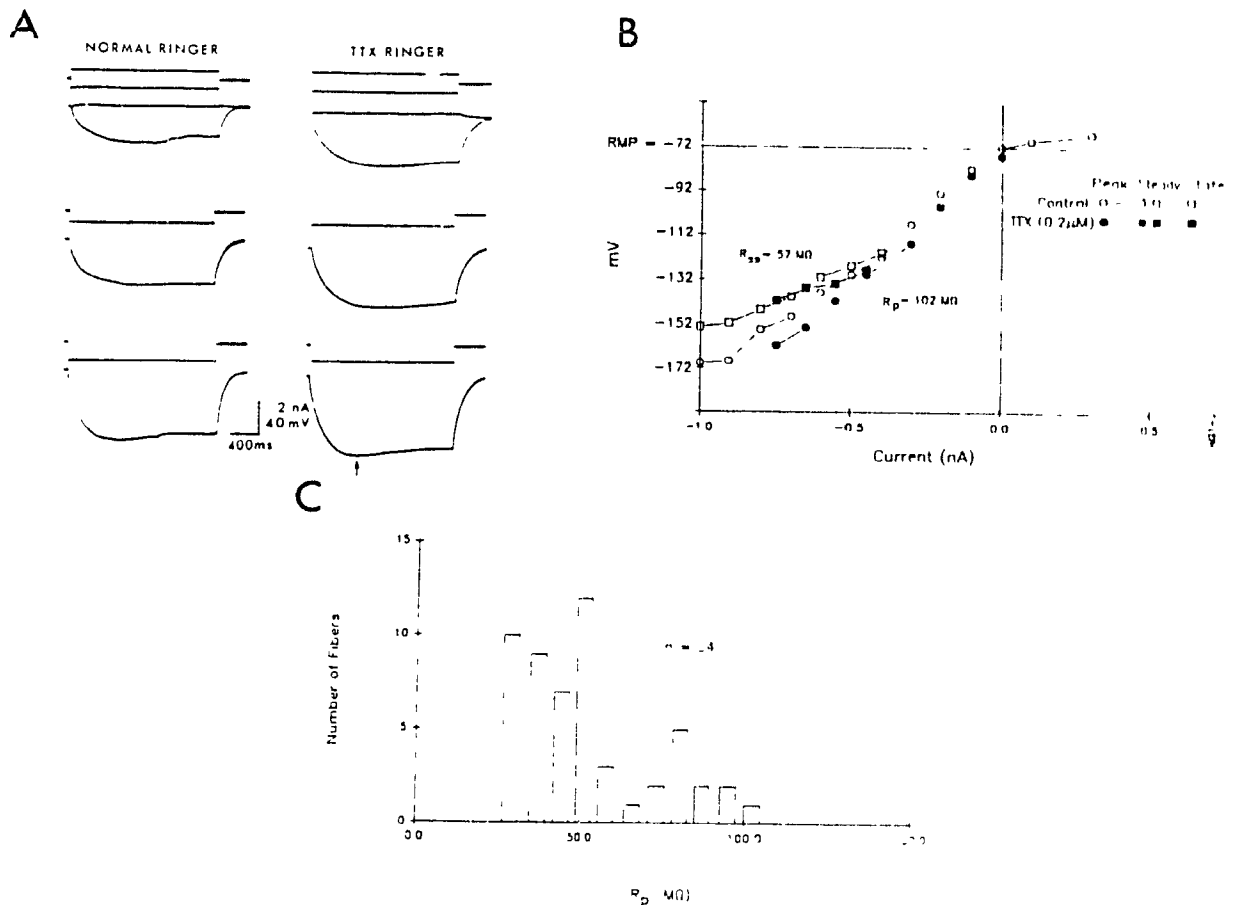


**FIGURE 2.2** Voltage-current relationship recorded in a large myelinated primary afferent axon. Samples **A** and plot **B** obtained in one fibre in both normal and TTX Ringer. Voltage values were measured at the peak (arrow, in **A**) and at steady state membrane potential (1.5 s in duration). Spontaneous activity is evident in voltage traces recorded in normal Ringer solution (left upper part). Note: the linear part of the V/I plot, between -95 and -130 mV, defined as peak resistance; an outward going rectification around resting membrane potential; an inward going rectification at membrane potential below -110 mV **C** Distribution of the peak resistances ( $R_p$ ) of primary afferents obtained in the presence of TTX- Ringer.

The longest charging time constant of ETP shortened with further hyperpolarization. Thus voltage responses to smaller currents, where the  $V/I$  is nonlinear (see below), had the longest time constant in the range of 100 - 500 ms, while the shorter one was  $< 20$  ms.

The discharging (off) phase of the hyperpolarizing ETPs was faster than the on phase, although this was not always as clear as seen on *FIGURE 2.2A*. An afterdepolarizing potential of several millivolts in amplitude, and lasting several hundreds of milliseconds to 5 seconds, was often observed following large hyperpolarizing ETPs (Padjen and Hashiguchi 1983; Chapter 3). In agreement with the complex time course of the charging phase of electrotonic potentials, the discharging phase could also be fitted by a number of time constants (one greater than 100 ms and the other  $< 20$  ms). However, unlike the charging phase, the "off responses" were not voltage dependent.

#### *Voltage-current relationship*

To obtain the voltage-current ( $V/I$ ) curves the values of membrane potential were measured at the peak of the voltage displacement ( $R_p$ , *FIGURE 2.2*, arrow in frame A) and at the steady state membrane potential ( $R_{ss}$ ) of electrotonic potentials in response to current pulses of 1.5 to 2.5 s in duration. Results of a typical experiment, in which the  $V/I$  relationship was determined first in the normal Ringer solution and then in the presence of  $0.2 \mu\text{M}$  TTX, are shown on *FIGURE 2.2A*. In the potential range more negative than  $-110$  mV, the  $V/I$  curve appeared to be linear. The slope for this primary afferent axon gave a peak resistance of  $102 \text{ M}\Omega$  (*FIGURE 2.2B*). There was no significant increase in  $R_p$  or  $R_{ss}$  recorded after blockade of synaptic transmission by TTX and/or



Manganese (TABLE 2). This indicated that the spontaneous synaptic activity does not account for the large variability in both resistance values observed among fibres with otherwise undistinguishable properties (same conduction velocities  $> 10$  m/s, membrane potential above  $-70$  mV, spikes with large overshoot).

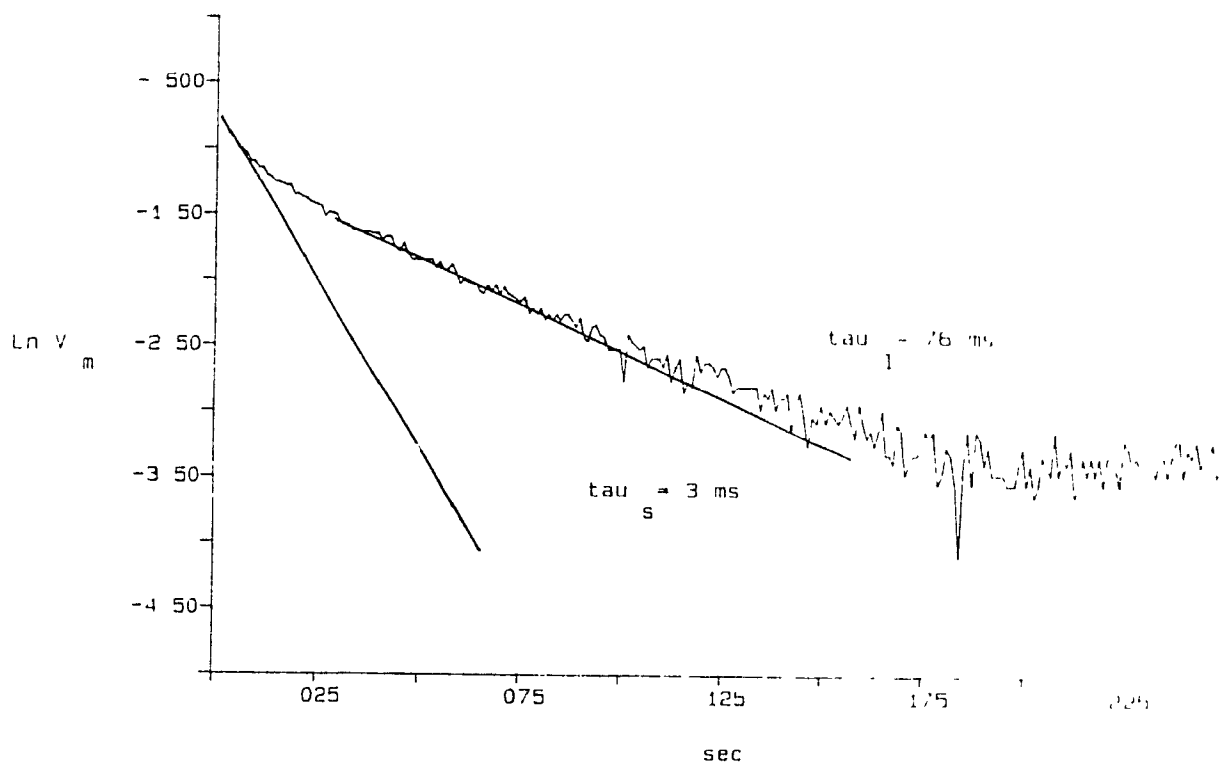


**FIGURE 2.3** Hyperpolarizing voltage response from the linear region of  $V/I$  plotted in semilogarithmic coordinates. At least two time constants are evident for this particular ETP,  $\tau_1$  of 76 ms and  $\tau_s$  of 3 ms. The time constants of charging were much greater than predicted by the charging of the nodal membrane.

The values of  $R_p$  ranged from 20 - 220  $M\Omega$  (average  $65.6 \pm 21.1$   $M\Omega$ ,  $n = 54$ ; in TTX Ringer **FIGURE 2.2C**). In all fibres an inward going rectification was present at membrane potentials more negative than  $-100$  mV (Padjen and

Hashiguchi 1983; Chapter 3).

Depolarizing current steps resulted in a distinct flattening of the V/I relationship indicating the presence of a strong rectification; fibres often could not be depolarized more than 10 mV.

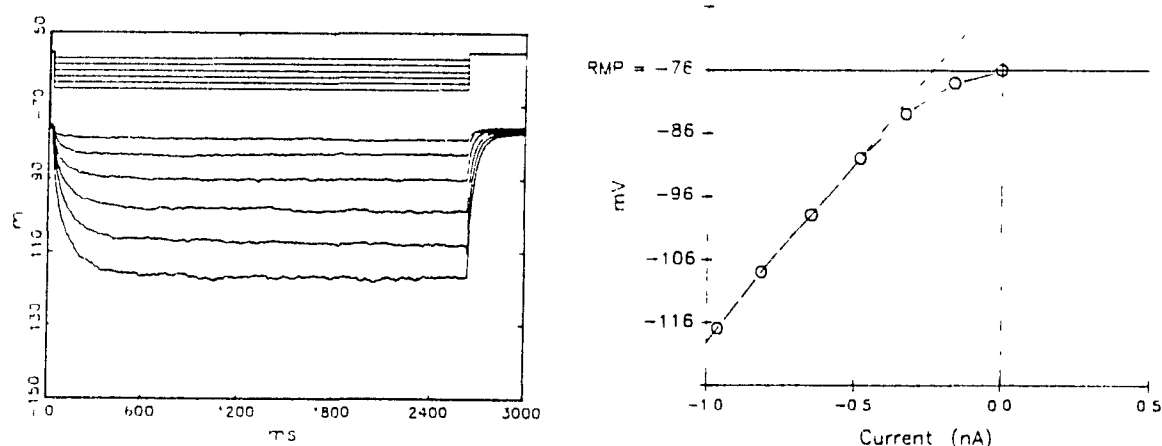


**FIGURE 2.4** Example of typical voltage-current relationship below resting membrane potential. Left: Voltage responses recorded from sensory axon. (Dotted line indicates resting membrane potential; Scale for current steps (top): 10 mV = 1 nA; traces obtained in the presence of 3 mM cesium and 0.2  $\mu$ M TTX in Ringer solution. Right: Plot of V/I relationship. Note the rectification below resting membrane potential.

As shown in *FIGURE 2.4* (recorded in the presence of TTX), there is rectification in the region below resting membrane potential, apparently at variance with the previous reports (Barrett and Barrett 1982; Hille 1971). In this fibre, the voltage displacement in response to injection of less than 0.20 nA was small, but further hyperpolarization initiated an increase in slope resistance at

the membrane potentials of more than  $-90$  mV. This rectification present in 50 of the 54 V/I relationships reported in this study, was unaffected by the addition of 3 mM cesium to the perfusion media (which blocked the anomalous rectification; see Chapter 3). However, 20mM TEA in the superfusate decreased the rectification (*FIGURE 2.5*) and depolarized the fibres from resting membrane potential on average  $7.0 \pm 1.7$  mV ( $n=4$ ). In the absence of anomalous rectification the resulting V/I intersected at  $-90 \pm 6.0$  mV ( $n=4$ ), on average, a value close to the reversal potential of potassium. This indicates that there is a potassium current active below resting membrane potential, which outwardly rectifies above the reversal potential of potassium and inwardly rectifies below the reversal potential of potassium. TEA had no significant effect on  $R_p$  (Control:  $73 \pm 31$  M $\Omega$ ; 20 mM TEA,  $79 \pm 31$  M $\Omega$   $p < 0.12$   $n = 4$ ; i.e. in the region where the V/I is normally linear). In the region below resting membrane potential to  $-120$  mV, Dubois (1981) and Grissmer (1986) have demonstrated the presence of a slowly activating, non inactivating potassium conductance ( $G_{K_S}$ ) in frog node of Ranvier and internode, respectively, which is sensitive to block by TEA. Our results suggest that  $G_{K_S}$ , or a conductance with similar properties to  $G_{K_S}$ , is responsible for the rectification observed in our preparation.

Barium ion has been shown to block a number of potassium conductances, some with characteristics similar to  $I_{K_S}$  (Hille 1984). Similar to TEA, barium ions (2 - 10 mM) depolarized the fibres (some 8-12 mV), abolished the rectification below resting membrane potential and reduced rectification above resting membrane potential (*FIGURE 2.6*). It had no effect on  $R_p$  or the anomalous rectification responsible for the sag in the voltage response.

For comparison, several recordings were done from the peripheral sites of dorsal roots, at least 10 mm from the spinal cord. The shape of the electrotonic potentials and nonlinear V/I relationship were the same as at the recording sites more proximal to the primary afferent terminals.

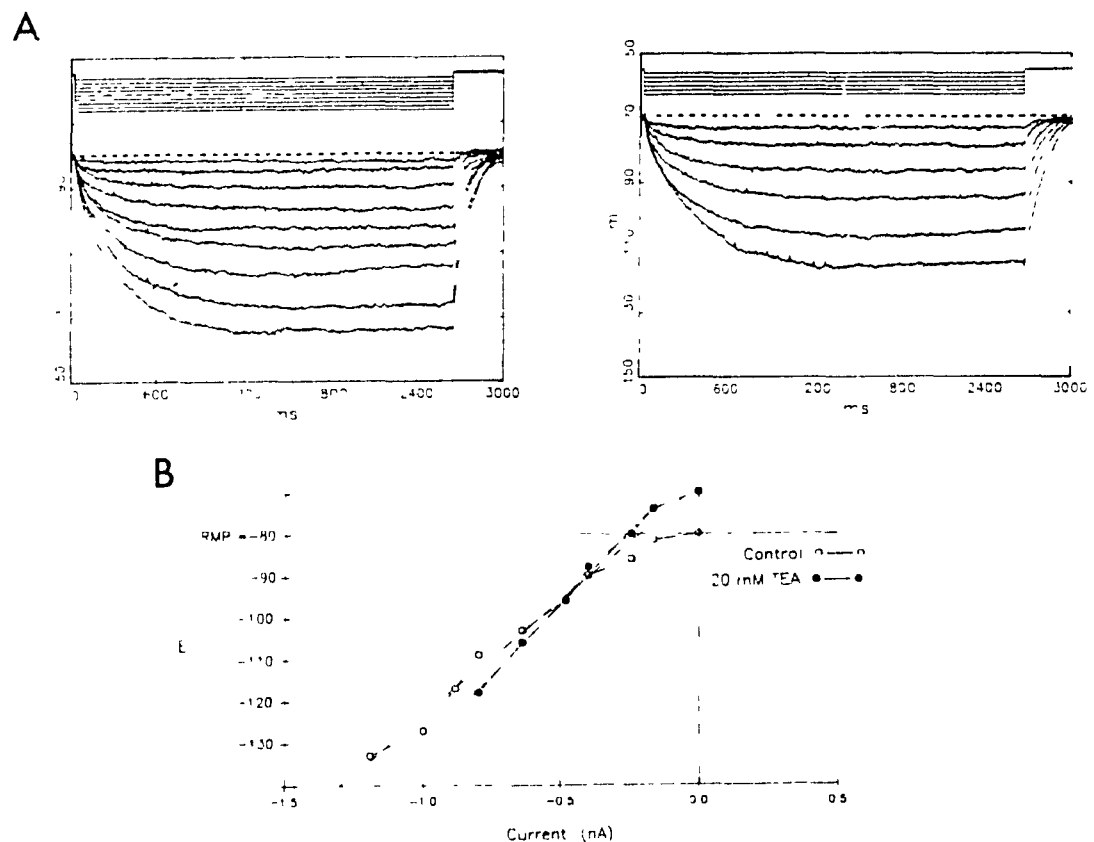


**FIGURE 2.5** Effect of TEA on the voltage/current relationship. **A** Control voltage responses before (left) and during superfusion with 20 mM TEA (right; dotted lines indicate resting membrane potential). **B** V/I relationship from data in **A**. Application of TEA causes the V/I relationship to become linear in the region below control resting membrane potential. Dashed lines fitted by linear regression (scale for current steps: 10 mV = 1 nA for both panels. Experiment done in 3 mM cesium-0.2  $\mu$ M TTX Ringer).

### Voltage-current relationship of motoneuron axons

Similar results were obtained from large myelinated motor axons recorded at the entry zone of the ventral root. In all of these axons, the V/I relationships showed both outward rectification around resting membrane potential and inward rectification at potential below -120 mV and thus appeared very similar to ones recorded from the primary afferents.

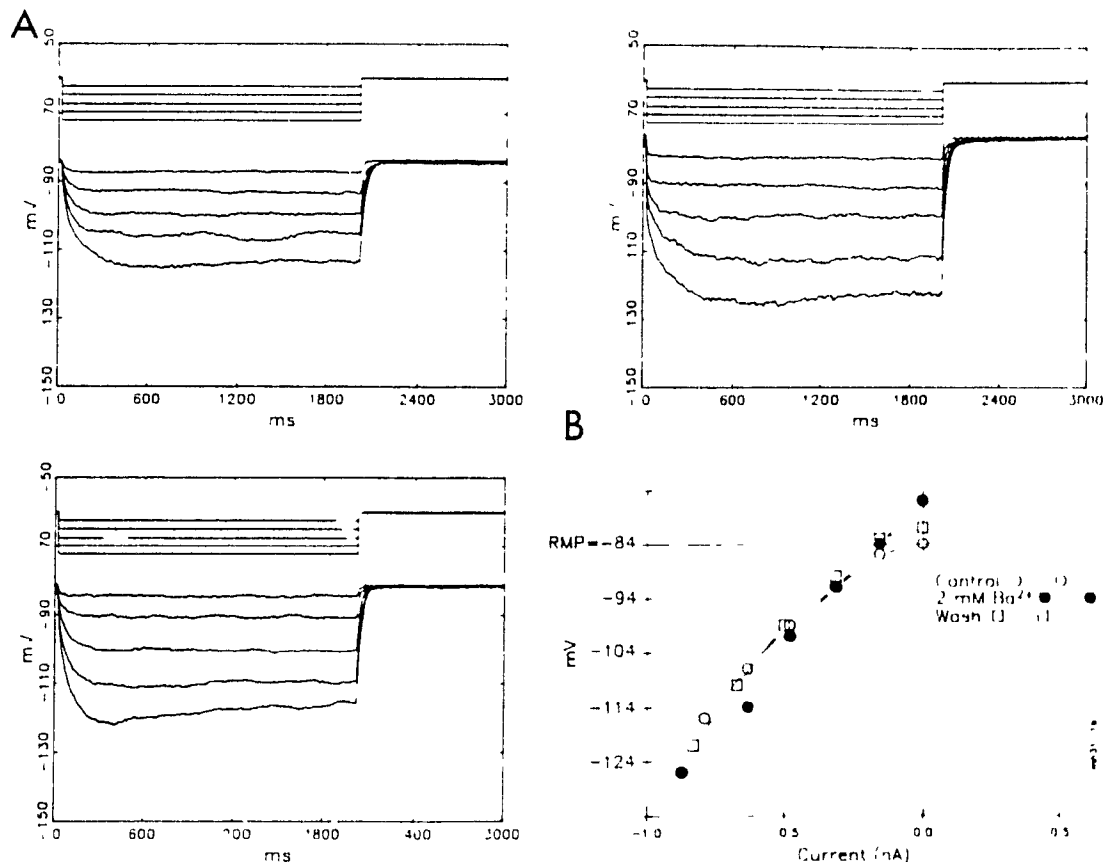


**FIGURE 2.6** Effect of barium on voltage current relationship. **A.** Control voltage responses show characteristic rectification (top left). After 20 minutes of superfusion with 2 mM barium ion in perfusate rectification was abolished (top right). Wash (+ 30 minutes) shows reversal of barium effects (bottom left). **B.** Plot of voltage current relationship for panels in **A.** Scale for current steps: 15 mV = 1 nA for all panels. Experiment done in 0.2  $\mu$ M TTX Ringer. Note that the V/I relationship is linear below resting membrane potential in the presence of barium (filled circles) and partially reversed during wash (open squares).

## II. Results of computer modeling

Some of the electrophysiological characteristics of myelinated axons observed in our experiments, in particular the charging time constants and the V/I relationship, did not qualitatively agree with the previous literature (Hille, 1971). We have developed a computational model, using Hodgkin-Huxley equations (see Methods), to examine our interpretations of the experimental data. Estimates of the effective capacitance were based on the parameters for both the nodal and internodal capacitance reported in Hille (1970) and Barrett and Barrett (1982), respectively. The slow potassium current reported in voltage-clamp studies of amphibian myelinated axons (Dubois 1981) was included in all calculations, except where noted.

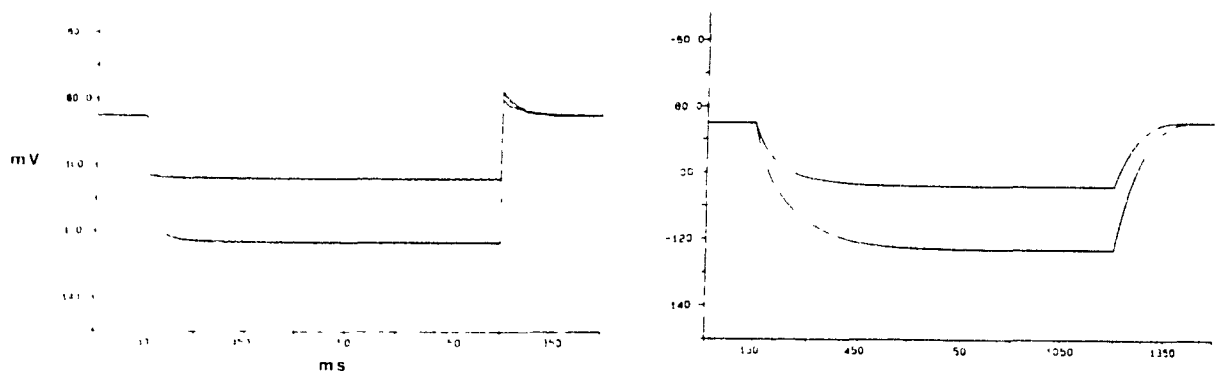


**FIGURE 2.7** Computer modeling of the ETP. Model using the effective capacitance of the node of Ranvier (Hille 1971; left panel) and the effective capacitance for the internodal membrane (Barrett and Barrett 1982; right panel). The ETP is at steady state much earlier than observed experimentally (left). However the latter model of the ETP better reflects the charging seen experimentally.

*Modeling of electrotonic potentials*

When the membrane potential responses to hyperpolarizing constant current pulses were calculated using the nodal capacitance, steady state was obtained much earlier than in experimental recordings (*FIGURE 2.7*). However, the charging was still much slower than that predicted by Hille 1971. In our model, it took approximately 150 ms to reach a steady state of -105 mV in response to a 0.3 nA current stimulus, and 200 ms to reach -125 mV in response to a 0.5 nA stimulus. Using the capacitance, calculated by Barrett and Barrett (1982) for the internodal region, the resulting plots better represented the experiment results (*FIGURE 2.7*). This implied that a larger (presumably internodal) capacitance can account for most of the long charging time constant, in agreement with Barrett and Barrett (1982) and Blight and Someya (1985), although the  $G_{K_S}$  is also likely to contribute.

The overshoot of resting membrane potential, observed at the end of the stimulus in the nodal model, is the result of the leak conductance temporarily being unopposed by  $G_{K_S}$ , which has been inactivated by the hyperpolarization. The decay of this overshoot is due to  $G_{K_S}$  turning back on and reestablishing a resting membrane potential of -85 mV. The capacitance dampens this overshoot in the internodal model.

In disagreement with experimental results, the model did not mimic the shortening of the initial charging time constants when the current intensity was increased, indicating that the time constant of the closing of  $G_{K_S}$  is not responsible for this decrease. The decrease in charging time is likely due to the activa-

tion of anomalous/inward rectification and the accompanying decrease in resistance (Chapter 3).

### *Modeling of the V/I relationship*

*FIGURE 2.8* compares the two computed models both using the same large capacitance value; in the standard model (no  $G_{K_S}$ ; left) the leakage current carries all of the membrane current in the potential range lower than -75 mV, whereas the modified model includes the gating parameters for the slow potassium conductance, activated at membrane potentials more positive than -120 mV ( $I_{K_S}$ ).

Qualitatively, the V/I relationship obtained with parameters of a standard internode is different from the V/I obtained in our experiments (compare with *FIGURES 2.4, 2.5 and 2.6*). However, the modified model has outward going rectification below resting membrane potential, simulating the rectification seen experimentally in the same potential range. In fact, comparing the plots of the V/I relationship of the two models one sees that it essentially models the pharmacology of TEA and barium. The results of computations also suggest that  $I_K$  below -100 mV ( $E_K$  in the model) may be responsible for some inward rectification as well, since the voltage responses below -100 in the standard internode are greater than in the "modified" internode.



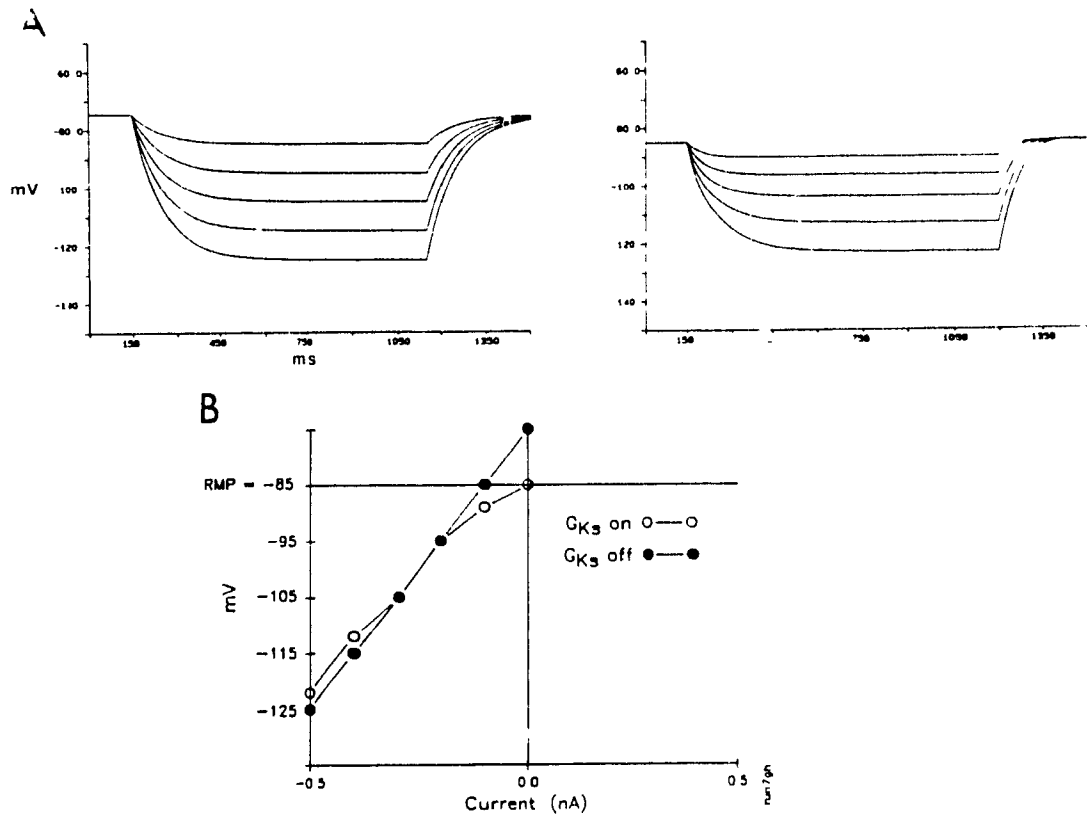


**FIGURE 2.8** Computer modeling of the current voltage relationship. **A.** Voltage-current relationships calculated for the standard axonal membrane (left) and for a modified membrane (right) which includes parameters for the slow potassium conductance. **B.** Plot of the computed voltage/current relationship showing non linear shape when  $G_{Ks}$  is included in the model. Note that the two models simulate the voltage/current relationships obtained in experiments using TEA and barium ion.

## DISCUSSION

Using intracellular microelectrode recording and standard "current-clamp" technique we have identified two electrophysiological characteristics of the frog myelinated axons: 1) a non-linear voltage-current relationship with distinct outward rectification; 2) an unusually long charging time of the hyperpolarizing ETPs. While both findings appear to differ from the description of axons in the classical literature, the second observation confirms previous reports (Barrett and Barrett 1982; Blight and Someya, 1985; Padjen and Hashiguchi, 1983). The complexity of the charging is to be expected, since the charging time reflects at least two capacitive components, nodal and internodal, in parallel with the leak resistance(s), and the time and voltage dependent resistances (deactivation of  $G_{K_S}$  and activation of the inward rectification). These results were not limited to the terminal region or the vicinity of motoneurons, in the case of primary afferents and motor axons, respectively, since they were also obtained in recordings from peripheral nerves.

The non-linear voltage-current relationships found in our experiments indicate involvement of voltage dependent membrane process(es) in electrotonic potentials. The rectification above resting membrane potential reflects the activity of the three potassium conductances, which have been identified in voltage clamp studies in both the node of Ranvier and the internodal membrane ( $G_{Kf1}$ ,  $G_{Kf2}$ , and  $G_{K_S}$ ; Dubois 1981; Grissmer 1986). This study provides evidence, based on the pharmacological data using TEA and barium and the results of computational tests, that the rectification below resting membrane potential is due to the slow potassium conductance  $G_{K_S}$ .

Our results also indicate that  $G_{K_S}$  partially governs the resting membrane potential, since blockade of  $G_{K_S}$  by TEA depolarized the fibre. These results, including a) the calculations of the reversal potential of potassium ( $E_K = -100$ ; assuming  $[K]_i \approx 115$  mM); b) the behaviour of our computational model which used the  $E_K$  calculated above, imply that the leakage current reversal potential must be at least 25 mV more positive than the reversal of potassium (i.e.  $G_{K_S}$ ), in order to account for the measured resting membrane potential of these fibres. This indicates that some other ion (sodium or chloride perhaps) is involved in setting the resting membrane potential, in addition to potassium. Alternatively, there may be a series leakage pathway as suggested by Baker et al. (1987). Our results imply that the true resting membrane potential of the myelinated axons may be some 5-15 mV more negative than -70 mV, a value usually assumed in voltage-clamp studies. The measured values reflect the contribution of both nodal and internodal membranes, the latter having a higher membrane potential than the nodal one (Chiu and Ritchie 1984).

Further studies of the model indicate that the net membrane conductance, which may be related to the effective resistance ( $R_p$ ), is determined by the positive leakage conductance at potentials more negative than -120 (range where  $G_{K_S}$  is inactive). The scattered distribution of  $R_p$  (see *FIGURE 1 2C*) in fibres of the same conduction velocity and therefore the same size (Arbuthnott et al. 1980; Tasaki 1953), is likely due to differences in the leakage conductance. Other factors that may contribute to the scattered distribution of  $R_p$  are: 1) damage of the axonal membrane by microelectrode penetration; 2) damage to the myelin could create a leak pathway decreasing the effective resistance of the fibres. However, in view of the high resting membrane and action potentials,

and the general stability of the recording, it is hard to imagine that damage would act selectively on the voltage-current relationship to cause the nonlinearity. Anomalous or inward rectification may also contribute (see Chapter 2).

The slow charging of hyperpolarizing ETPs could be partially accounted for in the computational model by the slow deactivation of the  $G_{K_s}$ . The computed ETPs were qualitatively similar to those recorded *in vitro* only when a large effective capacitance was used. The source of this large capacitance is either internodal membrane charged via a shunting internodal leakage resistance (Barrett and Barrett 1982), or alternatively by a low resistance path that shunts charge into the myelin sheath (Blight 1985). This capacitance is believed to be responsible for the slow afterdepolarization observed following an action potential (Barrett and Barrett 1982; Blight and Someya 1985; Poulter et al. 1989). Our experimental results support this hypothesis, since none of the identified conductances could explain the long time constant of charging.

In conclusion, our results support the existence of a slow potassium conductance operating in myelinated axons, which is responsible for outward rectification at potentials above the reversal potential of potassium. It may also contribute to the long charging time constant of hyperpolarizing ETPs which is, however, better accounted for by the charging of a large internodal effective capacitance. The physiological role of this slow potassium conductance operating below resting membrane potential is still uncertain. In the region positive to resting membrane potential, it appears to modify spike frequency adaptation and accommodation (Poulter and Padjen 1988; Poulter et al. 1989). One may also expect that the slow course of primary afferent depolarization could further activate the slow potassium conductance. This in turn could contribute to

sodium conductance inactivation and thus cause failure of presynaptic spike generation and contribute to presynaptic inhibition (Padjen and Hashiguchi 1983).

**A STUDY OF ANOMALOUS (INWARD) RECTIFICATION IN FROG  
SENSORY MYELINATED AXON**

by

Michael O. Poulter and Ante L. Padjen

(Submitted to The Journal Of Neurophysiology)

### *SUMMARY AND CONCLUSIONS*

1. Anomalous or inward rectification was studied in intact large frog myelinated axons, attached to hemisected spinal cord, by intracellular microelectrode recording and current clamp technique.
2. In response to a negative current step, which hyperpolarized the membrane 10-40 mV below resting membrane potential, all fibres showed a characteristic attenuation of the voltage response or a "sag" after an initial peak voltage deflection. This "sag" developed 300 to 600 ms after the start of the pulse. In addition, a depolarizing afterpotential (ADP; 1 - 5 mV in amplitude; 500 ms-10 sec. in duration) was evident following a current pulse, in which inward rectification had been activated.
3. The "sag" was blocked by external application of cesium ion (3 mM), but it was insensitive to external application of barium ion (2 - 10 mM). The blockade of the "sag" was accompanied by a disappearance of the DAP and an increase in the charging time constant of the membrane.
4. Replacing the external sodium ion with choline increased the slope resistance at steady state. Reducing the external potassium ion concentration increased both the peak and steady state slope resistance. These results indicate that the anomalous (inward) rectification is a mixed ionic conductance, dependent on potassium and sodium ions in the external media.
5. The function of this conductance may be to regulate the post tetanic hyperpolarizing potential produced by a high frequency train of action potentials, since

blockade of anomalous rectification with external cesium ions led to a prolongation of the post tetanic hyperpolarizing potential. Cesium also blocked the depolarizing afterpotential (DAP) that followed the post tetanic hyperpolarization.



## INTRODUCTION

Anomalous or inward rectification ( $G_{AR}$ ), first described by Katz (1949) in crayfish muscle, was identified as a conductance, which activates in a range hyperpolarized to resting membrane potential. Voltage responses resulting from injection of hyperpolarizing current steps show a characteristic attenuation after an initial maximum. This "sag" in the voltage response is seen in many different excitable membranes ranging from invertebrate oocyte to vertebrate heart, skeletal muscle, and neuronal membranes (Bader and Bertrand 1984; Binah et al. 1988; Constanti and Galvan 1983; Crepel and Penit-Soria 1986; Hagiwara and Takahashi 1974; Halliwell and Adams 1982; Mayer and Westbrook 1983; O'Neill 1983; Spain et al. 1987). Their diverse distribution is not matched by a diversity in attributes, and all inward rectifying conductances reported so far can be classified as belonging to one of two types. The first type (referred to as Type 1 in this paper) activates relatively fast, is primarily permeable to potassium ions and is blocked by extracellular application of barium or cesium ions. The type 2 conductance activates slowly, is permeant to sodium and potassium ions, and is blocked by extracellular cesium, but not barium ions.

In addition, Type 1  $G_{AR}$  differs from Type 2  $G_{AR}$ , in that the range of membrane potentials, at which Type 1 is activated, can be altered by changing the external potassium concentration. Thus, by increasing the concentration of external potassium ions the  $V_m$  of the activation curve for Type 1  $G_{AR}$  shifts with the reversal potential of potassium. This results in the conductance always activating within a few millivolts hyperpolarized to the reversal potential of potassium. This attribute tends to keep the magnitude of the  $G_{AR}$  conductance relatively constant (Constanti and Galvan 1983; Hagiwara and Takahashi 1974;

Hestrin 1981; Leech and Stanfeld 1981). In contrast, Type 2  $G_{AR}$  increases in magnitude when the external potassium concentration is raised, as the reversal potential of potassium moves further away from the voltage range, at which the conductance is activated (Halliwell and Adams 1982; Mayer and Westbrook 1983; Spain et al. 1987).

Studies on the functional relevance of these conductances have been done on a number of invertebrate, as well as, vertebrate preparations. In invertebrate oocytes, there is evidence that activation of this conductance prevents further fusing of sperm cells with a recently fertilized egg (Hagiwara and Jaffe 1979). Its presence in heart is thought to underlie pacemaker activity (Brown and Di Francesco 1980; Di Francesco 1981; Maylie and Morad 1984). In neurons,  $G_{AR}$  has been suggested to modulate synaptic transmission (Kandel and Tauc 1966), whereas in skeletal muscle, it has been hypothesized to aid the spread of conduction through the transverse tubules (Ashcroft et al. 1985). Recent studies by Schwindt et al. (1987) have suggested that  $G_{AR}$  modulates the post tetanic afterhyperpolarizing potential (AHP) activated by a train of action potentials and therefore, can influence cell excitability.

One of the objectives of this study was therefore to classify and investigate the function of the previously uncharacterized anomalous rectification in frog myelinated axon (Padjen and Hashiguchi 1983). Some of the experimental results obtained were analyzed and interpreted with the aid of a computer model, which utilized Hodgkin and Huxley type equations developed for AR. Results have been presented in a preliminary form in Poulter and Padjen (1988a) and Padjen and Poulter (1989).

## METHODS

### *Experimental*

Details of the microelectrode recording technique and experimental conditions are described in Padjen and Hashiguchi (1983) and Poulter et al. (Chapter 2). All recordings, from which the V/I relationships were obtained, were done in normal frog Ringer with tetrodotoxin added ( $0.25 \mu\text{M}$ ; TTX-Ringer) to block action potentials and to minimize synaptic activity.

In experiments, where trains of action potentials were required to generate afterhyperpolarizing potentials, isolated dorsal root fibres were used and perfused with Normal frog Ringer solution at  $10^\circ$  to  $14^\circ$  C. containing in mM: NaCl, 115; KCl, 2;  $\text{CaCl}_2$ , 2; HEPES buffer (pH adjusted to 7.3), 10; dextrose, 11 (NR). Stimulation of the fibre was accomplished by intracellular injection of 0.5 ms pulses of suprathreshold current at 50 Hz for 30 seconds.

Results calculated are expressed as the mean  $\pm$  standard error of the mean, unless otherwise specified. Significance of differences were evaluated by paired t-test analysis.

Replacement of sodium by choline Ringer solution produced a depolarization of RMP, which was accounted for by a liquid junction potential, rather than a real effect of sodium replacement.

*Computer Simulations*

Computation of voltage-current relationship and the effect of current steps on electrotonic potentials were obtained by solving standard Hodgkin-Huxley equations applied to myelinated axons (Dodge 1963). The gating equations for  $G_{KS}$  were taken from Dubois (1981).

Hodgkin-Huxley type of equations for the anomalous rectifying conductance were empirically developed to reflect voltage responses under current clamp conditions. The voltage dependence ranged from -100 mV ( $a_{\infty} = 0$ ) to -160 mV ( $a_{\infty} = 1$ ) and the conductance activated with one or two time constants  $\tau_1 = 10$ -12 ms,  $\tau_2 = 450$  - 600 ms.

*Gating Equations for anomalous rectifier conductance*

$$a_{\infty} = \alpha/(\alpha + \beta) \quad (1)$$

Equations for  $G_{AR}$  (fast and slow components)

$$\alpha_{AR} = .0075/A\{\exp(0.8\Theta_{\alpha})-1\} \quad (2)$$

$A = 1$  and  $50$  for fast and slow time constants  
respectively

$$\Theta_{\alpha} = (80 + E_m)/15 \quad (2a)$$

$$\beta_{AR} = .005\Theta_{\beta}/B\{\exp(\Theta_{\beta})-1\} \quad (3)$$

$B = 1$  and  $75$  for fast and slow time constants  
respectively

$$\Theta_{\beta} = -160 - E_m/5 \quad (3a)$$

TABLE 3.1 Parameters used in model

Conductance	$E_{rev}$ (mV)	$G_0$ (nSiemens)
leak	-75	10
$G_{KS}$	-100	40
$G_{AR}$	-55	slow: 300    fast: 10

Other Constants:

Voltage sensitive sodium conductance = 0

Capacitance = 1 nF

temperature 15°

## RESULTS

All fibres, upon which this study is based ( $n = 50$  in TTX-Ringer with axon attached to spinal cord; 5 in NR isolated dorsal root) showed a "sag" when hyperpolarizing pulses of sufficient magnitude were used. The average resting membrane potential (RMP) for fibres in the presence of TTX Ringer was  $-77.0 \pm 7.8$  mV (mean  $\pm$  SD,  $n = 50$ ). The voltage responses illustrated in *FIGURE 3.1A* depict the characteristic attributes of the hyperpolarizing electrotonic potentials (ETP) recorded from these fibres. Activation of the AR, based on the presence of a "sag" in the ETP, required current pulses to last at least 300 - 600 ms and the membrane to be hyperpolarized 10 - 40 mV below RMP. In this voltage range, the voltage response attenuated after an initial peak and a steady state voltage response was attained some 1200-2100 ms later. The time required to reach steady state was shorter as the membrane was more hyperpolarized. In addition, voltage responses with a pronounced "sag" often possessed a depolarizing afterpotential (DAP) (1 - 3 mV) lasting 500 ms - 10 seconds after the current pulse was terminated (small and slow developing in *FIGURE 3.1A*; also see *FIGURE 3.3*). Slope resistances were measured at the peak of the voltage responses ( $R_p$ ) and at the end of the pulse when the response was at steady state ( $R_{ss}$ ) *Figure 3.1B*. A histogram of the steady state resistance for the 50 fibres recorded in the presence of TTX is shown in *FIGURE 3.1C*.

### *Effect of extracellular cesium and barium ions*

The effect of cesium ion (3 mM) addition to the superfusion fluid was tested for its ability to block the "sag" resulting from AR. Application of cesium in-

creased the steady state slope resistance, which was accompanied by the abolishment of the sag in 5 of 6 fibres. An example of a  $V/I$  curve (*FIGURE 3.2*) for one fibre before and after cesium treatment depicts an increase in the  $R_p$  and  $R_{ss}$  ( $R_{ss}$  now equivalent to  $R_p$ ).

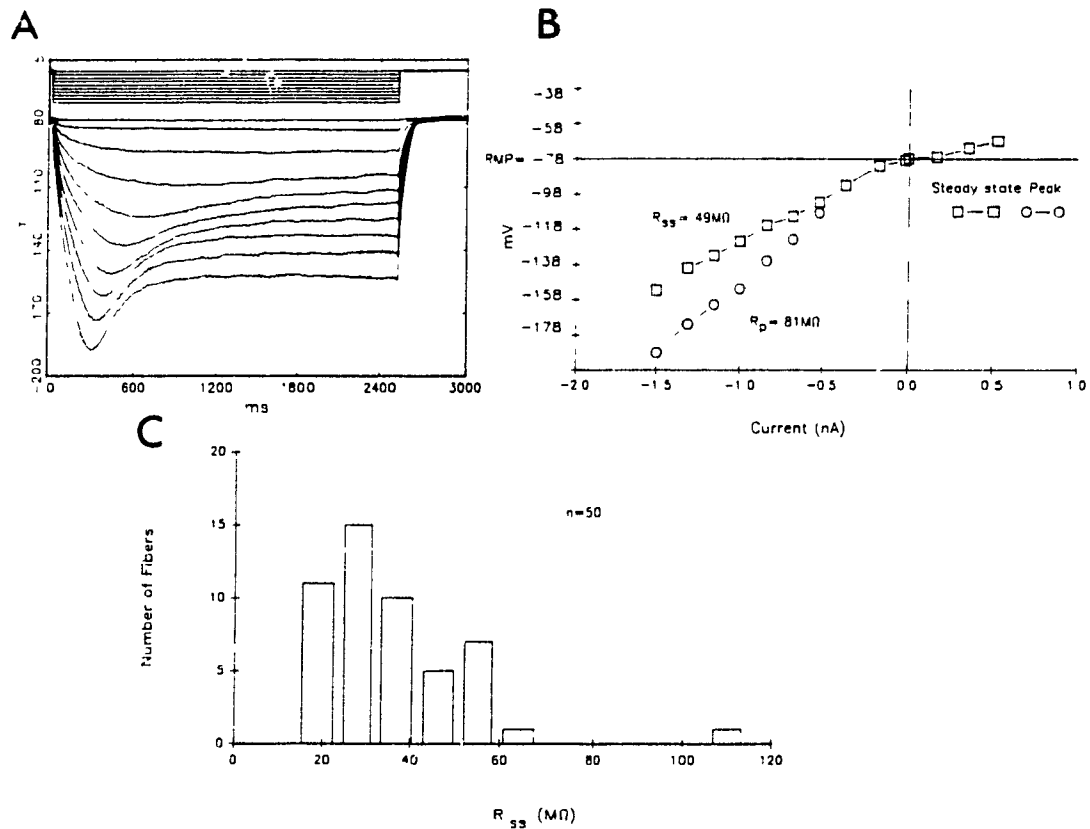


**FIGURE 3.1** Voltage responses to hyperpolarizing current pulses are attenuated by activation of inward or anomalous rectifying conductance. **A** Example of voltage responses from one fibre recorded in the presence of TTX-Ringer (current  $10\text{mV} = 1\text{ nA}$ ). **B** Plot of the voltage/current relationship of the responses shown in panel 1A. The decrease in the peak resistance indicates the turning on of an inward conductance, which rectifies the voltage responses. **C** Histogram of all steady state resistance values calculated for this study ( $31.1 \pm 10.8\text{ M}\Omega$ , mean  $\pm$  SD,  $n = 50$ ; done in TTX-Ringer).

On average,  $R_p$  and  $R_{ss}$  increased from  $63.2 \pm 11.4$  and  $42.2 \pm 5.8$ , respectively, to  $114 \pm 19.2$  and  $113 \pm 23.9$  (mean  $\pm$  SE in  $M\Omega$ ;  $n = 6$ ,  $p < 0.01$  and  $p < 0.005$ , respectively). However, there was no change in the rectification in the region above and just below RMP, indicating that extracellular cesium ions did not affect any conductances activated in the region around RMP. *FIGURE 3.3* shows that the small DAP evident after the current pulse in the control became a hyperpolarizing after potential. It also demonstrates that the time constant of charging of the ETP also increased. The V/I relationship in the region where  $G_{AR}$  is activated was unchanged by superfusion with Ringer, which contained 2.0 mM barium ions (*FIGURE 3.4*).

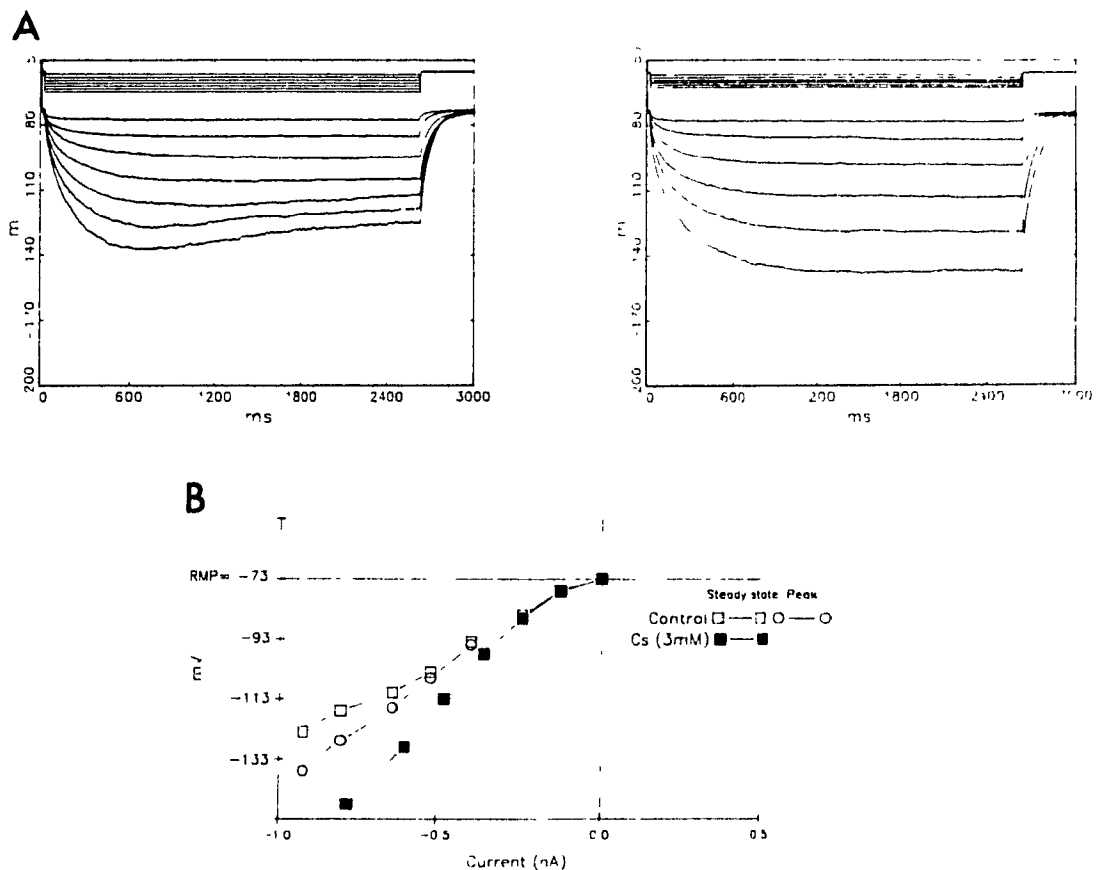


**FIGURE 3.2** Effect of external cesium ion on anomalous rectification **A** Control Voltage responses (left) Voltage responses after 5 min perfusion with Ringer solution containing 3 mM cesium chloride (right) The "sag" is abolished and the time constant of the initial charging phase is greatly increased. **B** The V/I relationship for the fibre depicted in **A**.



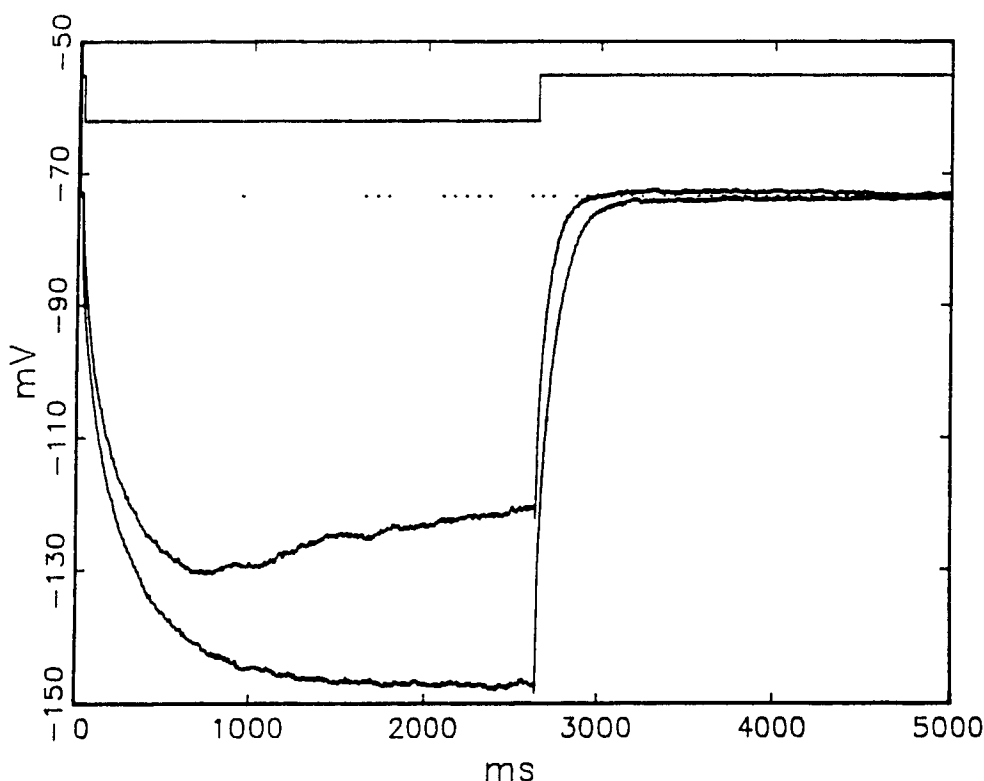


**FIGURE 3.3** Effect of cesium on the DAP. The small DAP which is evident after  $G_{AR}$  is activated is abolished when  $G_{AR}$  is blocked by extracellular application of cesium chloride.

#### *Ionic dependence of anomalous rectification*

Insensitivity to block by barium implied the presence of a Type 2  $G_{AR}$  in these fibres. In other neurons Type 2  $G_{AR}$  is defined as a mixed sodium and potassium ion conductance and so, Ringer solutions with modified ionic compositions were used to examine the ionic dependence of the "sag" and the ADP:

1) The voltage responses of a fibre before and after sodium replacement with choline illustrate that the "sag" was significantly attenuated (**FIGURE 3.5A and B**). The DAP was decreased and the fibre repolarized faster (**FIGURE 3.5C**).  $R_p$  was not significantly greater (control,  $R_p$ :  $45.6 \pm 9.4$ ; 0 sodium,  $R_p$ :  $59.2 \pm 12.5$ ;  $M\Omega$  mean  $\pm$  SE;  $n = 5$ ,  $p < 0.06$ ) whereas  $R_{ss}$  was significantly

increased, indicating that there was a decrease in conductance associated with the "sag" (control  $R_{ss}$ :  $24.2 \pm 5.3$ ; 0 sodium  $R_{ss}$ :  $33.0 \pm 6.4$ ;  $M\Omega$  mean  $\pm$  SE;  $n = 5$ ,  $p < 0.025$  FIGURE 3.5D).

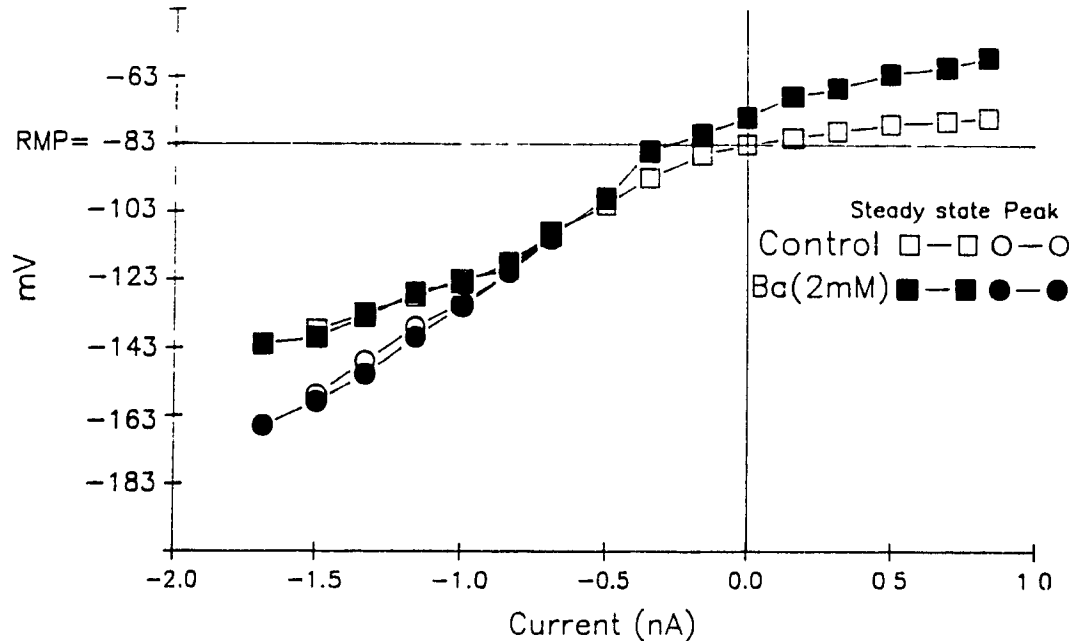
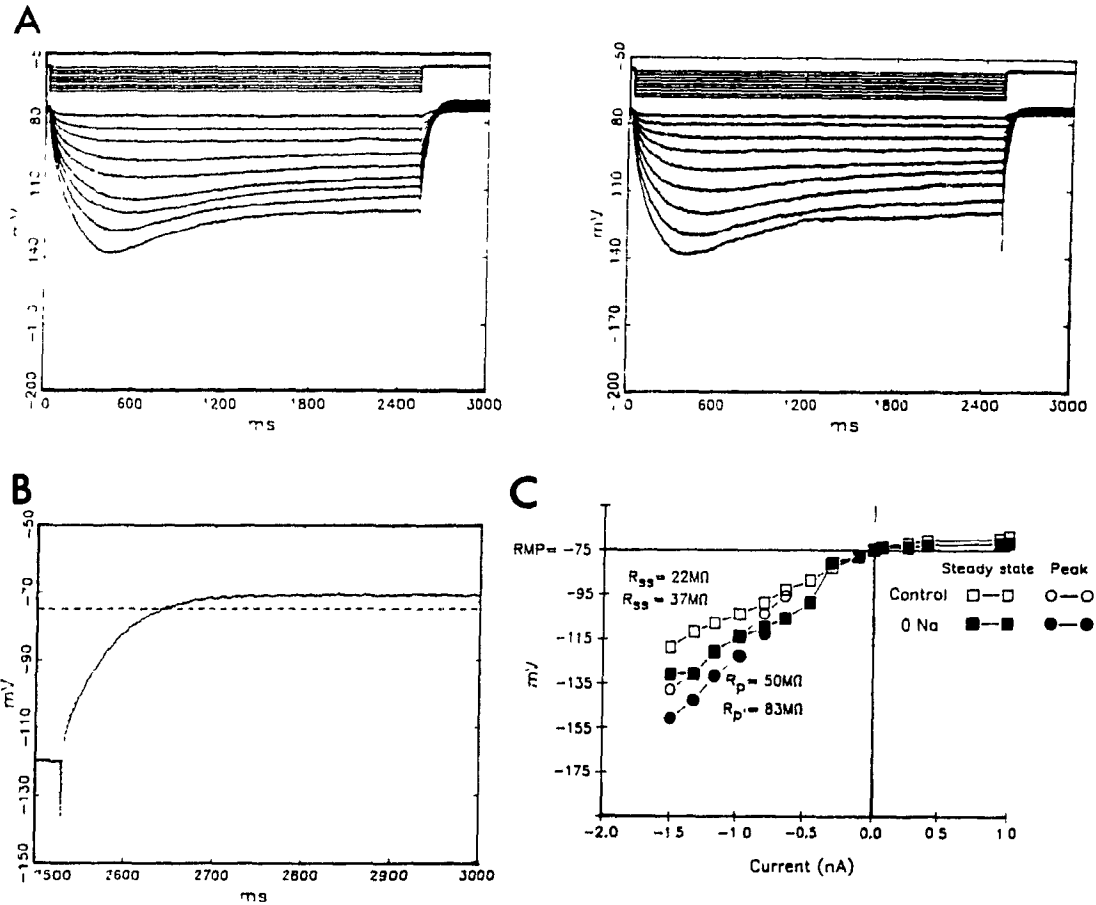


FIGURE 3.4 Effect of externally applied barium ion on  $G_{AR}$ . Superfusion of the preparation with Ringer solution containing 2 mM Barium chloride has no effect on the  $V/I$  relation in the region where  $G_{AR}$  is activated. (note the decrease in rectification in the region around resting membrane potential.)

2) Reducing the potassium concentration to 0.1 mM increased both  $R_p$  (control  $R_p$ :  $50.8 \pm 8.5$ ; 0.1mM potassium  $R_p$ :  $77.6 \pm 14.6$ ;  $M\Omega$  mean  $\pm$  SE;  $n = 5$   $p < 0.02$ ) and  $R_{ss}$  (control  $R_{ss}$ :  $31.0 \pm 4.8$   $M\Omega$ ; 0.1 mM potassium  $R_{ss}$ :  $53.0 \pm 7.35$ ;  $M\Omega$  mean  $\pm$  SE;  $n = 5$ ,  $p < 0.02$ ; FIGURE 3.6A & 3.6B) and therefore decreased the inward rectification. In addition, the DAP was increased in duration (not shown) in low potassium, implying that the potassium component normally limits the duration of the DAP. These two sets of results are consistent with  $G_{AR}$  being a mixed sodium and potassium conductance.



**FIGURE 3.5** Effect of sodium ion replacement. **A** Control (left) and 0 sodium voltage responses (right), respectively (scale for current record 10 mV = 2 nA) **B** (left) Detail of the off phase of the voltage response shows DAP is attenuated (control: solid line, 0 sodium: dotted line, Resting Membrane Potential: dashed line) **C** voltage/current curve for same fibre. The increase in the slope resistance  $R_p$  was not seen in all fibres whereas, the increase in  $R_{ss}$  was consistent.

3) Raising the external potassium concentration gave results that were not as straightforward as results obtained with the two prior ion manipulations. Both  $R_p$  (control  $R_p$ :  $45.6 \pm 6.2$ ; 8.0 mM potassium  $R_p$ :  $52.7 \pm 10.2$ ;  $M\Omega$  mean  $\pm$  SE;  $n = 8$ ) and  $R_{ss}$  (control  $R_{ss}$ :  $38.8 \pm 11.2$ ; 8.0 mM potassium  $R_{ss}$ :  $37.4 \pm 12.8$ ;  $M\Omega$  mean  $\pm$  SE;  $n = 8$ ) were not significantly different (not shown). In addition, another phenomenon was observed. *FIGURE 3.7* shows the record of a fibre whose charging was unstable and this "instability" was enhanced by increasing the external potassium to 8 mM (*FIGURE 3.7A* right). Blocking  $G_{AR}$  with cesium (3 mM) enhanced the instability even further (*FIGURE 3.7B* left). This effect of raised external potassium (decreasing stability) was also observed in a number of fibres which possessed no initial instability (4 of 8 tested). Returning to normal potassium Ringer before washout of cesium abolished this instability (*FIGURE 3.7B*, right). Furthermore, in 3 of 8 fibres raising potassium abolished the "sag", increased the charging time constant and decreased  $R_{ss}$  of the fibre. This could be interpreted as an enhancement of  $G_{AR}$  so large that the peak voltage response was obscured. Thus, although the effects of raised potassium were complex, it was possible in some cases to observe an enhancement of  $G_{AR}$ .

### *Functional aspects of $G_{AR}$*

It has been suggested that activation of  $G_{AR}$  can prevent excessive hyperpolarization of the cell membrane due to electrogenic pumping of sodium or the prolonged activation of a potassium conductance (Hille 1984; Schwindt et al. 1988). To test this possibility we examined the effect of blocking  $G_{AR}$  (with cesium in NR) on the post tetanic hyperpolarization recorded from axons in

isolated dorsal roots. Using short (0.5 ms) intracellular depolarizing pulses, a 50 Hz train of stimuli for 30 seconds produced a complex response consisting of a 10 to 15 mV hyperpolarization which decayed in two phases: a fast phase (lasting 200-500 ms) and a slower phase (lasting 3 - 5 seconds), followed by a 1 - 3 mV depolarization (lasting 2 - 4 seconds). Addition of 3 mM cesium ion to the perfusing fluid changed the biphasic decay to a monophasic decay, greatly prolonged the post tetanic hyperpolarization and abolished the depolarization following the post tetanic hyperpolarization (FIGURE 3.8).

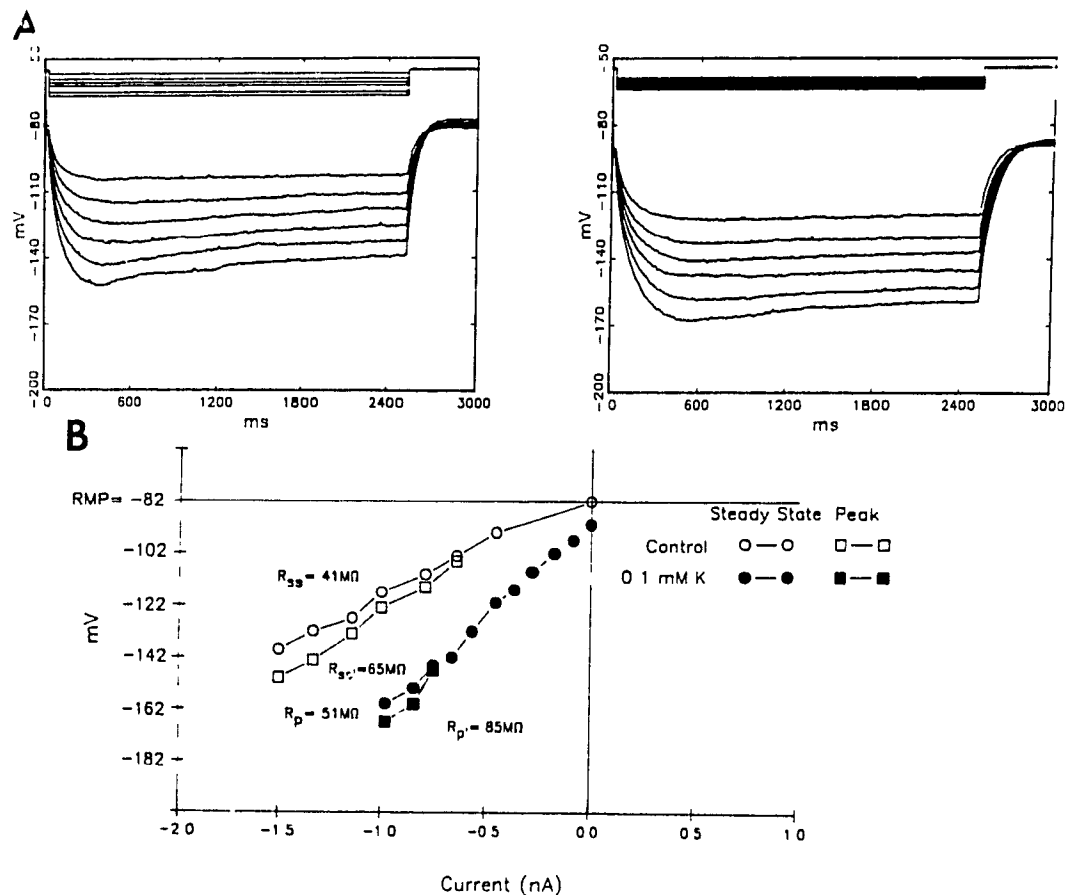


**FIGURE 3.6** Effect of reducing the external potassium ion concentration. **A** Control responses (left) Responses in 0.1 mM potassium (right; scale for current record 10 mV = 2nA) **B** Voltage/Current relationship. Reduction of external potassium concentration increased the peak and steady state resistance.

The time course of this prolongation closely followed the blockade of the

$G_{AR}$ . Partial blockade of the "sag" and the DAP in the ETP was accompanied by a partial elimination of the fast component of the post tetanic hyperpolarization, a prolongation of the post tetanic hyperpolarization and an attenuation of the depolarization following the post tetanic hyperpolarization (FIGURE 3.9A and B, respectively). Thus,  $G_{AR}$  appears to function in such a way as to limit the post tetanic hyperpolarization. These results are similar to those demonstrated in other neuronal preparations (Baker et al. 1987; Schwandt et al. 1988).

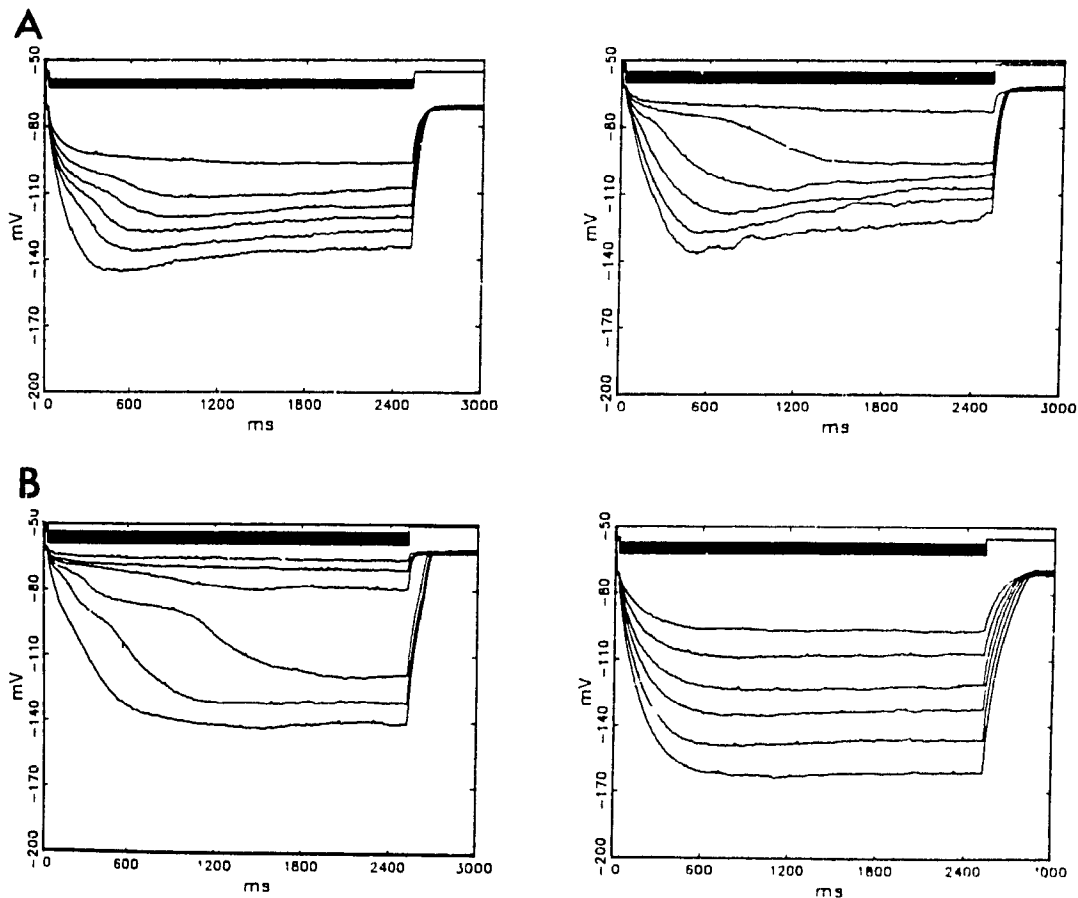


**FIGURE 3.7** Effect of raising the external potassium ion concentration on electrotonic potentials. **A** Control responses show an unusual instability in the charging phase of the ETP (left), which was enhanced when the external potassium conductance was increased to 8 mM. **B** Blocking  $G_{AR}$  with 3 mM cesium ion enhanced the instability further (left). Switching to normal potassium before washout of cesium abolishes the instability (right).

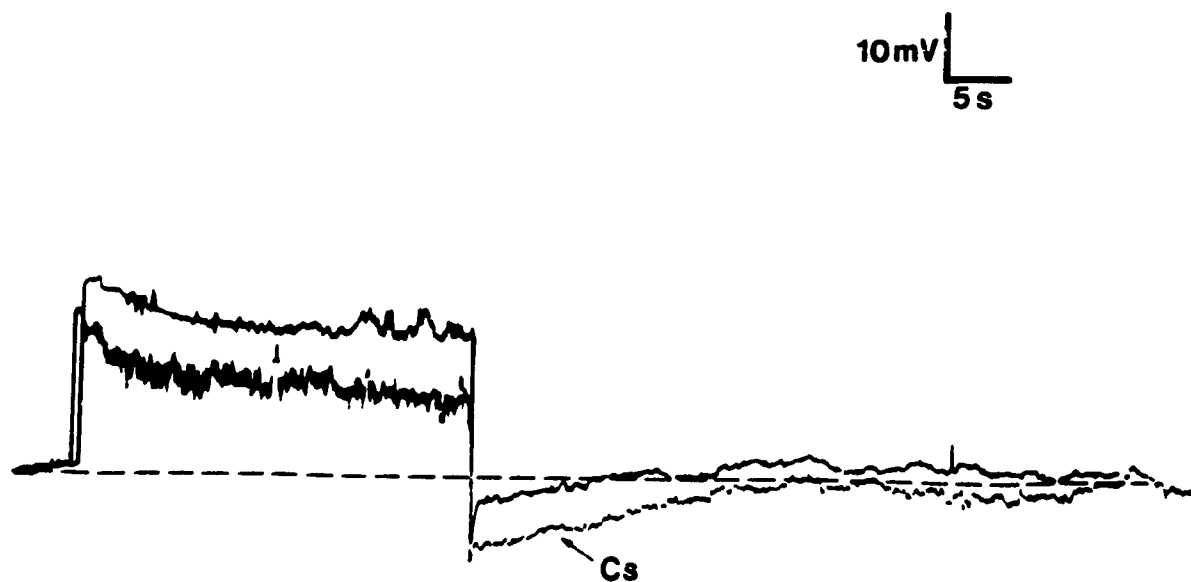


**FIGURE 3.8** Effect of cesium on the post tetanic afterhyperpolarizing potential. Chart record of the action potential train stimulated by the short supramaximal 0.5 ms pulses at 50 Hz for 30 seconds. Addition of 3 mM cesium ion to the extracellular medium prolongs the afterhyperpolarizing potential and blocks the depolarizing afterpotential elicited by the tetanus.

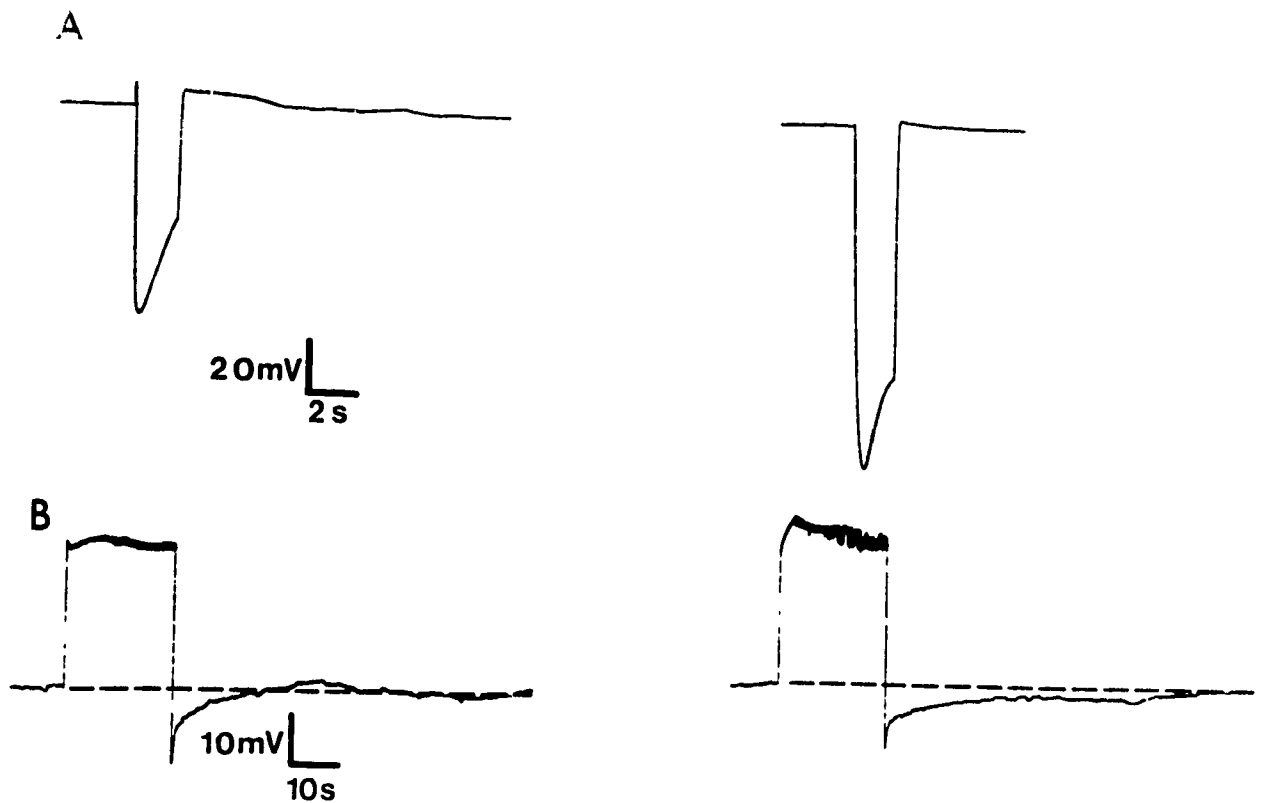


**FIGURE 3.9** Partial blockade of anomalous rectification is accompanied by partial blockade of the fast component of the post tetanic afterhyperpolarization. **A** (left) Chart record of Control ETP. **A** (right) After  $\approx 2$  minutes of perfusion with Ringer containing 3 mM cesium ion. The "sag" is partially blocked and the DAP is abolished. **B** (left). Chart record of control post tetanic AHP. **B** (right) Partial blockade of fast phase of AHP and complete block of DAP follows effects of cesium above.



## DISCUSSION

This study is the first to characterize the anomalous or inward rectification present in frog large myelinated primary afferent fibres. This rectification appears to have similar characteristics to the inward rectifying conductance reported in other excitable cells (Halliwell and Adams 1982; Mayer and Westbrook 1983; Spain et al. 1987). It is activated slowly, blocked by cesium ions but not by barium ions, and is reduced by decreasing the external potassium or sodium ions. All these observations suggest that the conductance is the Type 2  $G_{AR}$  defined by Schwindt et al. (1988). The slowness of its activation kinetics is likely an explanation as to why voltage clamp experiments have failed to demonstrate it, since voltage steps lasting 1500-2500 ms are required for its full development; a condition that would likely lead to significant shifts in the ion concentrations of the extracellular space obscuring measurement of the current (Binah et al. 1988).

Block by cesium ions of Type 2 anomalous conductance in mouse dorsal root ganglia (DRG) has been shown to be voltage dependent in the lower range of cesium concentrations (approximately 200  $\mu$ M), whereas at higher cesium concentrations ( $> 1$  mM), the degree of blockade was voltage independent (Mayer and Westbrook 1983). In contrast, cesium blockade of Type 2 conductance in hippocampal CA1 cells was found to be voltage dependent throughout the range of cesium concentrations (100  $\mu$ M - 3 mM; Halliwell and Adams 1982). In the present study, use of current clamp technique precludes a direct assessment of this possibility. However, in our preparation, if cesium blockade were voltage dependent, one would expect that a "sag" would be present in the range of membrane potentials, where the conductance is first activated, where-

as, when the membrane is more hyperpolarized the "sag" would disappear reported in Baker et al. (1987). However, this type of response was never seen in the voltage range where the sag was evident; thus it appears that blockade of  $G_{AR}$  by 3 mM cesium was voltage independent.

The reversal potential or driving point for a conductance could in theory be estimated, if not observed, from the intersection of  $V/I$  curves. In the case of  $G_{AR}$  this would mean estimating  $R_{ss}$  in the control  $V/I$  and  $R_{ss}'$  after cesium treatment (Werman 1969). In the case described in *FIGURE 3.2* the apparent reversal potential of  $G_{AR}$  was -90 mV. This result is difficult to reconcile with the evidence that  $G_{AR}$  is mediated by sodium and potassium ions. It would also be difficult to account for the presence of the DAP. The possibility exists that the DAP could result from an accumulation of ions in the external space and the reversal potential is as indicated from the  $V/I$ . However, two experimental results argue against this explanation. First, in control conditions, the inward rectifying conductance would tend to oppose an accumulation, since it is accompanied by a flow of potassium and sodium ions from the extracellular space. If accumulation of ions was significant, despite this ion flow, then blockade of  $G_{AR}$  would be expected to potentiate ion accumulation and therefore the DAP. Cesium blockade of  $G_{AR}$ , in fact, abolished the DAP. Secondly, reduction of the DAP when sodium was substituted with choline reveals that the DAP is dependent on sodium ions, clearly excluding an accumulation of sodium ions as a factor. Finally, simple calculations, estimating the possible effects of the currents used in these experiments ( $< 2$  nA), indicate that significant shifts of ion concentrations in the extracellular space should not be expected (Attwell et al. 1979). Therefore, one is likely to conclude that the DAP results from the slow inactivation of a conductance, whose reversal potential is

more positive to resting membrane potential. If the DAP is the slow closing of  $G_{AR}$  then one would place the  $E_{AR}$  more positive to resting membrane potential in agreement with voltage clamp studies, which found  $E_{AR}$  to be in the range of -50 to -60 mV (Adams and Halliwell 1983; Mayer and Westbrook 1983; Spain et al. 1987).

The increase in  $R_p$  observed when either cesium was present or potassium was reduced in the external media implies that  $G_{AR}$  is at least partially activated at the peak of the control hyperpolarizing ETP. One way this may occur is through the activation of  $G_{AR}$  with two time constants, similar to reports in Mayer and Westbrook (1983) and Spain et al. (1987). This hypothesis is not directly measurable under current clamp conditions, since the time constants of the voltage responses reflect the combination of both passive capacitive elements as well as the activation/inactivation time constants of conductances present in myelinated axons (Chapter 2). To examine contributions of these factors, we have used a computational model to generate V/I relationships. A single effective capacitance value for the axonal membrane was used (cf. Chapter 2). Inward rectification was modeled with one or two time constants of activation (see Methods).

The bottom set of traces in *FIGURE 3.10A* presents the computed ETPs with  $G_{AR}$  shut off. Its V/I relationship is graphed in *FIGURE 3.10B* top and bottom (filled squares) for comparison with the ETPs and V/I relationship computed with  $G_{AR}$  activated 1) with one time constant (*FIGURE 3.10A* top & *B* top: triangles) and 2) with two time constants (*FIGURE 3.10A* middle & *B* bottom; circles). A "sag" in the computed hyperpolarizing voltage response could only be reproduced when one of the time constants of activation was

longer than 450 ms. Using only one time constant, the  $V/I$  relationship was qualitatively of the same shape as seen experimentally (*FIGURE 3.10B* top, compare with *FIGURE 3.1, 3.2, 3.4, 3.5, 3.6*). However, only a small increase in  $R_p$  was observed when  $G_{AR}$  was shut off. The model of  $G_{AR}$  with two time constants generated a family of ETPs similar in appearance to experimental results (compare *FIGURE 3.10A* middle to *FIGURE 3.1A*): there was a larger increase in  $R_p$  after removal of  $G_{AR}$ , which is more in keeping with the large increase in  $R_p$  seen after blockade with cesium. However, the  $V/I$  relationship for the model with two time constants of activation was distinctly non-linear in the regions where experimental data were linear (compare *FIGURE 3.10B* bottom to *FIGURE 3.1B*).

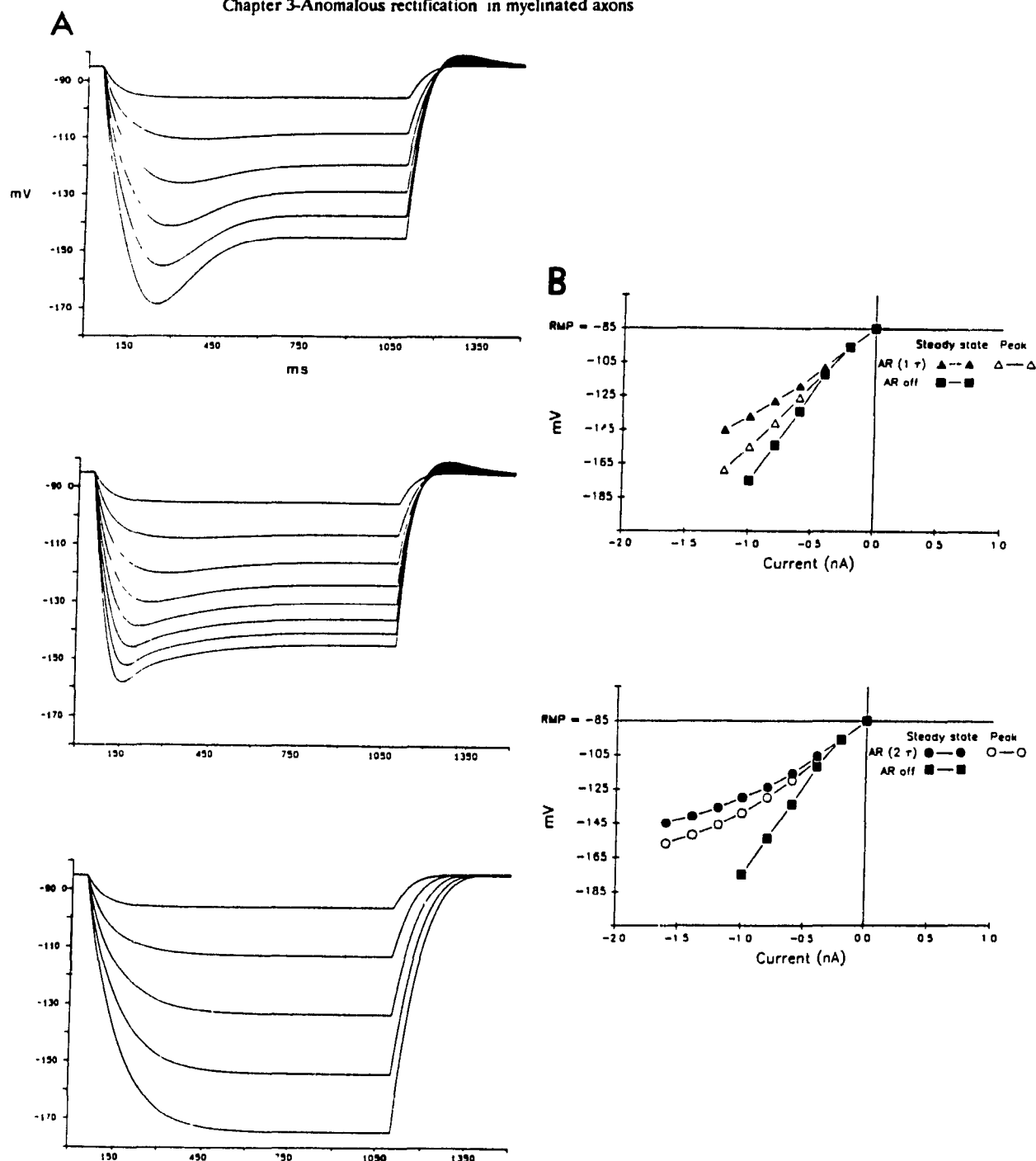


**FIGURE 3.10.** Comparison of single and double time constant activation of  $G_{AR}$  in a computer model. **A** Top: Voltage responses in which  $G_{AR}$  activates with a single 400-600 ms time constant; Middle: Voltage responses in which  $G_{AR}$  activates with an additional 10-12 ms time constant; Bottom: Voltage responses in the absence  $G_{AR}$  **B** Plots of V/I relationships; Top: V/I plot for single time constant activation (triangles) and V/I plot with  $G_{AR}$  turned off (squares) Bottom: V/I plot for double time constant activation (circles) and in the absence of  $G_{AR}$  (squares). V/I plot obtained with the single time constant activation best fit experimental observations.

This discrepancy suggests that, like the results reported by Halliwell and Adams (1982),  $G_{AR}$  in axonal membranes activates with only one time constant.

### *Physiological role of $G_{AR}$*

All the evidence indicates that  $G_{AR}$  in many cells is active in the voltage range negative to resting membrane potential. This limits its role to physiological mechanisms or phenomena that are recognized to occur in this range of membrane potential. In myelinated axons, and likely in other cells, two phenomena seem to be in question: slow potassium conductances and electrogenic pumping.

The fast conductances ( $G_{Kf1}$  and  $G_{Kf2}$ ; Dubois 1981) are activated in a range of membrane potentials, where  $G_{AR}$  appears to be inactive. Also, tail currents of both fast conductances decay much faster than  $G_{AR}$  activates (Dubois 1981; Grissmer 1986). The slow potassium current ( $G_{Ks}$ ; Dubois 1981) has a voltage dependence, which overlaps with the voltage range where  $G_{AR}$  appears to be activated (between -120mV and -100 mV). However, its activation and inactivation time constants would likely make it only susceptible to interaction with a fast activating component of  $G_{AR}$  (if it exists).

Based on the use of cesium ion to block  $G_{AR}$ , our results suggest that  $G_{AR}$  may regulate the length of the post tetanic afterhyperpolarization in myelinated axons. This activity is very likely generated primarily by electrogenic pumping (Barrett and Barrett, 1982; cf. Bergman et al. 1980) as is the case in many other cells (Koketsu 1971; Schwindt et al. 1988), as well as, potassium conductances. It is unlikely that the  $G_{AR}$  regulates this hyperpolarization

which itself is not otherwise limited by ionic gradients. Although there is only a slight overlap between the hyperpolarization induced by high frequency stimulation and the region where  $G_{AR}$  is activated, this interaction may be potentiated by a significant accumulation of potassium ions in the extracellular space. This accumulation would consequently shift the reversal potential more positive, away from the voltage range, where the Type 2  $G_{AR}$  is active, with a consequent potentiation of the conductance (Halliwell and Adams 1982; Mayer and Westbrook 1983; Spain et al. 1987).

Another role suggested for  $G_{AR}$  is the stabilization of the membrane potential when there is an accumulation of extracellular potassium ions (Hille 1984). This study may support this notion, since raising the potassium ion concentration of the external medium decreased the "stability" of the membrane potential, and blocking  $G_{AR}$  enhanced this instability even further. Therefore, under conditions, such as repetitive firing or anoxia accompanied by potassium ion accumulation,  $G_{AR}$  may function to maintain membrane potential and conditions favourable for the generation of action potentials.

Interestingly, some inward rectification may be due to the slow potassium conductance, if the reversal potential of potassium was shifted significantly above the region where  $G_{KS}$  is active (Chapter 2).

In summary, this study has characterized some properties of the anomalous or inward rectification present in frog myelinated primary afferent fibres: it can be classified as Type 2  $G_{AR}$ , since it is dependent on external sodium and potassium ions, it is blocked by cesium ions and not by barium ions and activates comparatively slower than Type 1  $G_{AR}$ . Its physiological role in axons

be classified as Type 2  $G_{AR}$ , since it is dependent on external sodium and potassium ions, it is blocked by cesium ions and not by barium ions and activates comparatively slower than Type 1  $G_{AR}$ . Its physiological role in axons may be to attenuate long lasting afterhyperpolarizations and to maintain and stabilize the membrane potential in a range, which supports action potential generation.



**DENDROTOXIN BLOCKS ACCOMMODATION IN FROG MYELINATED AXONS**

by

**M.O. Poulter, T. Hashiguchi and A. L. Padjen**

(Published in the Journal of Neurophysiology 62:174-184, 1989)

## SUMMARY AND CONCLUSIONS

1. Intracellular microelectrode recordings from large sensory and motor myelinated axons in spinal roots of *Rana pipiens* were used to study the effects of dendrotoxin, a specific blocker of a fast activating potassium current ( $G_{Kf1}$ , Benoit and Dubois 1986).
2. Dendrotoxin reduced the ability of myelinated sensory and motor axons to accommodate to a constant stimulus. A depolarizing current step, which normally evoked only one action potential, after dendrotoxin treatment (200-500 nM) produced a train of action potentials. These spike trains lasted  $29 \pm 2.8$  ms on average in sensory fibers ( $n = 18$ ) and  $40.2 \pm 4.5$  ms in motor fibers ( $n = 9$ ).
3. After dendrotoxin treatment, in addition to a reduction in the ability to accommodate to a constant stimulus, a slowing in the rate of action potential generation was evident (spike frequency adaptation).
4. Dendrotoxin had no effect on the rising phase of conducted action potentials evoked by peripheral stimulation. Together with a lack of effect on the absolute refractory period, these results indicate that dendrotoxin does not affect sodium channel activity.
5. The steady state voltage/current relationship was unchanged in response to hyperpolarizing current pulses; however, there was a significant increase in cord resistance in response to depolarizing current steps, demonstrating that DTX

decreases outward rectification.

6. A computer model based on Hodgkin and Huxley equations was developed, which included the three voltage dependent potassium conductances described by Dubois (1981). The model reproduced a major part of the experimental results: removal of the conductance termed  $G_{Kf1}$  reduced the accommodation in the early phase of a continuous stimulus, indicating that this current could be responsible for the early accommodation. The hypothesis that the slow potassium conductance,  $G_{Ks}$ , regulates late accommodation and action potential frequency adaptation is also supported by the computer model.

7. In summary, these results suggest that in amphibian myelinated sensory and motor axons the activity of potassium conductances can account for accommodation and adaptation without involvement of sodium conductance activity.

## INTRODUCTION

The wide variety of voltage dependent potassium conductances appear to be important in regulating the functional properties of neuronal membranes (Adams and Galvan 1986). In early descriptions of myelinated axons, activation of the outward rectifying current was attributed to a single class of voltage dependent potassium channels, equivalent to the activation of the potassium current in the squid axon described by Hodgkin and Huxley (1952a). However, several lines of evidence obtained in recent years have demonstrated that myelinated axons are endowed with more than one type of potassium channel (Dubois 1981; Grissmer 1986; Ilyn et al. 1980; Neumcke et al. 1980). In the amphibian large myelinated axon, Dubois (1981) has described three subclasses of potassium conductances with different kinetics and different sensitivity to pharmacologic agents: two fast activating conductances ( $G_{Kf1}$ ,  $G_{Kf2}$ ), blocked by both 4-AP and TEA, and a slow activating conductance ( $G_{Ks}$ ) that is blocked only by TEA.

Potassium conductances have been speculated to be important regulators of neuronal excitability by virtue of regulating accommodation or spike frequency adaptation (Dubois 1981; Neumcke et al. 1980). For example, Dubois (1981) has speculated that the relative proportion of the two fast conductances ( $G_{Kf1} \gg G_{Kf2}$ ) in sensory and motor fibers may account for the greater accommodation in motor fibers. However, the identification of potassium conductances that could be responsible for accommodation and/or adaptation in myelinated axons have only recently begun to be elucidated.

A purified fraction of the venom of the South African green mamba snake

(*Dendroaspis angusticeps*), dendrotoxin (DTX), has been shown to be a potent and selective blocker of potassium currents in a variety of tissues (Benoit and Dubois 1986; Harvey and Anderson 1985; Penner et al. 1986, Feltz and Stansfeld 1988; Stansfeld et al. 1986; Weller et al. 1985). In voltage clamp experiments on the frog node of Ranvier, Benoit and Dubois (1986) have shown that DTX selectively blocks the potassium conductance designated  $G_{Kf1}$  without affecting the other potassium conductances or the sodium current. The specific blockade of the  $G_{Kf1}$  conductance afforded the opportunity to examine and compare the effects of this toxin on the functional properties of motor and sensory axons and elucidate what role this conductance plays in the normal function of these axons.

The microelectrode technique (Padjen and Hashiguchi 1983) used in these studies is not amenable for voltage clamp analysis, but, unlike the latter technique, it allows recording from undissected axons; therefore, it is likely that the recordings obtained better reflect the excitability *in vivo*. In addition, to extend and evaluate our interpretation of experimental results, we have correlated experimental results with a computational model (Dodge 1963) of axonal membranes. The computational model utilized Hodgkin-Huxley formulations of the gating parameters fit to reflect the voltage clamp data for the three potassium conductances described by Dubois (1981). Preliminary results have been reported (Poulter and Padjen 1986).

## METHODS

### *Experimental procedure*

The recording methods used in this study have previously been described in detail in (Padjen and Hashiguchi 1983). Briefly, the hemisected spinal cord isolated from *Rana pipiens* was placed in a chamber (200  $\mu$ l volume) and perfused with 1) normal Ringer (containing in mM: 115 NaCl, 2 KCl, 2 CaCl<sub>2</sub>, 10 dextrose; pH 7.2-7.35 adjusted with 10 mM HEPES buffer); 2) Ringer in which the Ca<sup>2+</sup> concentration was reduced to 0.2 mM and 2.0 mM Mn<sup>2+</sup> was added to block synaptic transmission (Mn Ringer); 3) normal Ringer in which tetrodotoxin (0.25  $\mu$ M) was added to block sodium conductance. Except where noted, all experiments were done in Mn-Ringer at 15°C. The sensory (DRF) and motor fibers (VRF) were drawn through slits in the side of the perfusion chamber into a mineral oil filled chamber where they could be stimulated by extracellular platinum electrodes. Intracellular recording electrodes filled with 3 M KCl (resistance 35-50 M $\Omega$ ) were used to impale large myelinated fibers (conduction velocity > 15 m/s) near the entry zone of DRF or VRF. Fibers were considered suitable for use only when the membrane potential was stable, more negative than -75 mV and the conducted action potential amplitude greater than 85 mV. Records were stored in a digitized form on videotape using PCM and video recorder (Benzanilla 1985) for further off-line computer analysis (Modular Instruments Inc. interface and IBM-AT computer). Plots of computer records were done on a Hewlett-Packard X-Y plotter.

Due to the limited amount of toxin available, DTX stock solution was added directly into the bath after temporarily shutting off the flow of perfusate (final

bath concentration 250 and 500 nM in experiments on VRF and DRF, respectively). Incubation with the toxin was maintained for 30 minutes at 15°C. This has no noticeable effect on the viability of the preparation (cf. Collier et al. 1982). At the concentrations used, DTX effects appeared irreversible and were still present up to 24 hours after incubation.

Whenever appropriate, results were expressed as mean  $\pm$  standard error (s.e.) and their significance evaluated using a *t*-test analysis.

Purified DTX was obtained as a gift from J. Oliver Dolly, Department of Biochemistry, Imperial College of Science and Technology, London, and was purified as in (Dolly et al. 1984).

## RESULTS

As previously shown with partially purified toxin, DTX application produced convulsive discharges (Collier et al. 1982; Harvey and Anderson 1985; Harvey and Gage 1981). Increases in spontaneous activity and bursts of action potentials were evident within 30 minutes of DTX application, as seen by Harvey and Gage (1981) and Dolly et al. (1984). However, as shown in *FIGURE 4.1* Mn-Ringer, known to block synaptic transmission, abolished this activity. There was no change in membrane potential upon application of DTX to a preparation already perfused by Mn-Ringer.

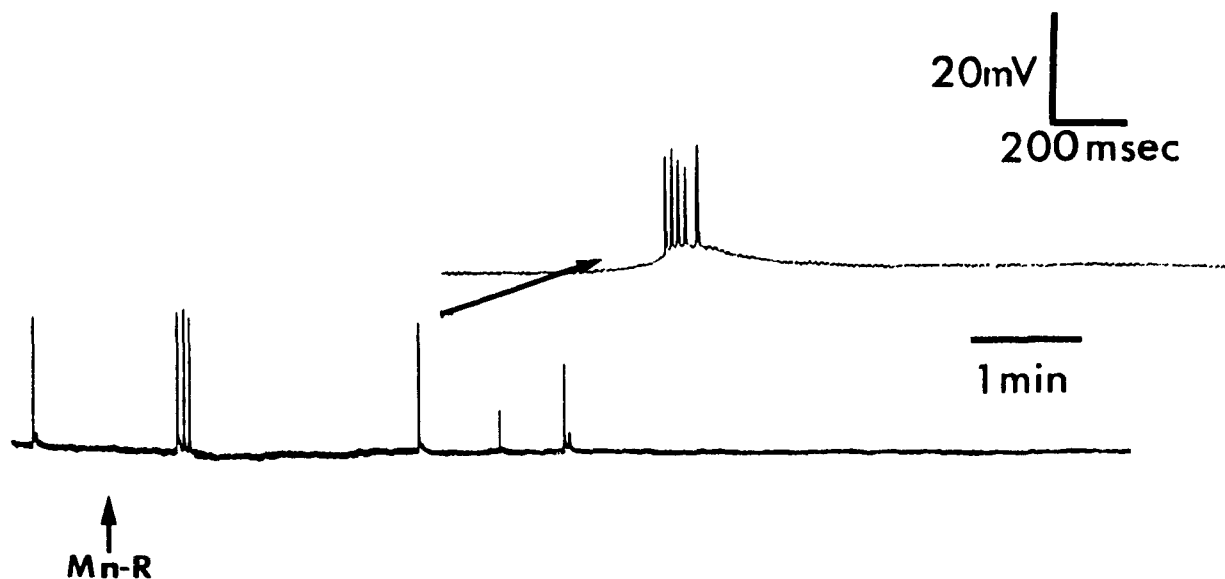


*FIGURE 4.1* Spontaneous convulsive discharges after DTX treatment. After DTX treatment, bursts of action potentials are recorded from primary afferents in normal Ringer solution. The bursts disappear after blockade of synaptic transmission by adding Mn (2mM) to the Ringer solution.



*Effect of DTX on repetitive activity.*

The differences in the accommodating properties of sensory and motor fibers studied in normal Ringer are well documented (Erlanger and Blair 1938; Schmidt and Stämpfli 1964) and so, studies were done to compare the effect of DTX on the excitability of these two types of fibers. Intracellular depolarizing current steps were injected into the fibers before and after DTX treatment to assay for differences in repetitive activity. In Mn-Ringer, both DRF and VRF control fibers ( $n = 17$ ) produced only one action potential in response to a depolarizing current step (*FIGURE 4.2A*). Moreover, no additional action potentials could be generated by injections of current up to 10 times the threshold current (not shown). In normal Ringer solution and in the same range of current injected, less than 5% of sensory fibers (no motor fibers) elicited more than one action potential.

After incubation with DTX, depolarizing pulses of similar magnitude generated a burst of action potentials at the beginning of the current step as illustrated in *FIGURE 4.2B*. Therefore, DTX reduced the accommodation to the stimulus in both types of fibers. There was no change in the voltage threshold for generation of the first spike in a current pulse after DTX treatment in either DRF or VRF (Control  $70.0 \pm 3.7$  mV; DTX  $69.0 \pm 4.5$  mV  $n = 17, 27$ , respectively). This indicates that DTX did not exert its effect by decreasing threshold for action potential generation. However, the maximal number of action potentials generated in the motor fibers was significantly greater than in sensory fibers ( $4.4 \pm 0.8$  and  $2.9 \pm 0.4$ , respectively;  $p < 0.03$   $n = 9, 18$ , respectively).

In addition, the trains of action potentials lasted significantly longer in VRF than in DRF ( $40.2 \pm 4.5$  and  $29.6 \pm 2.8$  ms, respectively;  $p < 0.04$   $n = 9, 18$ , respectively). The instantaneous interspike frequency of the first two action potentials and the applied current were positively correlated in both types of fibers (not shown); however, the maximum spike frequency produced in VRF and DRF were not different.

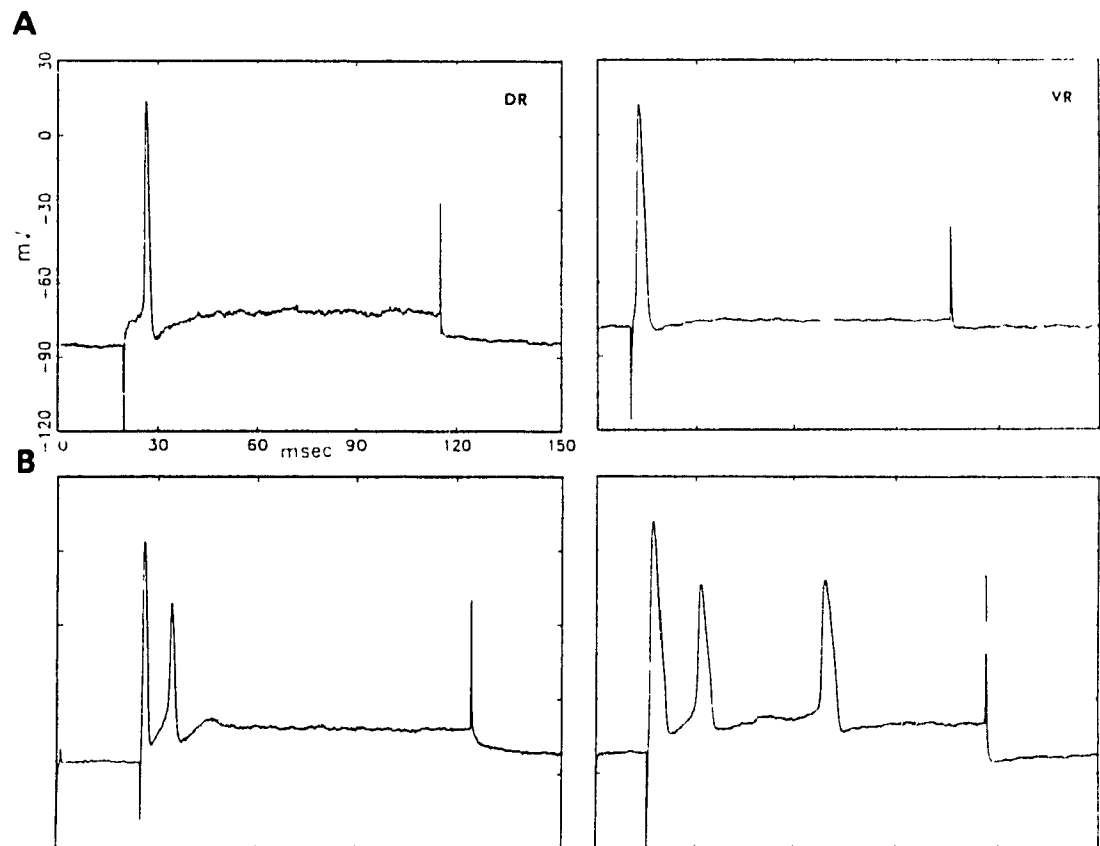


**FIGURE 4.2** Effect of DTX on accommodation of sensory (DR) and motor (VR) fibers. **A)** In control, a depolarizing pulse (100 ms) generates only one action potential in both DRF (left) and VRF (right), i.e. there is prominent accommodation; **B)** Treatment with DTX (500 nM for DRF; 250 nM for VRF) results in a decrease in accommodation; the same current pulse generates trains of action potentials, lasting  $29.6 \pm 2.8$  and  $40.2 \pm 4.5$  ms for DRF and VRF,  $n = 18, 9$ , respectively.

*FIGURE 4.3A* shows a sample of a typical record from a VRF: increasing stimulus current intensity resulted in a decrease in the second interspike interval, which nevertheless was greater than the first interspike interval. With a further increase in current stimulus, when more action potentials were generated, the firing frequency appeared to decline to a minimum and firing eventually ceased. The corresponding interspike frequency for various currents was calculated and plotted as shown in *FIGURE 4.3B*. Thus, fibers showed early and late spike frequency adaptation and were able to accommodate to a stimulus later in the current step.

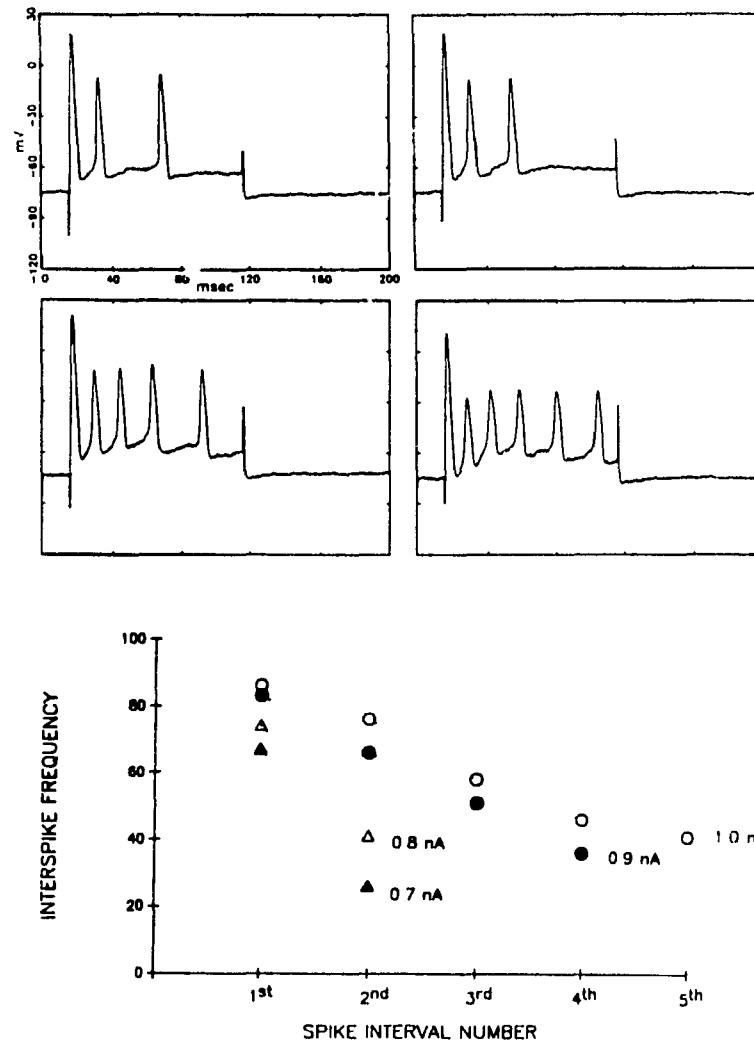


**FIGURE 4.3** The effect of increasing stimulus strength on DTX treated motor axons (VRF) A) Increasing the current of a 100 ms step results first in an increase in the firing frequency and then an increase in the number of spikes generated (left to right 0.7, 0.8, 0.9, 1.0 nA, respectively) B) Plot of the interspike frequency (Hz) versus the spike interval number at different current intensities. The decrease in spike frequency illustrates spike frequency adaptation.

#### *Effect of DTX on action potentials*

There was no change in the amplitude and the upstroke  $dV/dt$  of the first action potential in a train, resulting from an extended current pulse in DTX treated axons.

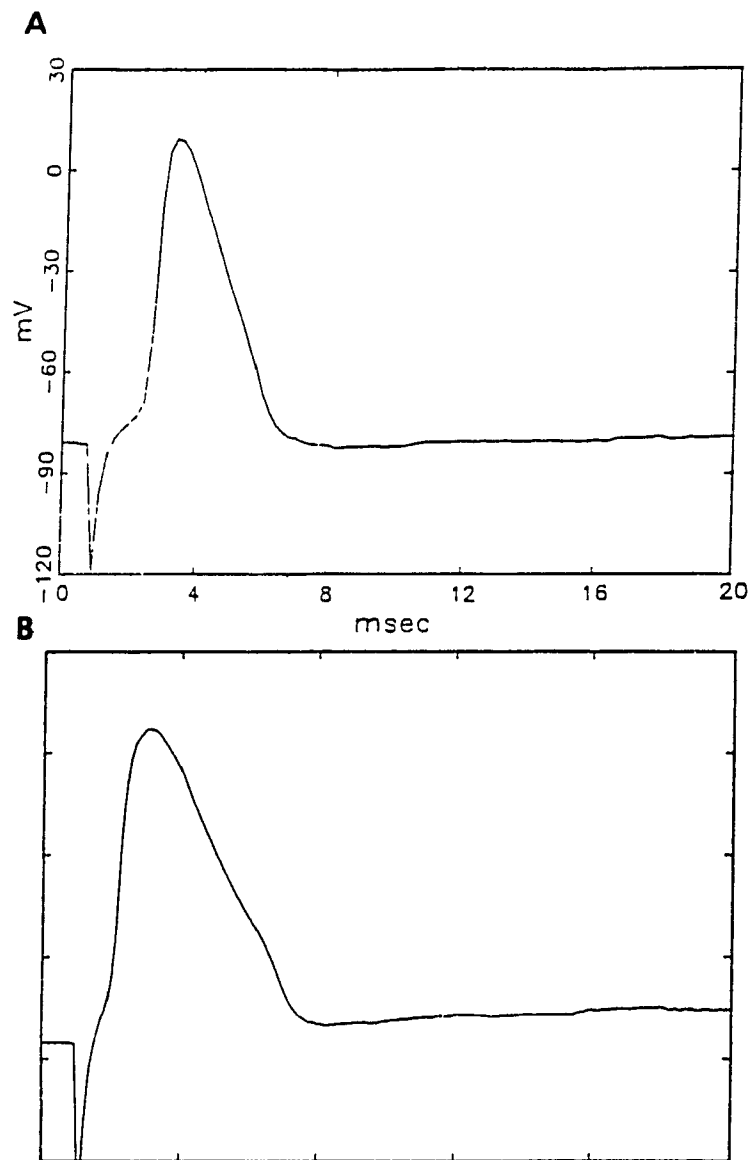


**FIGURE 4.4** Effect of DTX on duration of an action potential recorded from a motor axon. **A)** Control **B)** After DTX treatment. The rate of repolarization is slower after DTX treatment (a similar change was observed in VRF conducted action potentials not shown).

Subsequent action potentials in the train decreased in amplitude and became prolonged. The first action potential in a VRF but not DRF train was prolonged after DTX treatment, as illustrated in *FIGURE 4.4*.

Stimulation by a single short pulse of the peripheral end of spinal roots resulted in a single conducted action potential in both control and DTX treated preparations (*FIGURE 4.5*). In contrast, the same stimulus produced a burst of conducted action potentials in 4-AP treated rat myelinated axons (Kocsis et al. 1987), despite both agents apparently having similar pharmacological specificity (see *DISCUSSION*). DTX did not attenuate the upstroke  $dV/dt$  of the conducted action potentials: in control DRF and VRF,  $dV/dt$  was  $235 \pm 40$  and  $255 \pm 37.5 \text{ V}\cdot\text{s}^{-1}$ , respectively; in DTX treated preparations,  $dV/dt$  was  $270 \pm 28$  and  $278 \pm 12 \text{ V}\cdot\text{s}^{-1}$ , respectively ( $n = 5-12$ ).

Short (0.2-0.5 ms) intracellular injections of depolarizing current pulses also resulted in a single action potential. A double pulse technique, using supramaximal short pulses (2 x threshold) and varying the interpulse interval, was used to test the absolute refractory period. No difference was detected between untreated and DTX treated axons. The lack of effect of DTX on  $dV/dt$  and the refractory period indicates that DTX had no effect on the activation or inactivation of the sodium conductance. These results agree with those reported by Benoit and Dubois (1986) who also found that DTX had no effect on the sodium current in the frog node of Ranvier.

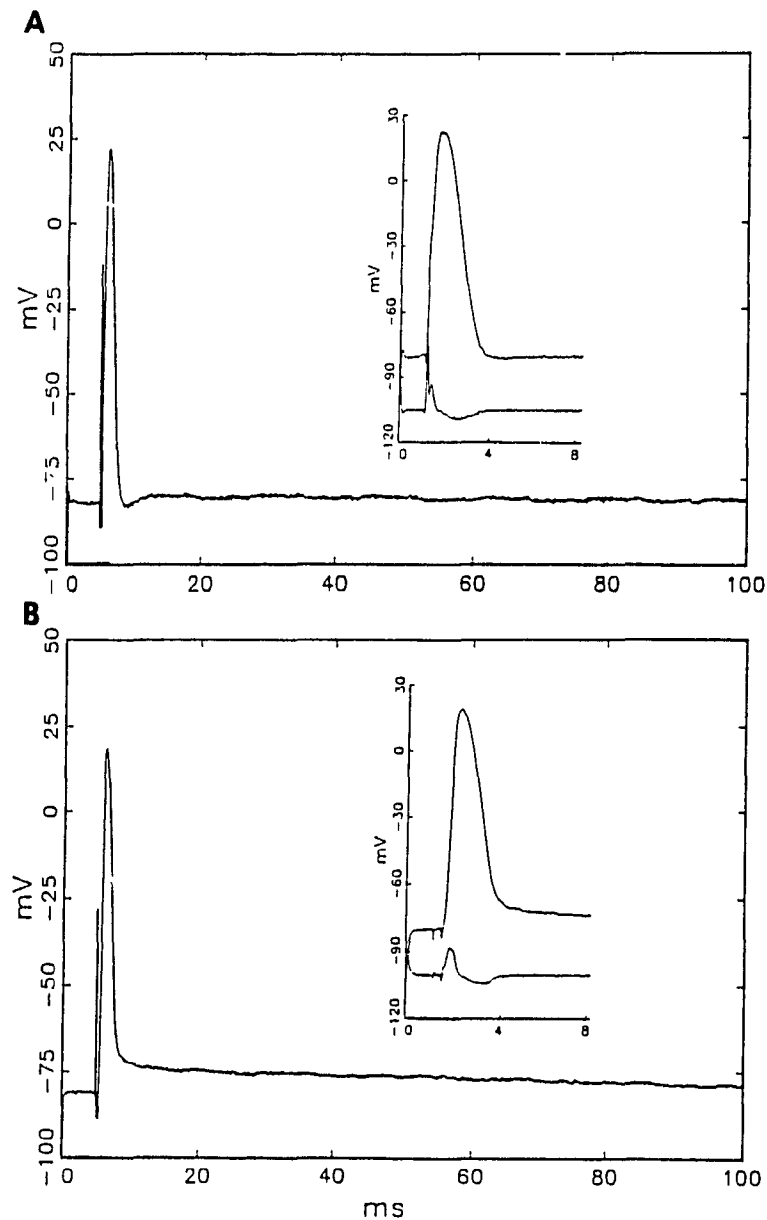


**FIGURE 4.5** Sample of DRF conducting spike with  $dV/dt$  before and after DTX treatment. DTX had no apparent effect on the upstroke of the action potential, and  $dV/dt$  measurement showed no significant difference in the magnitude (scale  $10 \text{ mV} = 200 \text{ V} \cdot \text{s}^{-1}$ ). **A)** Control; **B)** After DTX treatment. DTX treated fibers consistently had an afterdepolarizing potential that was rarely seen in control fibers.

The afterdepolarizing potential (ADP) (Barrett and Barrett 1982), usually

recorded in DRF, appeared to be larger in DTX treated fibers. Occasionally, preparations with small or no apparent ADP developed a prominent one after exposure to DTX (*FIGURE 4.5*). This observation was similar to reports of an increase in the ADP after TEA treatment (Barrett et al. 1988) and was likely the result of an increase in membrane resistance (Blight 1985) in the region above resting membrane potential following DTX treatment.

#### *Effects of DTX on voltage-current (V/I) relationship*

The V/I curves of myelinated axons, plotted for the steady state voltage responses to injected current, showed a characteristic outward rectification in the region positive to resting membrane potential (Padjen and Hashiguchi 1983). In control fibers, the maximal displacement of membrane potentials by depolarizing current steps (up to 1 - 2 nA) at steady state never exceeded 8-12 mV in Mn-Ringer or TTX-Ringer. A linear region below -100 mV was used to express the effective resistance of the fiber ( $R_p$ ) (Chapter 1;  $R_e$  in Padjen and Hashiguchi 1983). Inward rectification at membrane potentials below -130 was evident as a sag in the voltage response (Chapter 2; Padjen and Hashiguchi 1983; Poulter and Padjen 1989). After DTX treatment, neither  $R_p$  nor the inward rectification was altered. However, the outward rectification was significantly attenuated after exposure to DTX; the membrane could often be depolarized up to 25 mV above resting membrane potential. The V/I cord resistance calculated from the minimum current required to give a maximal voltage response for d.r.f control fibers was  $5.4 \pm 0.9 \text{ M}\Omega$  and DTX treated  $16.5 \pm 6.4 \text{ M}\Omega$  ( $p < 0.001$ ,  $n = 17, 12$ , respectively). *FIGURE 4.6* shows one such experiment on a DRF done in the presence of tetrodotoxin ( $0.25 \mu\text{M}$ ) to block spike generation. The current required to give a maximal voltage deflection of



10 mV was 1.0 nA before DTX treatment; whereas, after treatment, the fiber could be maximally depolarized to 13 mV by 0.6nA of current (approximately a 2 fold increase in the cord resistance). Similar results were observed in the motor fibers in the Mn-Ringer: Control  $1.3 \pm 0.1 \text{ M}\Omega$ ; DTX treated  $8.4 \pm 3.3 \text{ M}\Omega$   $p < 0.005$ ,  $n = 6$  and  $8$  for VRF, respectively.

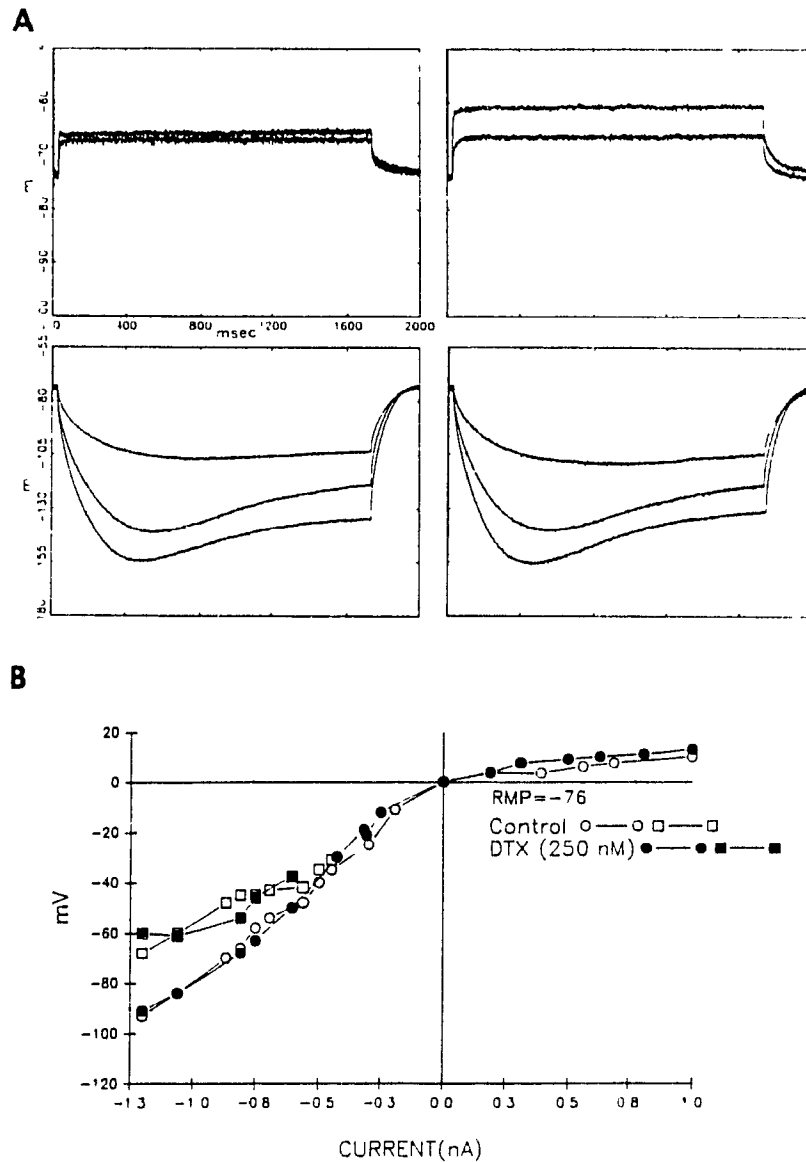


**FIGURE 4.6** Sample of voltage/current (V/I) responses of a single DRF before and after DTX application in the presence of 0.25  $\mu$ M tetrodotoxin. **A)** After DTX treatment (right) samples of the voltage record show no change in the response to hyperpolarizing pulses including the sag characteristic of the activation of the anomalous rectifying conductance, but a small increase in the voltage response in the depolarizing direction was evident. **B)** A plot of the steady state V/I relationship. The linear portion of the curve is unchanged (circles), as well as, the response measured at steady state (squares). In the depolarizing direction there is a small but significant decrease in the outward rectification.

## DISCUSSION

The studies of large myelinated axons of the frog described in this paper provide evidence that accommodation of action potential generation in the early part of a continuous stimulus is regulated by one of the fast-activating potassium conductances, described as  $G_{Kf1}$  by Dubois (1981). These conclusions are based primarily on the use of dendrotoxin (DTX), a specific blocker of this conductance in myelinated axons (Benoit and Dubois 1986).

Voltage clamp analyses of DTX effects in other excitable membranes have demonstrated that the action of DTX is selective for incompletely or slowly inactivating potassium conductances (Penner et al. 1986; Schauf 1987; Feltz and Stansfeld 1988; Stansfeld et al. 1986). These conductances have similar activation and inactivation kinetics to the axonal  $G_{Kf1}$  conductance. One exception to these findings was reported by Halliwell et al. (1986), who found that DTX blocks the current designated  $I_A$  in pyramidal cells of the CA1 region of rat hippocampus. Thus, the pharmacological spectrum of DTX action appears to identify a family of potassium currents characterized by fast activation kinetics. One might speculate that they are of a common origin, perhaps the result of alternative splicing of a single gene resulting in a number of different primary DNA transcripts, similar to that reported by Schwarz et al. (1988) and Tempel et al. (1988).

Differential effects of potassium channel blockers, e.g. 4-aminopyridine (4-AP) and tetraethylammonium (TEA), led to the proposal that pharmacologically distinct potassium channels may regulate functional characteristics of a varie-

ty of large myelinated axons (Bergman et al. 1968; Kocsis et al 1987). In rat optic nerve, Kocsis et al. (1987) have shown that 4-AP led to a widening of the action potential, whereas TEA attenuated the after-hyperpolarizing potential, which may modulate excitability.

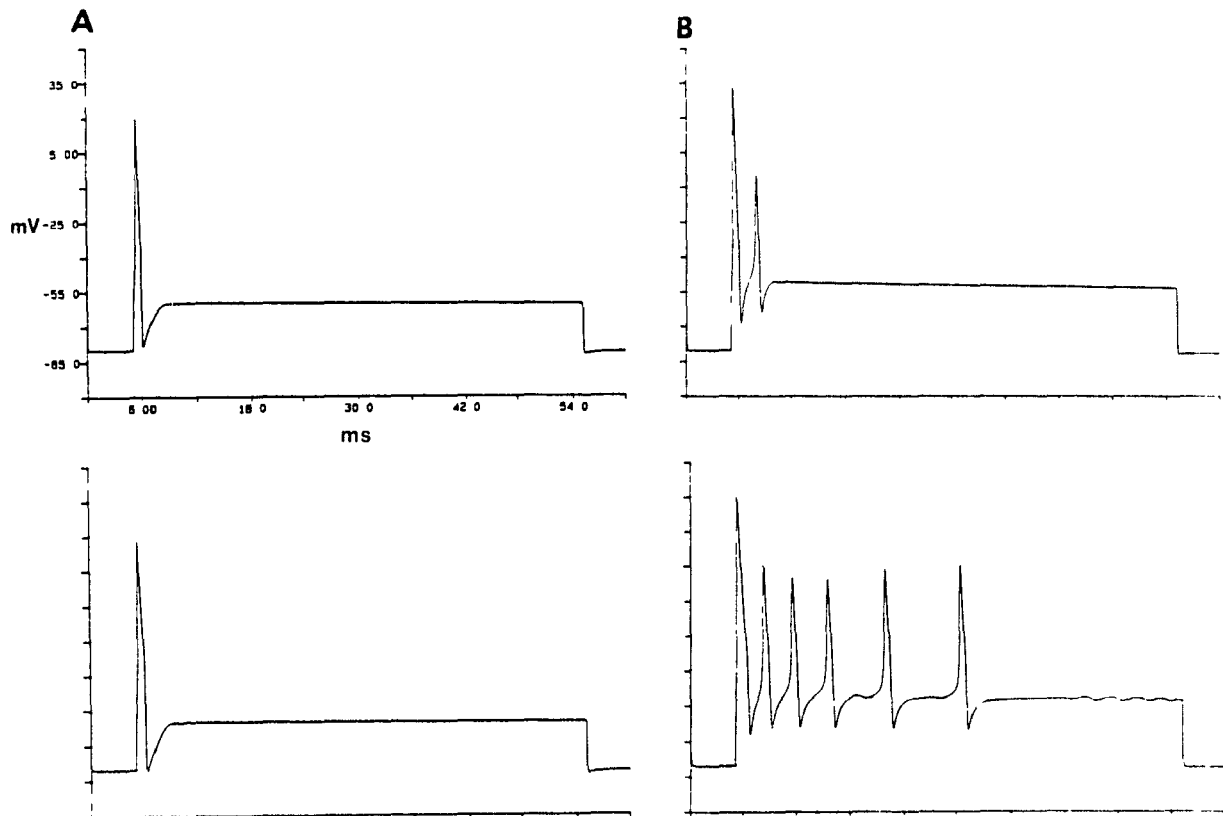


**FIGURE 4.7** Computer generated simulations of voltage responses from axonal membrane. **A)** Control responses (all potassium currents included in the model): DRF (top left) and VRF (bottom left) fibers generate only one action potential. **B)**  $G_{Kf1}$  set to zero. Action potential generation is similar to that seen after DTX treatment: VRF (bottom right) fiber generates more spikes, shows early adaptation and accommodates after approximately 30 ms while the DRF (top right) fiber accommodates more quickly (approximately 10 ms). Current pulse of 1.2 nA, starting at 5.0 ms and ending at 55 ms from the beginning of the trace.

Similarly, in rat myelinated spinal root axons, blockers of potassium channels selectively alter different aspects of excitability: TEA and Ba<sup>2+</sup> reduced accommodation of the rat myelinated axon, whereas 4-AP led to an increased excitability in response to a brief stimulus (Baker et al. 1987). Since DTX specifically blocks only G<sub>Kf1</sub>, unlike the less selective action of 4-AP, which affects both fast-activating currents (Dubois 1981), our results further define this functional classification of potassium currents sensitive to 4-AP.

A comparison of the pharmacology of DTX and 4-AP sensitive K<sup>+</sup> currents in various excitable membranes suggests that sensitivity to blockade by 4-AP and DTX varies directly with the time constant of inactivation (Dolly et al. 1987). Thus, in nodose ganglion, DTX and 4-AP blocked a rapidly activating and slowly inactivating current (and reduced action potential accommodation) at concentrations below that affecting the faster inactivating I<sub>A</sub> current (Stansfeld et al. 1986). A common characteristic of I<sub>A</sub> currents and G<sub>Kf1</sub> is their voltage-dependence: e.g. both activate between -80 and -30 mV. Together with their fast kinetics of activation, the voltage dependence is the main determinant of the functional role of these currents (Rogowski 1985). As one might expect in all tissues where spiking properties were measured, DTX reduced accommodation (Halliwell et al. 1986; Harvey and Gage 1981; Feltz and Stansfeld 1988) including myelinated axons as reported in this study.

Although Schauf (1987) reported a slowing of the rate, at which sodium channel inactivated in *Myxicola* giant axon, this was accomplished by internal application of DTX. In contrast, the reports of external application of DTX on frog nerve fibers (Benoit and Dubois 1986; Weller et al. 1985), studied by volt-

age clamp technique, demonstrated that DTX had no effect on the sodium current (in concentrations up to 850 nM). Our observations agree with these results, since the upstroke  $dV/dt$  of the single action potential, evoked by peripheral stimulation of the DTX treated motor or sensory root and the absolute refractory period, were not significantly different from control. For these reasons and others discussed below, alteration of the sodium conductance could not be considered the cause of the decrease in early accommodation.

To test the interpretation of our experimental results, a computational model of the axonal membrane was developed which included all the potassium conductances described by Dubois (1981). Both the fast and the slow potassium currents were represented in the relative proportions described by Dubois for motor and sensory fibers (Dubois 1981). In addition, the  $h$  gate was adjusted so that a continuous train of action potentials was produced when no potassium currents were included in the calculations, as previously done by Bromm & Frankenhaeuser (1972) (see *APPENDIX: Conditions for Repetitive Activity*).

The model reproduces all major experimental results fairly well:

1. A single action potential is generated with a depolarizing step of 1 - 2 nA (*FIGURE 4.7A*) under "control" conditions (all potassium currents present);
2. The train of action potentials is generated when the  $G_{Kf1}$  conductance is removed from the model (*FIGURE 4.7B*);
3. The length of the trains generated by the model without  $G_{Kf1}$  differs between motor and sensory fibers: 6 ms for DRF and 24 ms for VRF

Action potential generation accommodates in both fiber configurations despite the  $h$  gate reopening to a level where the sodium conductance is less inactivated at the end of the train ( $h \approx 0.25$ ) than at the beginning ( $h \approx 0.15$ , *FIGURE 4.8*). This indicates that, while the  $h$  gate level of inactivation is permissive in allowing action potential development early in the pulse, the shunting of depolarizing current by the remaining potassium conductances eventually accommodates the stimulus.

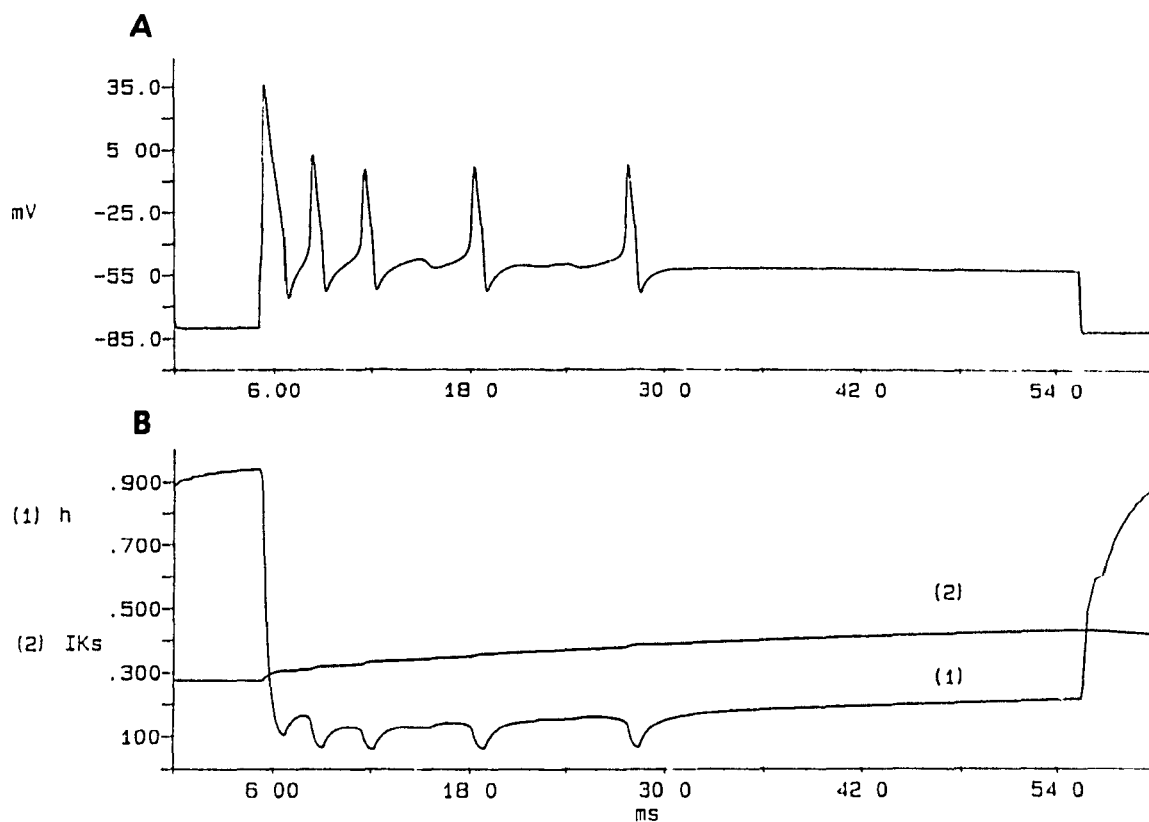


**FIGURE 4.8** Computer generated simulation of responses to a current step using model of ventral root axonal membrane without  $G_{Kf1}$ . **A)** Plot of action potentials and **B)** Plot of  $h$ -gate parameter (1) and of  $I_{Ks}$  (2), synchronized with **A**. The generation of action potentials eventually stops despite the reopening of the  $h$ -gate (**B1**) to a level greater than that required to generate action potentials early in the pulse. The time course of slow potassium current development (**B2**) coincides with the reduction in the rate of spike generation and accommodation. Removal of  $I_{Ks}$  resulted in a continuous train of spikes (not shown). Current pulse: 1.15 nA, starting at 5.0 ms and ending at 55 ms from the beginning of the trace.



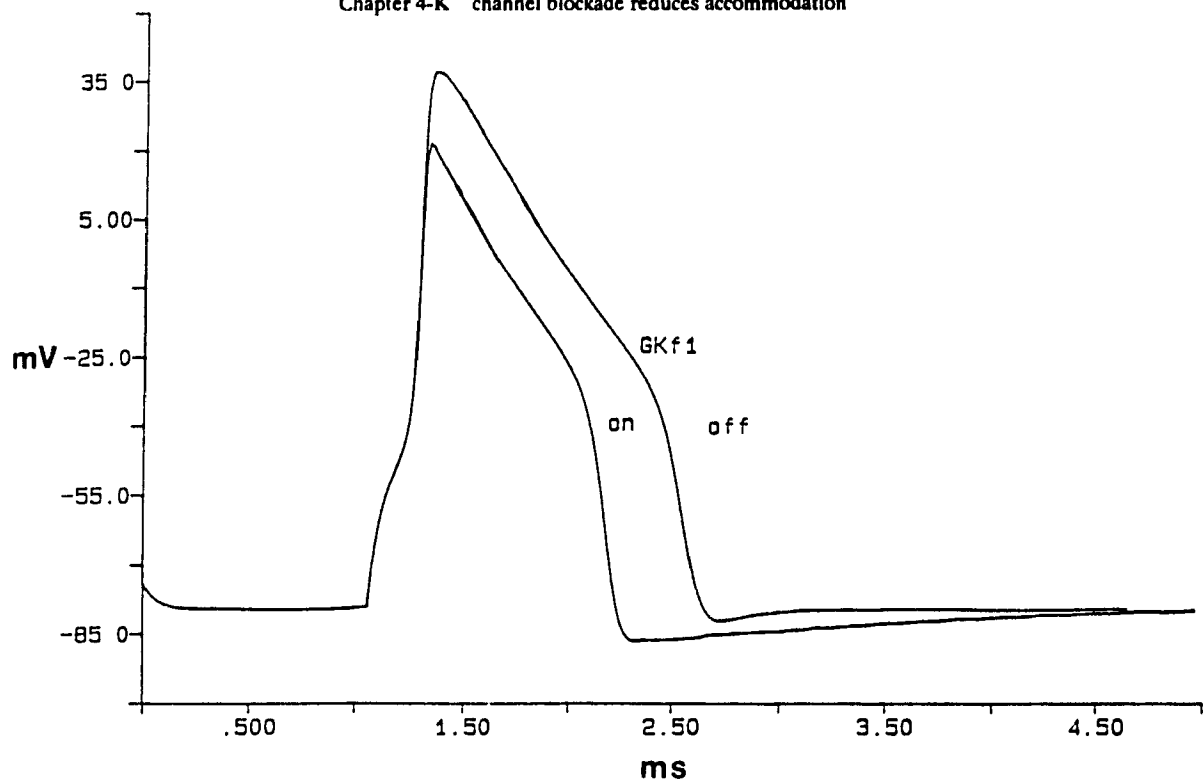


**FIGURE 4.9** Computed effect of  $G_{Kf1}$  on action potential in motor axons (VRF). Removal of  $G_{Kf1}$  slows action potential repolarization and increases spike height. Current pulse: 1.0 nA, 1.0 ms long, starting at 2.0 ms from the beginning of the trace.

DTX treatment removed accommodation to a constant stimulus on average for only 20-40 ms in both types of fibers; in addition, the frequency of action potentials in a train slowed, i.e., spike frequency adaptation was evident. Therefore, it would seem that the late phase of accommodation and adaptation is regulated by some factor(s) other than  $G_{Kf1}$ .

Although the experimental results suggest that the sodium conductance is unaffected by DTX, we have compared the effects of varying the  $h$  gate in other computational models to our experimental results. A single exponential activation and inactivation of the  $h$  gate did not predict late accommodation, since, depending on the level of inactivation, accommodation was either complete or the fiber generated a continuous train (Bromm and Frankenhaeuser 1972;

Frankenhaeuser and Huxley 1964: Valbo 1964). Also, the frequency of action potential generation was constant for a given stimulus level and increased the slower the  $h$  gate closed (Valbo 1964). A single exponential rate of inactivation of the sodium conductance only regulates the initial spike frequency, since the rate at which the  $h$  gate reopens will govern the absolute refractory period of the membrane (Bergman et al. 1968). For these reasons Krylov (1984) introduced a biexponential model of sodium channel inactivation, which altered the spike frequency within a train of action potentials and attenuated action potential generation later in a current stimulus. This model also predicted that spikes generated in a train would decline in amplitude, which is contrary to our observations and therefore, it does not adequately explain our experimental results.

From the above discussion, it appears that, at present, there is no relatively simple model of sodium channel inactivation which explains our experimental results. Excluding sodium conductance inactivation as a regulatory mechanism of the accommodation and late adaptation leaves potassium conductance activation as the next possibility. The rate at which the slow potassium conductance ( $G_{K_S}$ ) develops ( $\tau = 40$  ms) suggests that it may be responsible for late accommodation and adaptation. Our computational model, which included  $G_{K_S}$  (Dubois 1981) agrees with this interpretation. With  $G_{K_{f1}}$  set to zero, turning off of  $G_{K_S}$  resulted in continuous firing. Reducing the amount of  $G_{K_S}$ , reduced the spike frequency adaptation (decreased the slope of the interspike frequency vs. spike interval number).

It is interesting to note that Krylov and Makovsky (1978) proposed a model in which the activation of a then hypothetical slow potassium conductance

reproduced both a change in interspike frequency and, at higher depolarizing levels, late accommodation. They also suggested that a greater amount of a slow potassium conductance in VRF compared to DRF might account for the observed greater accommodation in VRF. However, experimental results show that the amount of  $G_{Ks}$  in both types of fibers is equal (Dubois 1981). More likely, it is the greater amount of  $G_{Kf1}$  in VRF, which accounts for its greater accommodation (Dubois 1981). Our experimental results support this hypothesis, since the greater blockade of the total potassium conductance in VRF after DTX treatment would explain the larger decrease in accommodation in this type of fiber.

It follows that the conductance,  $G_{Kf2}$ , may account for differences in spiking properties between DRF and VRF after DTX treatment. This conductance is partially activated at membrane potentials, where action potential generation occurs and so acts in an additive manner to  $G_{Ks}$ . The differences in behavior between DRF and VRF, such as, a larger number of action potentials in VRF and the lack of change in the rate of repolarization in DRF, could then be the result of the greater potassium conductance left unaffected in DRF. Again, the computer simulation agreed with this interpretation, since the duration of the action potential trains were different (see above) and the computed VRF action potential became longer in duration (*FIGURE 4.9*) after  $G_{Kf1}$  was removed, whereas the DRF action potential duration did not (not shown).

In summary, we provide further evidence that conductances, like the fast activating outward rectifying  $G_{Kf1}$ , may be functionally responsible for accommodation and that slow conductances, like  $G_{Ks}$ , are involved in spike frequency adaptation and the late phase of accommodation. These cellular mechanisms

seem to be important for coding of neural processing in excitable membranes, although the true meaning of their differences in sensory and motor axons could not be fully assessed in this study.

## APPENDIX

*Computer Model* The present model uses formulations for channel gating described by Hodgkin and Huxley (1952b). For computational purposes, the equations were approximated, as previously done by Dodge (1963). Total membrane current was calculated at the point of injection of current ignoring cable properties (i.e., changes are calculated only at one point of summation).

Equations for calculation of the net conductances:

$$I_m = I_{Na} + I_{Kf1} + I_{Kf2} + I_{Ks} + I_{leak} \quad (1)$$

$$I_{Na} = m^3 h G_{Na} (E_m - E_{Na}) \quad (2)$$

$$I_{Kf1} = n_{f1}^4 G_{Kf1} (E_m - E_K) \quad (3)$$

$$I_{Kf2} = n_{f2}^2 G_{Kf2} (E_m - E_K) \quad (4)$$

$$I_{Ks} = n_s G_{Ks} (E_m - E_K) \quad (5)$$

$E_m$  is the membrane potential for every iteration of the model. Equations describing  $\alpha$  and  $\beta$  of each gating parameter are defined by:

*Na channel equations*

$m$  gate:

$$\alpha_m = 1.6 \Theta_\alpha / (\exp(\Theta_\alpha) - 1) + 6.0 / (1 + (E_m + 25)^2 / 324) \quad (6)$$

$$\Theta_\alpha = (-37.5 - E_m) / 3.8 \quad (6a)$$

$$\beta_m = 4.05 \Theta / (\exp(\Theta_\beta) - 1) \quad (7)$$

$$\Theta_\beta = (37.5 + E_m) / 13.2 \quad (7a)$$

*h* gate:

$$\alpha_h = 0.14 \Theta / (\exp(0.8\Theta_\alpha) - 1) \quad (8)$$

$$\Theta_\alpha = (A + E_m) / 5.9 \quad (8a)$$

A = 74,76 for DRF and VRF, respectively

$$\beta_h = B / \exp((\Theta_\beta) + 1) \quad (9)$$

B = 4.0, 2.5 for DRF and VRF, respectively

$$\Theta_\beta = -(C + E_m) / 14.5 \quad (9a)$$

C = 12,14 for DRF and VRF, respectively

The constants for the *h* gate were different for the sensory and motor axon in order to simulate the well-described differences in the rate of repolarization of action potentials (Schwarz et al. 1983). In the motor axon Schwarz et al. (1983) described a double exponential rate of the *h* gate closing, where the relative proportion of the slow time constant at depolarized potentials predominates, thus accounting for the initial slower dV/dt of repolarization. We have approximated this by reducing the rate, at which *h* closes ( $\beta$ ) in VRF, and shifting the voltage dependence of *h* so that the level of inactivation in the VRF and DRF models were comparable.

The potassium conductances were defined by three sets of equations. The equations used by Dodge (1963) for defining the one conductance were altered to describe the two fast conductances ( $G_{Kf1}$  equations 10,11;  $G_{Kf2}$  equations 12,13). The equations for  $\alpha$  and  $\beta$  reported by Dubois (1981) were used for the

slow conductance ( $G_{K_S}$  equations 14,15).

*K channel equations*

$n_{f1}$ :

$$\alpha_{f1} = 1.25 \Theta_{\alpha} / (\exp(\Theta_{\alpha}) - 1) \quad (10)$$

$$\Theta_{\alpha} = -(50 + E_m) / 3.8 \quad (10a)$$

$$\beta_{f1} = 0.075 \Theta_{\beta} / (\exp(\Theta_{\beta}) - 1) \quad (11)$$

$$\Theta_{\beta} = (25 + E_m) / 13.2 \quad (11a)$$

$n_{f2}$ :

$$\alpha_{f2} = 0.34 \Theta_{\alpha} / (\exp(\Theta_{\alpha}) - 1) \quad (12)$$

$$\Theta_{\alpha} = -(10 + E_m) / 8.0 \quad (12a)$$

$$\beta_{f2} = 0.46 \Theta_{\beta} / (\exp(\Theta_{\beta}) - 1) \quad (13)$$

$$\Theta_{\beta} = (60 + E_m) / 12.2 \quad (13a)$$

$n_s$ :

$$\alpha_s = 0.028 \exp(E_m/33) \quad (14)$$

$$\beta_s = .0008 \exp(-E_m/33) \quad (15)$$

*Gate Equations*

$$m_{\infty}, h_{\infty}, n_{\infty} = \alpha / (\alpha + \beta) \quad (16)$$

$$\tau_{m,h,n} = 1 / (\alpha + \beta) \quad (17)$$

Figure 10 shows the voltage dependence of the fraction of current activated for  $G_{Kf1}$  and  $G_{Kf2}$ , and the time constant ( $\tau$ ) generated by equations (10, 11) and (12,13), respectively.

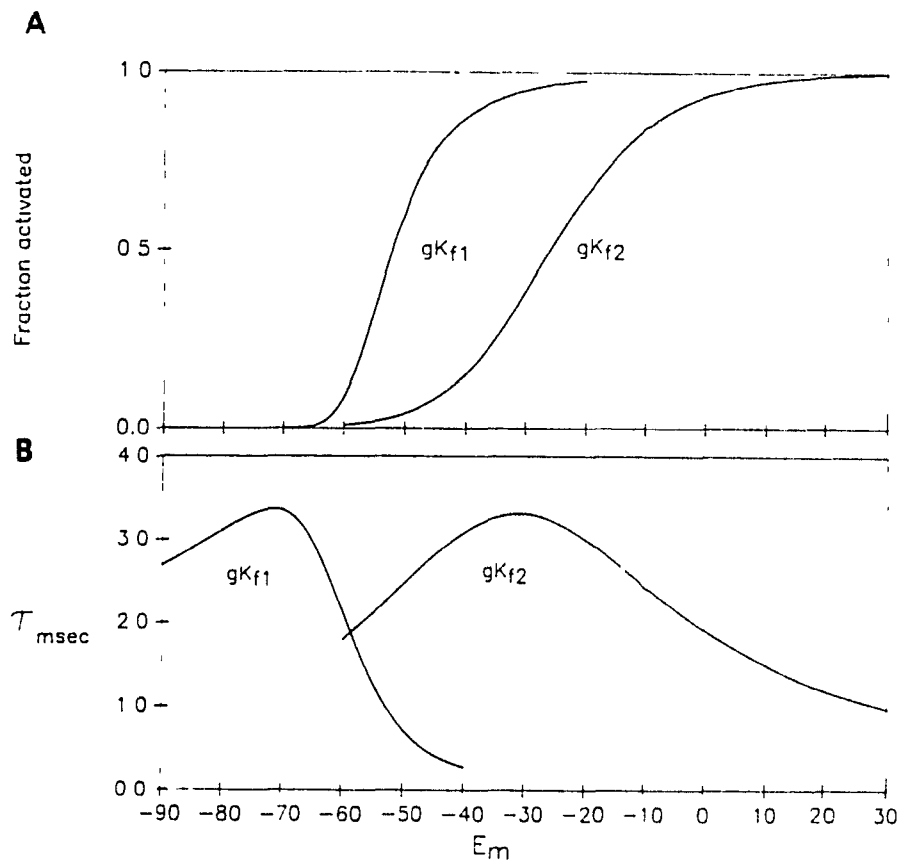


**FIGURE 4.10** Voltage dependence of fast potassium currents used in the computer model. The equations of Frankenhaeuser & Huxley (1964) and Dodge (1963) were empirically fitted to approximate the voltage dependence of the fast conductances reported by Dubois (1981; **A**) Using the equations:  $g_{Kf1} = n^4 G_{Kf1}$ ;  $g_{Kf2} = n^2 G_{Kf2}$ , the voltage dependence of the two fast conductances are plotted. **B**) Plot of the activation time constants for the two fast potassium currents.

### Constants

The magnitude of the sodium conductance used in the model was within the physiological range. The magnitude of the potassium conductance was chosen to be a median value in the range that either did not attenuate action potential



generation (at values less than 150 nS) when  $G_{Kf1}$  was removed, or that did not allow action potential generation at all (at values greater than 300 nS) .

Sodium:

$$Na_i = 16.74 \text{ mM} \quad Na_o = 110 \text{ mM}$$

$$P_{Na} = 3.9 \times 10^{-6} \text{ cm}^3 \text{ s}^{-1}$$

Potassium:

$$G_{Ktotal} = 225 \text{ nS} \quad E_{rev} = -90 \text{ mV}$$

Relative proportion of  $G_{Ktotal}$  for conductances  $G_{Kf1}$ ,  $G_{Kf2}$ ,  $G_{Ks}$ :

A) sensory axon: 28%: 53%: 19% (63:119:43 nS)

B) motor axon: 50%: 32%: 18% (112:72:41 nS)

Leak and Capacitance:

$$G_{leak} = 20 \text{ nS} \quad E_{rev} = -75 \text{ mV}$$

$$\text{Capacitance} = 2 \times 10^{-3} \text{ nF}$$

*Conditions for repetitive activity.*

The voltage dependence of  $h$  used in Dodge (1963) and Frankenhaeuser and Huxley (1964) does not generate continued spiking, in response to a continued stimulus. Therefore, the voltage dependence was altered so that the  $h$  gate reopened sufficiently for repetitive activity to be generated in the absence of all potassium conductances. When all potassium conductances were added back to the computations in the relative proportions for both types of fibers, there was only one action potential produced. The value used ( $h \approx 0.9$  @ -80mV) is close to the value used to generate repetitive activity in the computer model of Bromm and Frankenhaeuser (1972).

In addition to adjustment of the  $h$  gate required to produce repetitive activity, the level of potassium reversal was set at -90 mV. This level provided the necessary driving force to repolarize the "membrane" to a level where the  $h$  gate opened sufficiently to allow further action potential development. Since  $G_{Ks}$  is activated at "resting" membrane potential, it hyperpolarizes the "fiber". Therefore, it was necessary for the leak conductance to be adjusted so that there was no change in membrane potential when there was no current stimulus. A similar manipulation was used in the Frankenhaeuser and Huxley (1964) model for a computed action potential.

**VOLTAGE DEPENDENT POTASSIUM CONDUCTANCES REGULATE  
ACTION POTENTIAL REPOLARIZATION AND EXCITABILITY IN FROG  
MYELINATED AXON**

by

M.O Poulter and A. L. Padjen

(Submitted to Pfluegers Archives)

### *ABSTRACT*

Intracellular microelectrode recording technique was used to examine the effects of the potassium channel blockers 4-aminopyridine (4-AP) and tetraethylammonium (TEA) on the function of large sensory (dorsal root) myelinated axons of frog. Application of the blocker was accomplished by diffusional leak of the blocking agents into the intracellular space of the axon from the recording electrode. A decrease in outward rectification was evident within 5 minutes after impalement of a fibre indicative of the blockade of the potassium conductances. This blockade reached a maximum within 1 hour post impalement. There was a concomitant increase in action potential duration and excitability. Action potential widening was attributed to the blockade of the conductance  $G_{Kf2}$  by 4-AP. The increase in excitability was manifested in two ways: 1) a decrease in accommodation in the presence of 4-AP and/or TEA for a maximum of 200 ms and 2) a decrease in spike frequency adaptation when both 4-AP/TEA were present. The latter effect was attributed to the blockade of the conductance,  $G_{Ks}$ , by TEA. A computer model, based on Hodgkin-Huxley formulation of the sodium channel and three voltage dependent potassium conductances, was used to examine our interpretation of the experimental results. Our experimental and computational results imply that there is still another as yet undefined mechanism responsible for attenuation of action potential generation in large myelinated axons.

*INTRODUCTION*

Frog myelinated axons have been shown to be endowed with at least 3 types of voltage dependent potassium channels; two fast activating and slowly inactivating conductances that differ in their voltage dependence ( $G_{Kf1}$ ,  $G_{Kf2}$ ; Dubois 1981) and a slowly activating and inactivating conductance termed  $G_{KS}$  (Dubois 1981). Previous results from this laboratory have demonstrated that potassium channel blockade using dendrotoxin, an irreversible blocker of the fast activating potassium conductance  $G_{Kf1}$  (Benoit and Dubois 1986), blocks accommodation of action potential generation in frog myelinated axon for the early phase of a continued stimulus step (Poulter et al. 1989). Therefore, it was of interest to extend these studies by examining the effects of the well known potassium channel blockers 4-aminopyridine (4-AP) and tetraethylammonium (TEA). Voltage clamp studies of the potassium conductances present in the nodal (Dubois 1981) and the internodal axon membranes (Grissmer 1986) have shown 4-AP to be a selective blocker of both fast conductances ( $G_{Kf1}$  and  $G_{Kf2}$ ), whereas TEA blocks both the fast and slow conductances. By taking advantage of this selective pharmacology of these voltage dependent potassium conductances it was hoped that we could elucidate the function of these conductances in relatively intact large myelinated axons. In our previous studies we had hypothesized that the decrease in frequency of action potential generation (adaptation) results from the activation of the slow conductance termed  $G_{KS}$  (Poulter et al. 1989). Our hypothesis predicts that in the presence of 4-AP, which reduces accommodation, adaptation should be evident (when the slow conductance is unaffected). However, in the presence of both 4-AP and TEA adaptation would be reduced or abolished. A computer model which

includes these three voltage dependent potassium conductances was used to test and evaluate our conclusions. Preliminary results have been reported in Poulter and Padjen (1988b).

*METHODS*

The preparation used for these experiments was the hemisected frog spinal cord with dorsal spinal roots attached and perfused with normal frog Ringer solution at a constant 14°C to 17° C (Padjen and Hashiguchi 1983). Normal frog Ringer contained in mM: NaCl, 115; KCl, 2;  $\text{CaCl}_2$ , 2; HEPES buffer (pH adjusted to 7.35), 10; dextrose, 11. Intracellular recordings were obtained from large myelinated dorsal root fibres (conduction velocity > 15m/s) impaled at the dorsal root entry zone.

In normal Ringer solution extracellular application of 4-AP and/or TEA produced convulsive discharges due to enhanced synaptic transmission, making interpretation of the data impossible. Therefore, application of the two blockers (5-50 mM 4-AP; 10-20 mM TEA) was accomplished by adding them to the 3M KCl recording electrode solution allowing for passive diffusion into the intracellular space. Under these conditions, diffusional leak was believed to be the primary mechanism by which the blocking agent(s) entered the intracellular space. Assuming the tip of the electrode pipette to be conical, the following equation was used to calculate the rate of leak ( $q_D$ ) of the blocking agent(s) from the microelectrode (Purves 1981).

$$q_D = \pi D C_0 \Theta a$$

where:  $D$  = diffusion coefficient ( $1 \mu\text{m}^2 \text{ms}^{-1}$ )

$C_0$  = concentration of the drug in the microelectrode

$\Theta$  = the angle of the apex of the cone ( $4^\circ$ )

$a$  = the radius of the microelectrode opening ( $0.2 \mu\text{m}$ )

For example, an electrode containing 10 mM 4-AP and 20 mM TEA would achieve a concentration, after 10 min of impalement, of 1mM 4-AP and 2 mM TEA (assuming an intracellular volume of  $6.06 \times 10^{-15}$  liters).

Axons were considered suitable for experiments only when the membrane potential was stable, more negative than -70 mV and the action potential amplitude was greater than 85 mV. Records were stored on videotape in a digitized form, after filtering by a low pass 8 pole Bessel filter (set at 10 KHz) and A/D conversion rate (22 KHz, 16 bit resolution) using a PCM (Benzanilla 1985). For further off line computer analysis a Modular Instruments Inc. A/D interface and 286 microprocessor based microcomputer was used (A/D conversion rate 20 KHz; 14 bit resolution).

### *Computer Model*

The computational model used in this paper has been previously described in detail in Poulter et al. (1989) and only a brief description will be provided here. The approximations of Hodgkin and Huxley gating equations used in Dodge (1963) were altered to reflect the activation of  $G_{Kf1}$  and  $G_{Kf2}$  reported in Dubois (1981). The gating equations for  $G_{KS}$  were taken from Dubois (1981). The model calculates membrane potential under current clamp conditions in response to current steps of varying length.



## RESULTS

Impalement of a dorsal root axon with a microelectrode containing 5-50 mM 4-AP and/or 20 mM TEA decreased the outward rectification above resting membrane potential. A reduction in outward rectification was usually evident within 5 min of impalement, but a maximum decrease in outward rectification was usually observed only after 45 minutes to 1 hour post impalement (*FIGURE 5.1*). The shape of the V/I relationship obtained by injection of depolarizing current pulses is distinctly nonlinear and it is not possible to measure a slope resistance (Padjen and Hashiguchi, 1983; Poulter et al. 1989). Therefore, we have calculated cord resistances (in  $M\Omega$ ) from the minimum current required to evoke a maximum depolarization. Typically the resistance of the fibre increased by 8-10 fold (upon impalement  $6.4 \pm 2.0 M\Omega$ ; at time of withdrawal or loss, 30 min-1.5 hours later,  $49.3 \pm 10.6 M\Omega$ ).

The reduction in the outward rectification was also accompanied by an increase in the action potential duration and a decrease in the rate of repolarization, as measured by  $dV/dt$  (*FIGURE 5.2*). There was no difference in the rate of repolarization in fibres impaled with a 4-AP or a 4-AP/TEA containing microelectrode. This implies that blockade of  $G_{Ks}$  has no effect on action potential repolarization. Since blockade of  $G_{Kf1}$  with the specific blocker dendrotoxin (DTX; Benoit and Dubois 1986), has little effect on action potential repolarization (Poulter et al. 1989), this suggests that the conductance  $G_{Kf2}$  (also blocked by 4-AP) is responsible for action potential repolarization in dorsal root myelinated axon.

Intracellular injection of depolarizing current steps of 100-200 ms in duration were used to test the excitability of the axons. Upon impalement, fibres responded to current pulses by producing only one action potential. Multiple spiking could not be induced by increasing the stimulus up to 10 times the rheobase current. This type of response (not shown but similar in appearance to panel on top left in *FIGURE 5.3 A*) is typical of the excitability of a fibre impaled with an electrode containing no potassium channel blocker (Poulter et al. 1989). Approximately 10-15 minutes after impalement with either a 4-AP or 4-AP/TEA containing microelectrode the axons responded to increased current intensity by generating more action potentials, demonstrating a reduced ability to accommodate to the stimulus. Comparing the effects of these two microelectrode types, it was apparent that the 4-AP/TEA containing microelectrodes had a greater effect on accommodation than the microelectrodes containing 4-AP only. *FIGURE 5.3* shows the effect of 4-AP approximately 30 minutes post impalement; a maximum of 4 action potentials were produced and spiking was attenuated after approximately 50 ms. In fact, there was an attenuation of spiking, despite recovery of the action potential height in this particular fibre (panel bottom left). This suggests that, despite the sodium conductance becoming less inactivated some other process or processes are involved in accommodation. Results in *FIGURE 5.3B* were similar to those in *FIGURE 5.3A*, except that there are more spikes produced when both TEA and 4-AP were present in the microelectrode. Therefore, TEA decreased even further the ability of the fibres to accommodate to a stimulus.

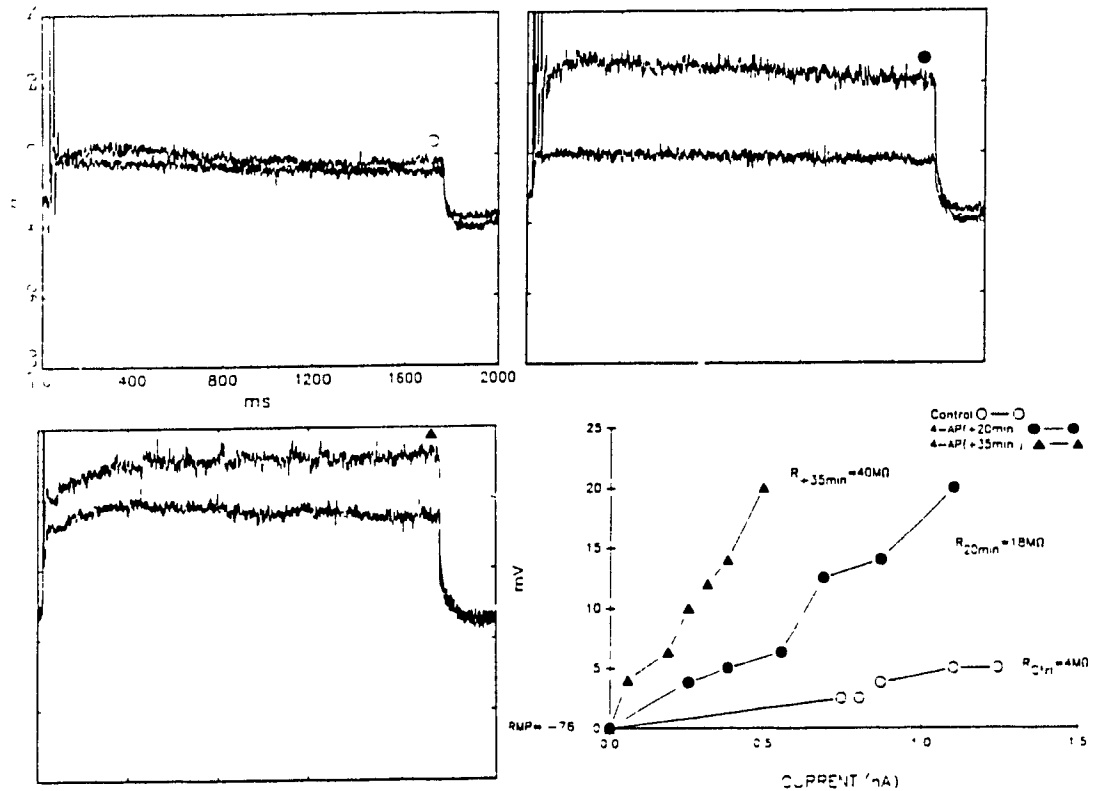


**FIGURE 5.1** Intracellular application of 4-AP blocks outward rectification. Samples of voltage responses from current clamp steps (1600 ms duration). Control response (top left; open circles) within 5 minutes of impalement of axon with electrode containing 10mM 4-AP. Voltage responses after 20 minutes of impalement (top right; filled circles) and 35 minutes (bottom left; filled triangles) demonstrate a progressive decrease in the outward rectification with time impaled. Lower right illustrates the V/I relationship obtained from a number of depolarizing steps. (Resistance values indicate cord resistances; equivalent current pulses are used in all panels).

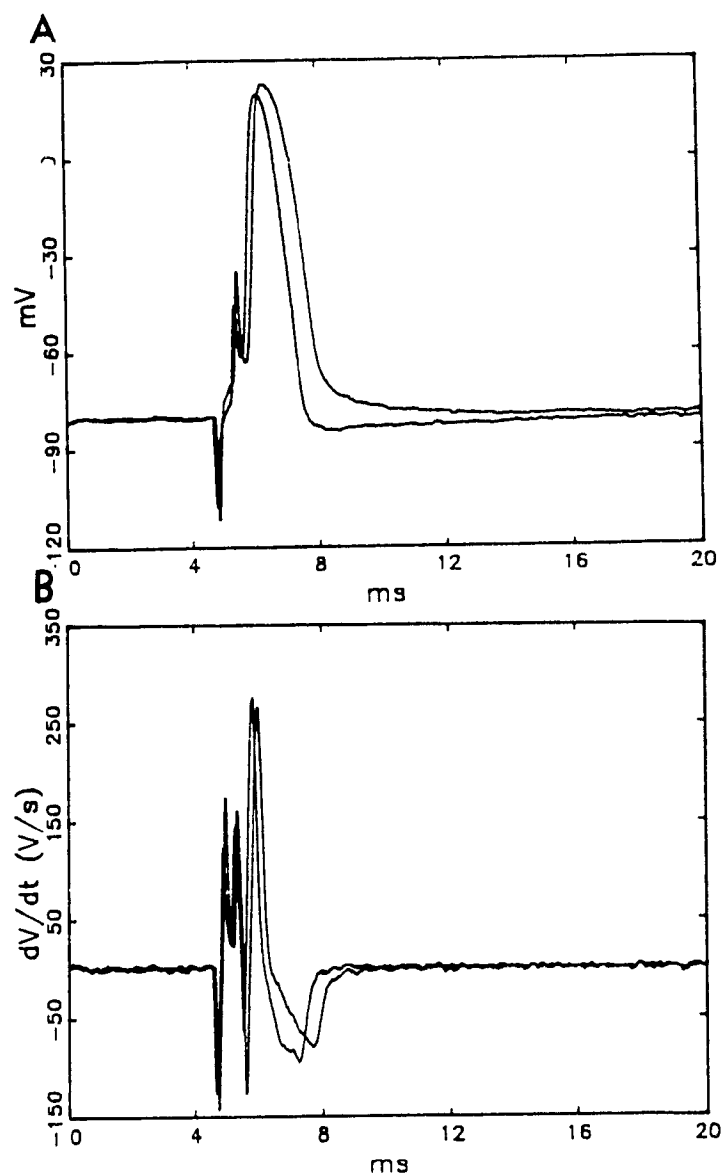


**FIGURE 5.2** Effect of 4-AP/TEA on action potential repolarization. **A** Generation of a single action potential by a short (0.5 ms) intracellular injection of depolarizing current produces a single action potential, which became wider within  $\approx 10$  min post impalement. The small fast AHP is abolished and an ADP of variable duration was observed **B** Computational differentiation of the action potential before and after an increase in resistance revealed a slowing of action potential repolarization; no significant effect was seen on the upstroke  $dV/dt$ .

Spike frequency adaptation could be assessed by plotting the interspike frequency (where  $1/\text{spike interval in ms}$  equals instantaneous spike frequency in Hertz) versus the spike interval number. In fibres impaled with microelectrodes containing 4-AP there was a decline in the frequency with each successive spike interval (*FIGURE 5.4 top*). However, in fibres impaled with 4-AP/TEA containing electrodes, this relationship was less steep. Nevertheless, spike generation stopped approximately 100 ms later (*FIGURE 5.3B*). Since the only difference between these two treatments is that the 4-AP/TEA microelectrode blocks  $G_{KS}$ , this result supports the hypothesis that  $G_{KS}$ , at least partially, regulates adaptation.

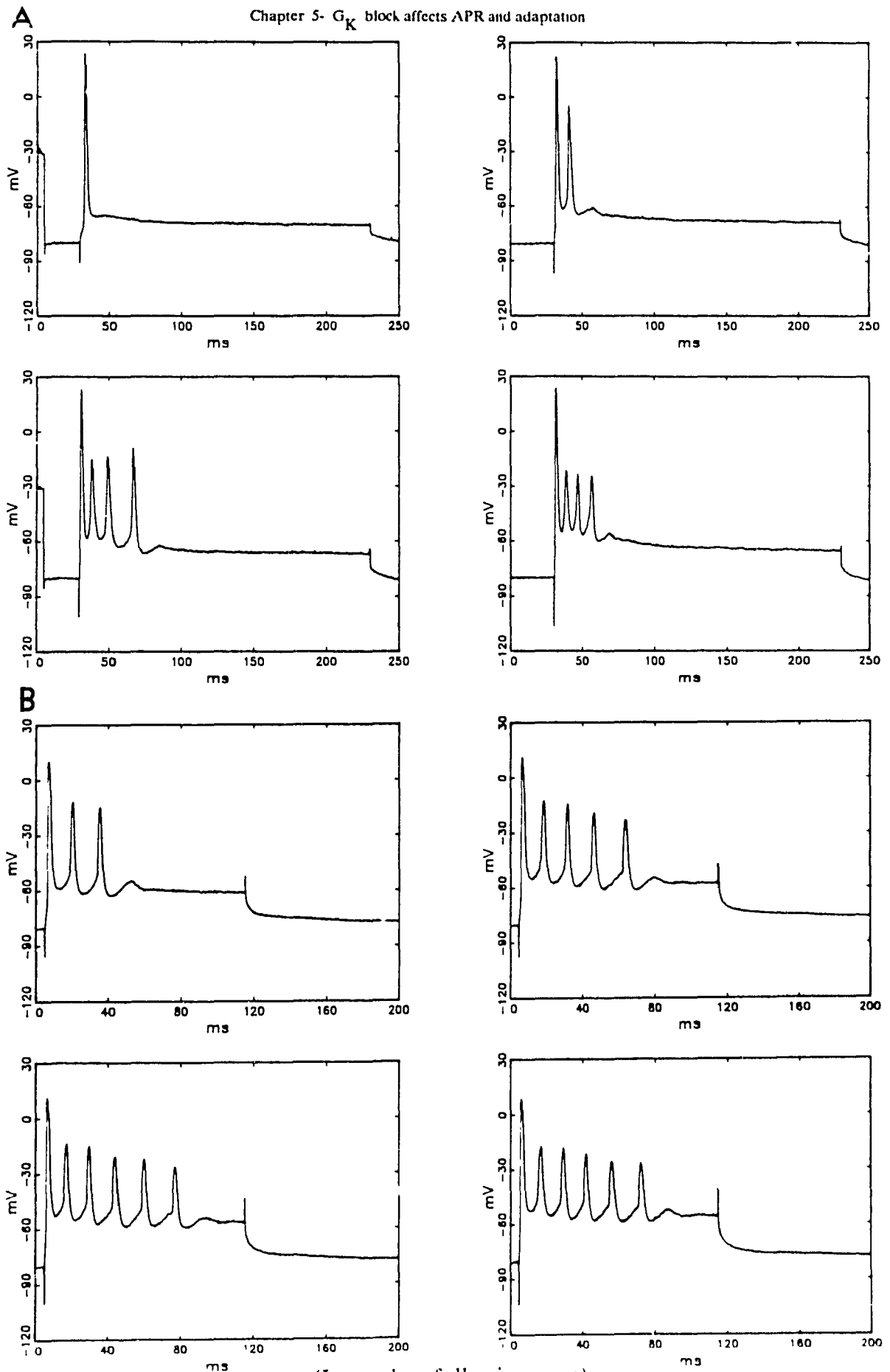


**FIGURE 5.3** Effect of 4-AP and TEA on action potential generation. **A** Response (top right) approximately 10 min after impalement at threshold. Increasing the current strength increased the number of spikes generated (left to right top to bottom). Bottom right shows a good example of the spike frequency adaptation within the current pulse. In addition, there is an apparent recovery of action potential amplitude implying that sodium channel inactivation is decreasing. **B** An equivalent set of current pulses was used to test the accommodating properties of an axon fibre impaled with an electrode containing 20mM TEA and 10 mM 4-AP. Electrodes containing 4-AP/TEA produced more spikes for a longer period of time than observed above with 4-AP alone.

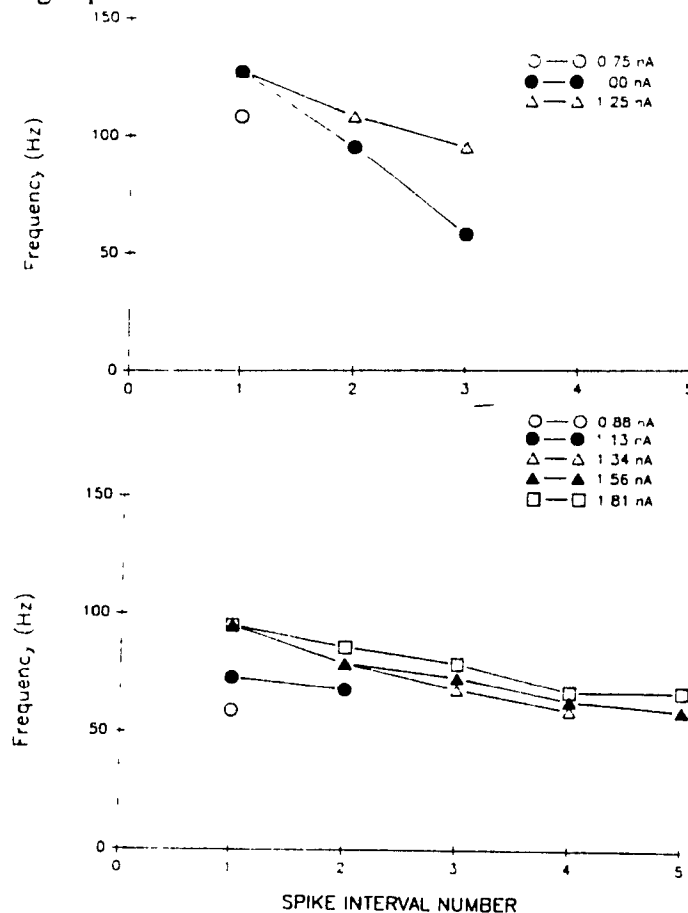


**FIGURE 5.4** Effects of 4-AP and 4-AP/TEA on adaptation. The interspike frequency versus the spike interval number illustrates the progressive decrease in the frequency of action potential generation. The rate of decrease in the frequency was greater in 4-AP treated fibres (top) than for 4-AP/TEA fibres (bottom).

### Computer Modeling

A computer model, which calculates the voltage of the nodal membrane in response to a current step was used to test our interpretation of the experimental results. Removal of the fast conductances from the model (equivalent to the action of 4-AP) demonstrates accommodation to the stimulus, as well as, spike frequency adaptation (*FIGURE 3.5A* top left). It is also evident that action potential generation is attenuated, despite the reduction in sodium conductance inactivation ( $h$ -gate opening) within the stimulus pulse. The spike recovery in *FIGURE 5.5* (top left) is similar to that observed in *FIGURE 5.3A* (bottom left). A reduction of  $G_{KS}$  to 25% of that in "control" reduces spike frequency adaptation (*FIGURE 5.5*, top right); setting the conductance equal to zero completely blocked both accommodation and adaptation (bottom left). A plot of the interspike frequency versus spike interval illustrates the reduction in adaptation as the amount of  $G_{KS}$  is reduced (*FIGURE 5.5*, bottom right). Thus, the model supports our interpretation of the experimental data, as far as the effects of 4-AP are concerned. However, the effects of TEA could not be accounted for by the computational model, since abolition of  $G_{KS}$  resulted in continuous firing. This behaviour of the computational model was independent of any alteration in the sodium channel parameters. Repetitive firing was all or none depending on the voltage dependence and time constant of the  $h$ -gate (cf. Valbo 1964). Since our model did not fully account for the observed pharmacology, it suggests that there must be some other mechanism(s) or factor, in addition to the voltage dependent potassium conductance, which modulate excitability in myelinated axons.



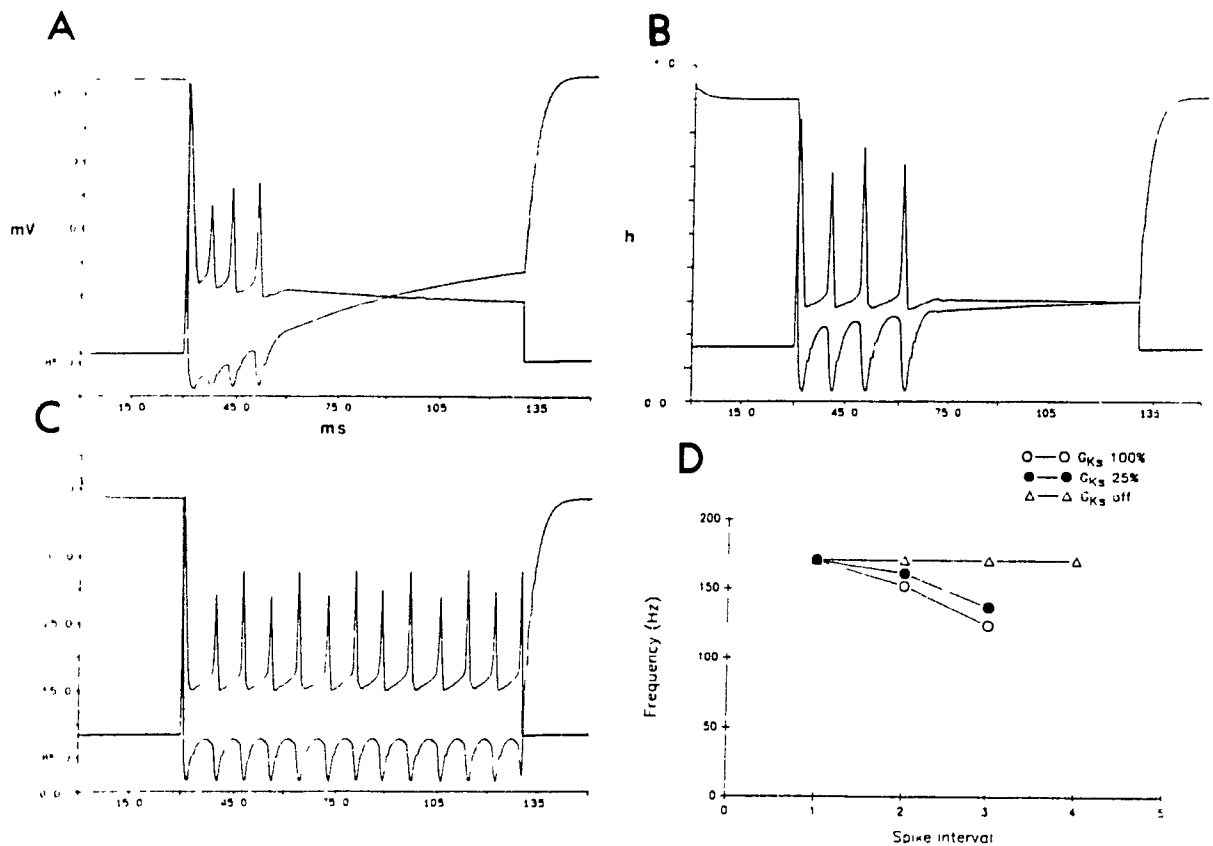


**FIGURE 5.5** Computer simulation of 4-AP and TEA pharmacology. Plots show computed action potentials and  $h$ -gate parameter (Y axis scale for action potentials **A** and  $h$ -gate parameter **B** is for all computer simulations). Panel **A** shows the effect of setting the conductances,  $G_{Kf1}$  and  $G_{Kf2}$ , equal to zero, simulating the action of 4-AP. **B** Setting  $G_{K_S}$  to 25% of its original value reduced spike frequency adaptation. **C** Setting  $G_{K_S}$  equal to zero resulted in continuous action potential generation with no spike frequency adaptation. (Alternating action potential height is due to computer sampling artifact). **D** Graph of frequency versus spike interval number shows a decrease in spike frequency which is dependent on the presence of  $G_{K_S}$  in the model.

*DISCUSSION*

In this study we have shown that intracellular application of 4-AP results in a slowing of action potential repolarization and a reduction in accommodation. A slowing in action potential repolarization is likely due to the blockade of the conductance  $G_{Kf2}$ , since blockade of  $G_{Kf1}$  alone did not lead to a substantial prolongation of a single action potential (Poulter et al., 1989). The reduction in accommodation is the result of the reduction in the outward rectification seen when the voltage dependent conductances  $G_{Kf1}$  and  $G_{Kf2}$  and  $G_{Ks}$  were blocked. The addition of TEA, which also blocks the conductance  $G_{Ks}$ , reduced accommodation further and attenuated spike frequency adaptation. Our interpretations of these results is based on the differences in specificity of these agents for the potassium channels, shown to exist in both the nodal and internodal regions of these axons (Dubois, 1981; Grissmer, 1986). All these effects were achieved by allowing the passive diffusion of these potassium channel blockers from the recording microelectrode. An estimate of the concentration achieved within the first 10-20 minutes of impalement indicates that the concentrations reached are large enough to significantly block these conductances (see Methods; Hille 1967; Dubois 1981; Grissmer 1986).

The identification of a voltage dependent potassium conductance, which plays a significant role in action potential repolarization in large myelinated axon disagrees with the commonly held belief that the resting "leak" conductance is primarily responsible for action potential repolarization (Schmidt and Stämpfli 1964; Hille 1984). Although it may be true that  $G_{Kf2}$  is important for action potential repolarization in the dorsal root fibres it may not be quite so important in ventral root fibres, since action potential widening was seen when

only  $G_{Kf1}$  was blocked (Poulter et al. 1989). This difference in responsibilities is more likely a function of the difference in their relative magnitudes, since  $G_{Kf1}$  represents a larger proportion of the total potassium conductance in ventral root axons, whereas  $G_{Kf2}$  is greater in dorsal root (Dubois 1981).

The most obvious effect of a blockade of these potassium conductances was the increase in excitability. This effect was quite striking, as one of the distinguishing characteristics of dorsal root fibres is the inability of prolonged supra-threshold intracellular current pulses to generate more than one action potential (Poulter et al. 1989). The reduction in the outward rectification and the concomitant increase in excitability demonstrates an important functional role of potassium conductances in regulating accommodation. However, it appears that this reduction may not be the only determinant in regulating accommodation, since spiking could only be maintained for a maximum of 100-200 ms. This observation indicates that some other mechanism(s) or factor causes the axon to accommodate to the stimulus. A number of possibilities exist which may account for the late phase of accommodation such as: 1) repeated action potentials remove the potassium channel block; 2) slow ( $\tau > 100$  ms), second order sodium channel inactivation or 3) the activation of a sodium dependent potassium conductance (Poulter and Padjen 1989).

1) The block by 4-AP has been shown to be voltage dependent. It is reduced by depolarization (Arhem and Johansson 1989; Hermann and Gorman 1981; Meeves and Pichon 1977; Ulbricht and Wagner 1976), and so it is possible that a train of action potentials could relieve the 4-AP block. A number of reasons argue against any significant voltage dependent unblocking in our experiments.

The first is that very large voltage clamp steps ( $> 100$  mV) are required to produce significant relief of block (Hermann and Gorman 1981). In our studies these voltages are reached only transiently, and the rate of unblock at these potentials ( $\approx 200$  ms; Ulbricht and Wagner 1976) is too slow to assume a significant relief of block. In addition, despite some removal of blockade Ulbricht and Wagner (1976) showed that, with 4-AP of  $\approx 1$  mM, substantial block still remained 100 ms after the start of the voltage step. However, it was recently reported that there may be an additional short time constant of unblock (Arhem and Johansson 1989), though this was observed only at concentrations of 4-AP of less than  $50 \mu\text{M}$ . The same study also indicates that the channel must first open in order for 4-AP to block, and subsequent unblocking occurs only if the depolarization is maintained. This observation is contrary to most reports of the action of 4-AP, which indicate, unlike TEA, that 4-AP likely blocks closed channels (in fact, the voltage dependence of unblock itself implies that closed channels are preferentially blocked). In contrast to the above studies, Dubois (1981) showed that for the range of membrane potentials, in which the two 4-AP sensitive currents normally operate ( $-80$  to  $30$  mV), the blocking effect of  $1$  mM 4-AP was voltage independent. Indeed, this fact was used to demonstrate and characterize the slow potassium current. Despite these arguments, if one were to assume that unblocking was significant and this phenomenon attenuated action potential generation, the behaviour of the axon would likely be quite different. After attenuation of action potential generation one would expect that block would again be reestablished; accommodation would be reduced and action potentials would be generated. This effect would likely manifest itself as some sort of bursting behaviour, which was never observed. Therefore, voltage dependent unblocking of the 4-AP sensitive currents is not thought to be a mechanism by which action potential generation was

attenuated. Finally, incomplete non voltage dependent block of  $G_{Kf1}$ ,  $G_{Kf2}$  or  $G_{KS}$  is not likely a factor since attenuation of spiking occurs long after the full activation of any residual current.

2) The possibility of a slow, second order inactivation of the sodium current has been suggested by Krylov (1984) to account for accommodation and spike frequency adaptation. A diminution of action potential amplitude, as seen in Fig. 3 B, is predicted by this mechanism and therefore, this may be a factor, which can lead to action potential accommodation. However, sodium channel inactivation with two time constants also predicts substantial adaptation, which is contrary to the experimental results. Further examination of this possibility could not be explored in our experiments.

3) Sodium dependent potassium conductances ( $G_{K(Na)}$ ) have recently been demonstrated in a number of different neurones (Bader et al. 1985; Dryer et al. 1989; Poulter and Padjen 1989, chapter 6; Schwirtdt et al. 1989). Furthermore, this conductance has been shown to modulate the excitability of cat neocortical neurones (Schwirtdt et al. 1989). Therefore, it is possible that activation of this conductance may be responsible for late accommodation. This possibility is difficult to assess in the absence of a specific blocker of  $G_{K(Na)}$ . Unfortunately, alteration of the conductance by changes in ionic composition of the perfusing media also alters the development of the sodium action potential and therefore obscures evaluation of the importance of the  $G_{K(Na)}$  in the regulation of repetitive firing (Poulter and Padjen 1989).

In agreement with previous studies (Baker et al. 1987; Kocsis et al. 1987;

Poulter et al. 1989), these results indicate that pharmacologically distinct potassium channels regulate a number of distinct properties in myelinated axons. Specifically, the voltage dependent fast conductance,  $G_{Kf}$ , was found to be responsible for action potential repolarization and the conductance  $G_{Ks}$  was important for the slowing of action potential generation during a prolonged stimulus. We have reported earlier (Poulter et al. 1989) that in the absence of potassium channel blockade the axon responds to depolarizing current steps by generating only one action potential. This is most likely due to the inability of high resistance electrodes required for these studies to pass sufficient current to generate multiple action potentials. Studies using extracellular stimulation (Bromm and Rahn 1969; Katz 1936), as well as, physiological stimuli (Catton 1976) have shown that dorsal root fibres are capable of sustained firing. Therefore,  $G_{Ks}$  may play a role in regulating firing when sufficient stimulus is applied.

**EVIDENCE FOR A SODIUM DEPENDENT POTASSIUM CONDUCTANCE  
IN FROG MYELINATED AXON.**

by

M.O. Poulter and A.L. Padjen

(Submitted to Pflügers Archives)

## *ABSTRACT*

After blockade of the voltage dependent potassium conductances, intracellular depolarizing constant current steps in frog myelinated axon generate trains of action potentials, lasting a maximum of 100 - 200 ms. Under these conditions a hyperpolarizing afterpotential (AHP) appeared. The purpose of this study was to investigate the properties of this AHP. It was found that the AHP was dependent on: 1) the number of sodium dependent action potentials generated either by a prolonged current step or by a train of short current pulses; 2) action potential broadening and 3) the level of depolarization during a current step. Application of tetrodotoxin prevented the activation of the AHP by any of the above stimuli. The AHP was unaffected by 1) 8-acetyl-strophanthidin, an agent which poisons the electrogenic pumping in the axon; 2) blocking calcium influx with 10 mM magnesium or 2 mM manganese; 3) EGTA in the recording microelectrode which buffers intracellular calcium. The AHP was shown to reverse at  $\approx -92.3$  mV. Increasing the external potassium concentration from 2 to 10 mM shifted the reversal potential +14.5 mV indicating that the AHP is potassium mediated conductance. Reducing the internal sodium concentration or replacing the external sodium concentration with lithium ion substantially reduced and/or abolished the AHP. These results are consistent with the presence a sodium activated potassium conductance in frog myelinated axons.



*INTRODUCTION*

Previous studies from this laboratory have shown that large myelinated frog dorsal or ventral root axons respond to depolarizing constant current steps by producing only one action potential. Furthermore, this ability to accommodate to a stimulus was shown to be primarily due to the activity of the three voltage dependent potassium conductances present in these fibres ( $G_{Kf1}$ ,  $G_{Kf2}$ , and  $G_{Ks}$  Dubois 1981; Poulter and Padjen 1988; Poulter et al. 1989; Chapter 5). After blockade of the voltage dependent potassium currents by DTX, 4-AP and/or TEA, trains of action potentials lasting a maximum of 100-200 ms were observed (Poulter and Padjen, 1988; Poulter et al., 1989; Chapter 5). Despite a substantial blockade (see Chapter 5; Hille 1967) of these conductances, trains never lasted longer than 200 ms indicating that some other phenomenon was responsible for this late accommodation. At the same time, it was noticed that following a test stimulus, in which a train of action potentials had been generated, there was an afterhyperpolarizing potential (AHP) lasting 150-350 ms. Therefore, the aim of this study was to establish the ionic dependence of this AHP and investigate what factors lead to its activation.

Previous voltage clamp studies have shown that the longest tail current for the voltage dependent potassium currents present in myelinated axon was in the range of 10-20 ms (Dubois 1981). Therefore, it seems unlikely that this AHP is due to the slow turning off of any residual conductance activated during the action potential train. Also, in the absence of evidence of there being calcium mediated conductances in these myelinated axons, it was considered very unlikely that the AHP is due to the activation of a calcium dependent potassium

conductance. Therefore, our investigation centered around testing the hypothesis that this AHP was the result of the activation of a sodium dependent potassium conductance, much like that reported in other tissues (Bader et al. 1985; Schwindt et al. 1989; Dryer et al. 1989).

## METHODS

The preparation used in this study was the isolated dorsal root fibre of the frog (*Rana pipiens*). The isolated 9<sup>th</sup> or 10<sup>th</sup> root was detached from the spinal cord at the dorsal root entry zone. The root with ganglia and a small length of sciatic attached was placed in a recording chamber (volume 200  $\mu$ l) and continuously perfused with normal frog Ringer solution (NR) consisting of (in mM): NaCl, 115; KCl, 2; CaCl<sub>2</sub>, 2; HEPES buffer (pH adjusted to 7.3), 10; dextrose, 11 at 15-18° C. Solutions, in which the sodium concentration was reduced, were replaced with choline chloride in order to maintain osmolarity. Lithium Ringer had the same ionic composition as normal ringer, except for the substitution of lithium chloride for sodium chloride.

Glass microelectrodes, filled with KCl (3 M) and 10 mM 4-AP and 20 mM TEA in order to block voltage dependent conductances in a single fibre had a D.C. resistance of 40 - 100 M $\Omega$ . An estimate of the amount of blocker which enters the fibre has been provided in Chapter 5. Electrodes were selected for their low noise and ability to pass up to 2 nA without rectification. Microelectrodes were connected to a fast amplifier made by Dagan Corp. An active bridge circuit allowed simultaneous current injection and recording through the same electrode ("current-clamp" technique). Results were analyzed from the chart record, oscilloscope traces and/or from the data digitized and stored on videotape using a PCM based A/D converter (conversion rate of 22 kHz at 16 bit resolution) after a low pass 8 pole Bessel filter set at either 5 or 10 kHz. Off line analysis was accomplished by A/D conversion of the video tape playback using a microcomputer based A/D converter (Modular Instruments Incorporated; 12 bit resolution).

## RESULTS

Since depolarizing current pulses do not normally generate multiple action potentials (Poulter et al. 1989), accommodation was reduced by addition of 4-AP and TEA to the recording microelectrode (Chapter 5), in order to facilitate action potential generation. Establishment of potassium conductance block is manifested by an increase in excitability. Increasing the current stimulus intensity results in the production of more action potentials within the current pulse. An increase in spike number was accompanied by an increasingly large afterhyperpolarizing potential (AHP, *FIGURE* 6.1 top). These AHPs were 200-400 ms in duration and, at resting membrane potentials in the range of -70 to -80 mV, were maximally 4-1 mV, respectively. Addition of TTX (0.25  $\mu$ M) to the perfusing solution resulted in the abolition of the action potentials and the disappearance of the AHP (*FIGURE* 6.1 bottom). The AHP could also be elicited by a high frequency train of action potentials generated by short depolarizing intracellular pulses. Dependence of the magnitude of the AHP on the number of action potentials is shown *FIGURE* 6.2. In a few recordings, when the impalement lasted  $\approx$  an hour and the potassium conductance blockade continued to increase, broadening of a single action potential ( $>5$  ms at half height) was sufficient to produce a significant AHP (*FIGURE* 6.3). In addition, if the outward rectification was substantially decreased (by blocking the potassium conductances) the axon could be depolarized to levels, where action potential trains ceased to be generated. The size of the AHP then became dependent on the membrane potential, to which the axon was depolarized. This phenomenon was also sensitive to TTX. An example of this action potential independent AHP and its sensitivity to TTX is shown in *FIGURE* 6.1 (compare the first

pulse at the top of figure to the first pulse on the bottom). Thus, the amplitude and the presence of the AHP is dependent on 1) the number of sodium dependent action potentials, 2) action potential broadening and/or 3) the level of depolarization during a current step.

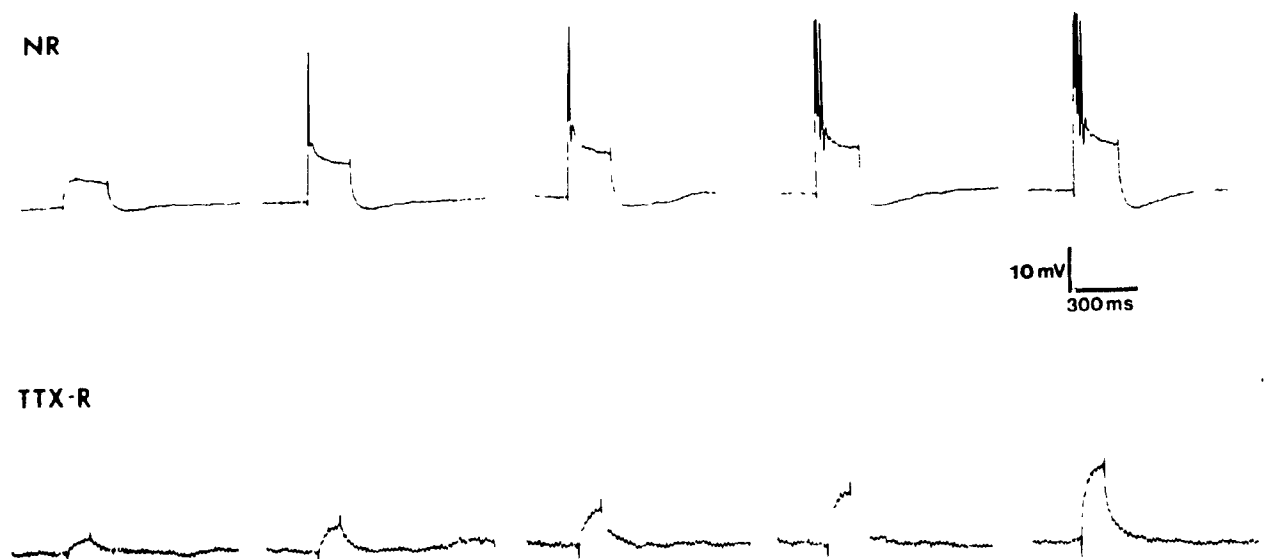


**FIGURE 6.1** Effect of action potential number and TTX blockade on AHP amplitude. Top. Increasing the intensity of a 200 ms current stimulus produced more action potentials and resulted in an increase in the AHP magnitude present after the pulse. Bottom. Blocking action potential generation by 0.25  $\mu$ M TTX was accompanied by abolishment of the AHP.

It has been recognized for some time that a prolonged train of action potentials in myelinated axons can elicit an AHP (Bergman et al. 1980; Barrett and

Barrett 1982; Ritchie 1970). This AHP is believed to result from the activation of an electrogenic pump by an increase in the internal sodium ion concentration. This electrogenic pumping in frog myelinated axons has been shown to be sensitive to a number of agents, which poison metabolic pumps (ouabain, and its analogues as well as lithium ions; Bergman et al. 1980). We used 8-acetylstrophanthidin (8-Ac-Stroph), a reversible analogue of ouabain, to examine its effect on AHP. As demonstrated in the (FIGURE 6.4), this agent had no effect on the AHP evoked by a current pulse, in which a few spikes had been generated. This implies that electrogenic pumping is not responsible for the AHP and by exclusion, it is likely mediated by a change in membrane conductance.

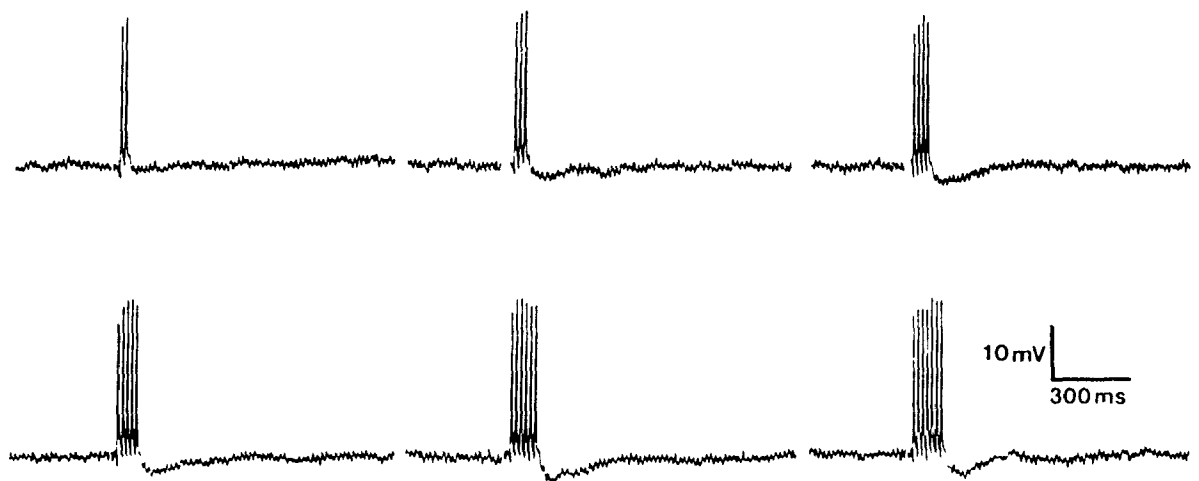


**FIGURE 6.2** Effect of increasing action potential number on AHP generation. Short intracellular stimuli at 70 Hz produce a transient AHP only after 3 action potentials are generated, which continues to increase with the number of action potentials generated. (action potentials truncated by strip chart recorder)

In order to establish voltage dependence and reversal potential of AHP, the

membrane potential of the axon was altered by injection of depolarizing and hyperpolarizing current, while superimposing 100 - 200 ms depolarizing current steps to generate spike trains and AHPs. Depolarizing the axon increased the AHP and sufficient hyperpolarization reversed the AHP. By plotting the amplitude of the AHP versus the membrane potential, the extrapolated reversal point was shown to be  $91.2 \pm 2.3$  mV ( $n = 5$  FIGURE 6.5 top), a value which closely corresponds to the equilibrium potential of potassium in myelinated axons. In agreement with this result, the reversal potential of the AHP could be shifted in the positive direction by increasing the external concentration of potassium to 10 mM ( $+14.5 \pm 1.5$  mV  $n = 3$ ; Fig. 5 bottom). These results indicate that the AHP is a potassium mediated conductance.

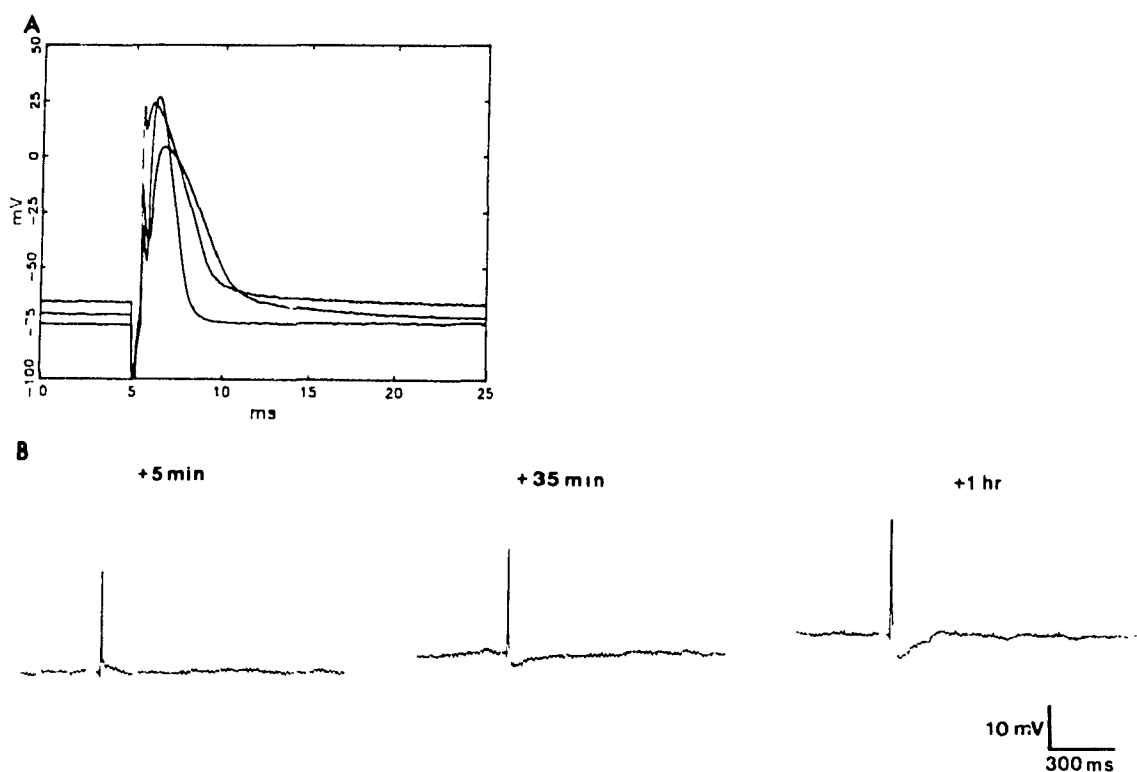


**FIGURE 6.3** Effect of action potential prolongation on the AHP. **A** Computer plot demonstrating the progressive widening of action potentials depicted in **B**. **B** Prolongation of the action potential duration was accompanied by the generation of an AHP. (Action potentials truncated by strip chart recorder)

It is well established that myelinated axons do not possess any voltage dependent calcium conductance (Stämpfli and Hille 1976) and therefore, it is not likely that this AHP is due to the activation of a calcium dependent potassium conductance ( $G_{K(Ca)}$ ) in the axon. Furthermore, it was not believed that the internal release of calcium triggered by action potentials was responsible, since electrodes containing 0.2M EGTA had no effect on the AHP (results depicted in *FIGURE 6.8* used these electrodes). However, it was remotely possible that the AHP resulted from the electrotonic spread of  $G_{K(Ca)}$  activated in the dorsal root ganglia or any residual terminal region left after excision of the dorsal root. Perfusion of a fibre with a Ringer solution containing 0.2 mM calcium and 10 mM Magnesium had no effect on the AHP (*FIGURE 6.6* top; + 10 min switch). Similar results were obtained using Ringer containing 2 mM Manganese. These results indicate that the AHP is independent of the influx or the internal release of calcium ions, which might activate a  $G_{K(Ca)}$  in the axon or elsewhere.

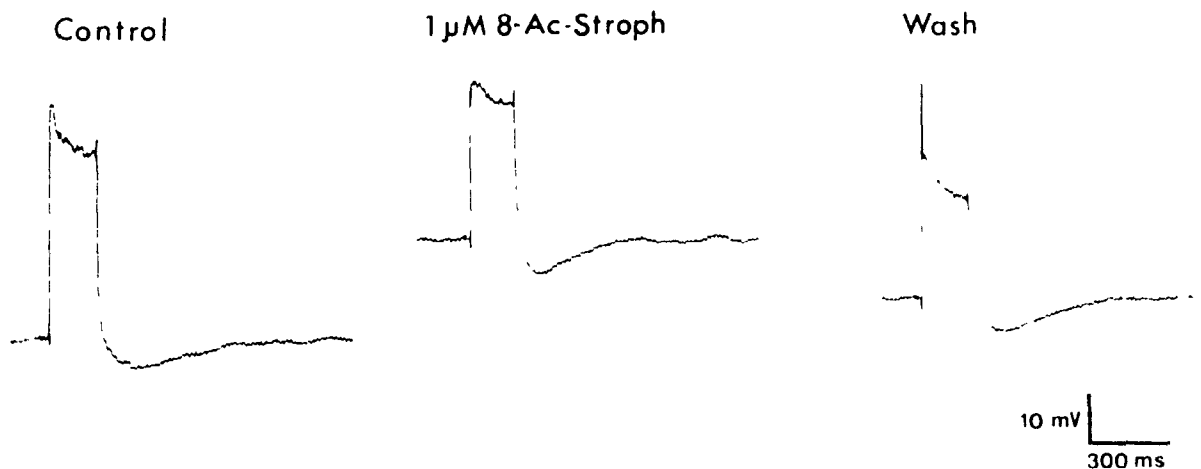


**FIGURE 6.4** Effect of 8-Acetyl-strophanthidin on the AHP. Application of an agent known to block the sodium electrogenic pump had no effect on the AHP. (Action potentials truncated by strip chart recorder)



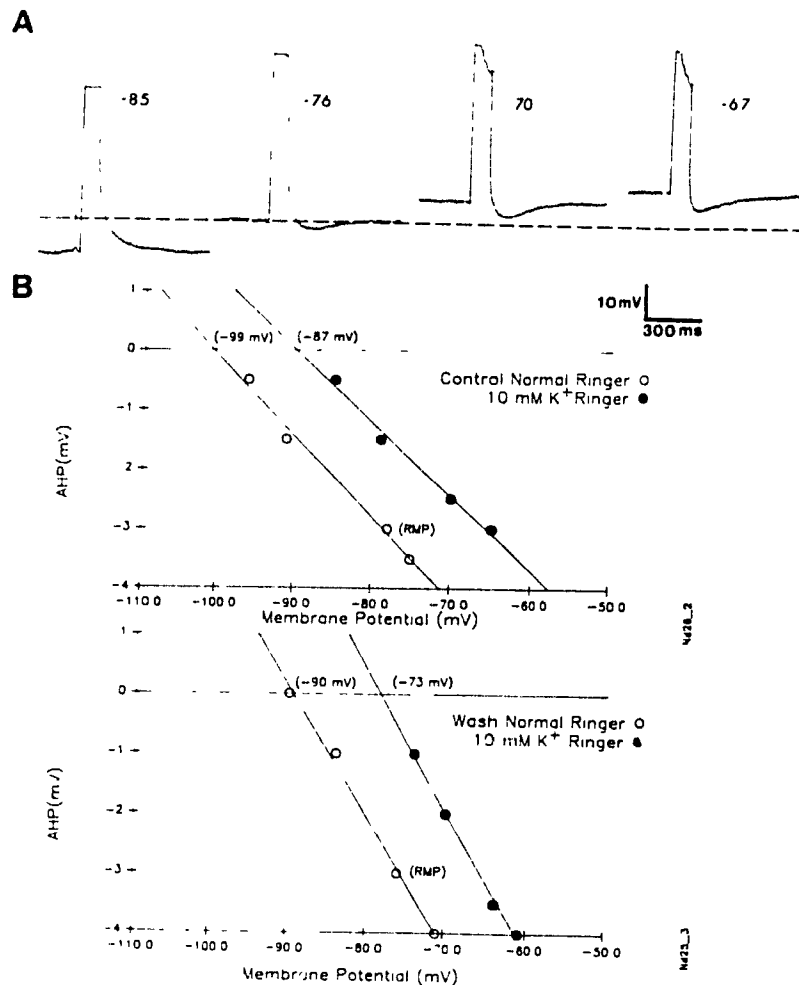


**FIGURE 6.5** Effect of an alteration in membrane potential and raising the external potassium concentration on the AHP. **A** Alteration of the membrane potential by constant current injection demonstrated that the AHP was increased when the fibre was depolarized and reversed when the fibre was hyperpolarized. (Action potentials truncated by strip chart recorder record) **B** Plots show that the extrapolated reversal point is shifted positive when the external potassium was increased to 10 mM. (Plots from different fibres than the one illustrated in A)

In light of reports of the presence of a sodium dependent potassium conductance ( $G_{K(Na)}$ ) in other sensory neurones (Bader et al. 1985) and in view of the results presented above, it seemed reasonable to hypothesize that this AHP was due to the activation of a  $G_{K(Na)}$ . This hypothesis would predict that the

AHP should be sensitive to the removal of extracellular sodium. By perfusing the preparation with a Ringer solution, where one half the sodium concentration was replaced with choline, it was possible to demonstrate that the AHP could be substantially reduced (*FIGURE 6.7*). The reversal potential of the AHP, monitored throughout the time of sodium replacement, was not changed. Therefore this reduction in the AHP was not due to an efflux of potassium following a reduction in extracellular sodium, like that reported by Schwindt et al. (1988) for cortical neurones.

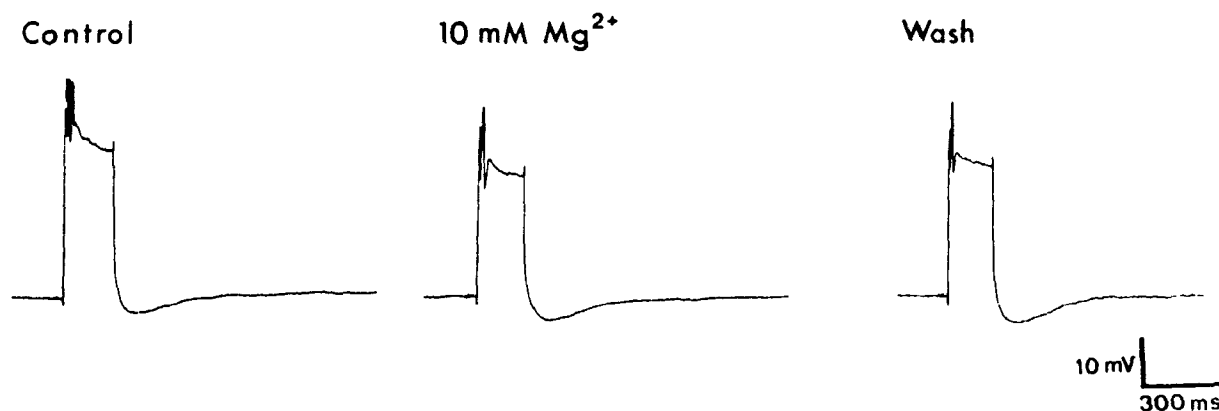


**FIGURE 6.6** Effect of calcium channel blockers on AHP. Perfusion with a Ringer solution containing 0.2 mM calcium and 10 mM Magnesium had no effect on the AHP. Similar results were obtained using Ringer containing 2 mM Manganese. (Action potentials truncated by strip chart recorder)

The  $G_K$  involved in the AHP generation could be a slow voltage dependent conductance activated by action potential(s), but not directly dependent on sodium ions. In order to rule out this possibility lithium ions were used as a replacement for sodium ions in the perfusing media. Sodium channel permeability to lithium ions is 93% percent of sodium (Hille 1984). As shown in *FIGURE 6.8*, replacing the sodium with lithium ions abolished the AHP despite fully

developed action potentials in the pulse (not visible in this chart record). This experiment also demonstrates that this conductance is not activated by lithium entry into the fibre, in agreement with results of Dryer et al. (1989).

This protocol also tested another possibility. Since the potassium channel blockers are being applied intracellularly their concentration fades with distance from the site of microelectrode insertion. Therefore, the AHP may be the result of electrotonic spread of a signal from a site where the voltage dependent potassium conductances are incompletely blocked. If this were true, one would predict that the AHP would be dependent only on the presence of conducting action potential(s) independent of the carrier ion. Since lithium mediated action potentials were unable to activate an AHP this mechanism is also ruled out.

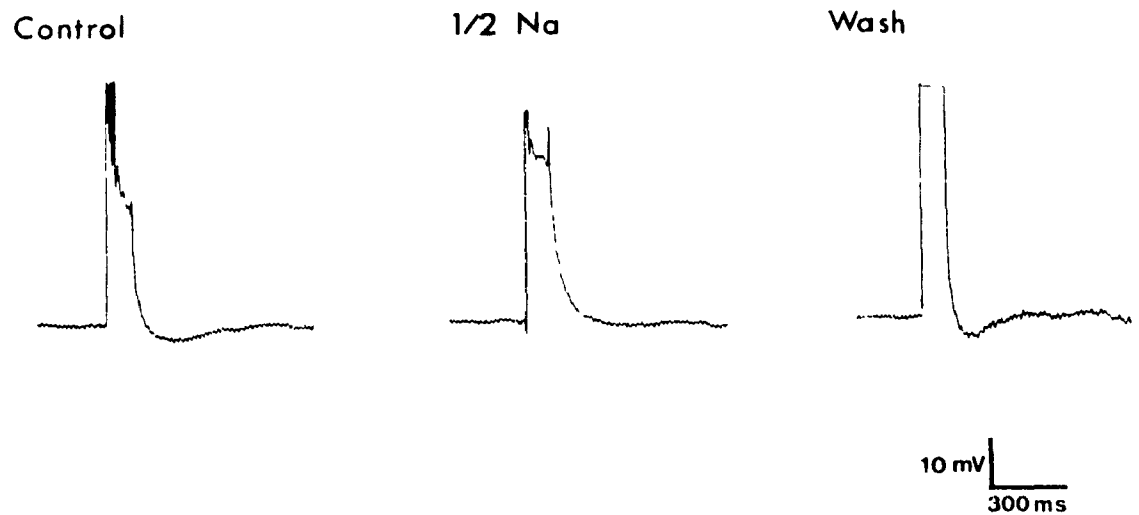


**FIGURE 6.7** Effect of reducing the sodium ion concentration in the external media on the AHP. Perfusion of a fibre with a Ringer solution with one half the sodium concentration replaced with choline resulted in a substantial reduction of the AHP. (Action potentials truncated by strip chart recorder)

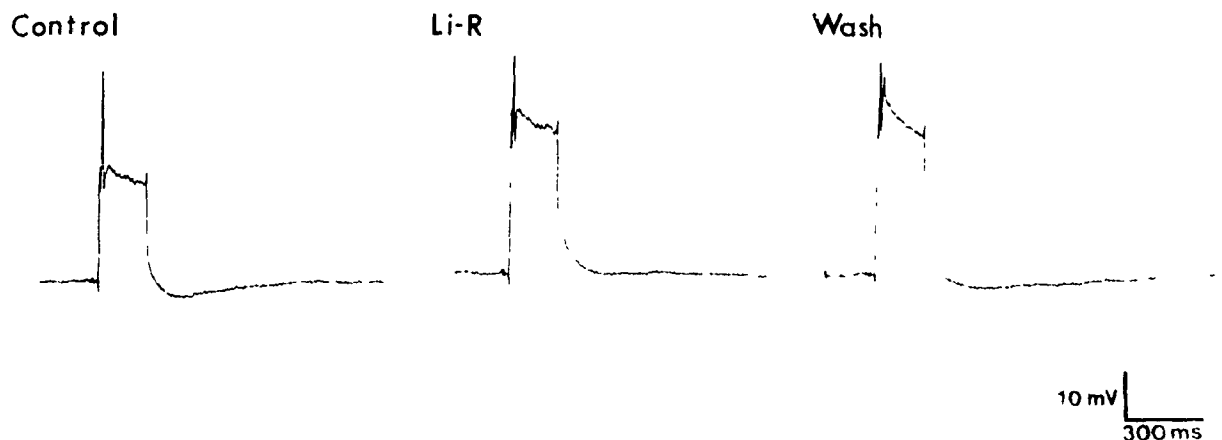


**FIGURE 6.8** Effect of lithium ion on the AHP. Replacing the sodium with lithium ion abolished the AHP indicating that, despite full development of spikes in the pulse, the AHP is dependent on the presence of sodium in the external medium. (Action potentials truncated by strip chart recorder)

## *DISCUSSION*

The results presented in this study are consistent with the presence of a sodium activated potassium conductance in frog myelinated axons. This conductance is activated by a number of action potentials, action potential prolongation or a substantial decrease in outward rectification; conditions which presumably promote an accumulation of sodium in the axon.

One of the more perplexing problems in rationalizing the existence and the activation mechanism of this conductance is the apparent contradiction between an insignificant increase in the total intracellular sodium ion concentration produced by action potential generation (Dryer et al. 1989; Hille 1984) and reports that millimolar concentrations of sodium are required to activate this conductance isolated in membrane patches (50 mM, Dryer et al. 1989; 12 mM, Haimann and Bader (1989). In the frog node of Ranvier, Bergman (1972) has shown that a 250 ms long train of 1 ms voltage clamp pulses shifted  $E_{Na}$  approximately 10 mV more negative. From this value one can calculate the apparent internal sodium concentration to be approximately 24 mM (an apparent increase of 8 - 12 mM from resting levels). The change in  $E_{Na}$  decayed in two phases: one fast ( $< 1$  sec time constant) and one slower phase lasting several seconds to minutes. The fast phase predominated in short volleys and was presumed to reflect diffusion of the sodium ions into the intracellular space from a local accumulation near the inner surface of the nodal membrane. The rate at which the sodium concentration decayed correlates with the time course of the AHP. This interpretation would thus reconcile the contradiction stated above, as far as  $G_{K(Na)}$  in axonal membrane is concerned. It may still be

necessary, as suggested by Dryer et al. (1989), that there is a close proximity of potassium and sodium channels in the axonal membrane, a condition similar to that required for calcium dependent potassium conductances (Pennefather and Goh 1988; Roberts and Hudspeth 1987).

A  $G_{K(Na)}$  with comparable properties has been demonstrated in Betz cells of the cat somatosensory cortex (Schwindt et al. 1989). However, the activation of  $G_{K(Na)}$  in myelinated fibres appears to be more rapid (5 - 100 ms, depending on action potential duration) than the  $I_{K(Na)}$  in Betz cells (1 - 2 s). This difference in the rate of activation might reflect a difference in the cell sizes and consequently different rates of build up of the internal sodium concentration, rather than a real difference in the channel characteristics. The density of sodium channels on a nodal membrane (3000 channels/ $\mu m^2$ ; Dubois and Schneider 1982) is presumably larger than on the Betz cell and therefore, the amount of sodium influx should be much larger. Considering the substantial difference in the volume of these cells (node =  $200 \mu m^3$ ; Betz cell =  $5 \times 10^5 \mu m^3$ ) it is not surprising to find sizable differences in kinetics of AHP. For example, it takes 1 - 2 s of high frequency firing to activate the AHP in Betz cells compared to one action potential for the node of Ranvier. Of course, one could not exclude that the  $G_{K(Na)}$  in myelinated axons is more sensitive to the rise in sodium ion concentration. If any case, its rate of activation in myelinated axons is intermediate between the fast one (1 - 2 ms) reported by Bader et al. (1985) and Dryer et al. (1989) and the slow one (1 - 2 s) reported by Schwindt et al. (1989).

Another factor that may contribute to the rise in the intracellular sodium

concentration and the generation of  $G_{K(Na)}$  is a TTX sensitive persistent sodium conductance demonstrated in the node of Ranvier by Dubois and Bergman (1975). This current is evident with voltage clamp steps lasting 160 - 300 ms and membrane potentials greater than -50 mV. The presence of such a current would account for the AHP observed in our studies under circumstances when the transient sodium current is inactivated. Activation of a similar current has been hypothesized to activate the  $G_{K(Na)}$  in Betz cells (Schwindt et al. 1989)

Although  $G_{K(Na)}$  may be important for the regulation of adaptation and/or accommodation in myelinated axon, these experiments were not designed to directly assess its role in regulating repetitive activity. If this conductance does terminate action potential generation, one might predict that the reduction of the AHP by lithium might lead to a decrease in accommodation. However, this was never observed, perhaps due to sodium channel inactivation following an additional decrease in outward rectification with lithium ions. On the other hand, this observation may indicate that activation of  $G_{K(Na)}$  may promote firing by minimizing inactivation of the sodium conductance following the membrane repolarization. It then may act as a safety valve limiting action potential generation later in stimulus.

In conclusion, this study demonstrates that a potassium mediated AHP is dependent on the presence of sodium ions in the external media. The AHP was not affected by agents, which normally block calcium influx ( $Mg^{2+}$  or  $Mn^{2+}$ ) into the neurones nor was it affected by agents, which prevent an internal increase in calcium (EGTA). Agents, which block the electrogenic pump also do not alter the AHP. These results are consistent with the activation of a sodium

dependent potassium conductance operating in frog large myelinated axons. Its function may be important for regulation of action potential generation during a prolonged stimuli.



## **DISCUSSION**

## *INTRODUCTION*

The development of myelinated axons represents a major evolutionary step. The ability of an organism to rapidly receive information from the periphery and respond as quickly confers great advantages to their ability to respond to external stimuli. For example, spindle fibres give muscle tension information from the periphery. The frequency and number of action potentials transmitted "tells" how much force to supply back to our muscles to resist the force of gravity so that we may stand erect, lie prone or sit. This information must be relayed quickly, efficiently and accurately. We cannot wait a second or two every time we change position to receive new tension information and then respond. Therefore, owing to myelinated axon's relative importance, from a teleological point of view, one might expect that the electrical properties of myelinated axons should be tightly regulated.

Until very recently axons were considered to be relatively unsophisticated structures, which were faithful servants (propagators) conducting the action potentials provided them. This view made axons a rather unique neuronal structure; they were the only neuronal structure which did not regulate their excitability. The work presented in this thesis, as well as other recent studies (cf. Black et al. 1990) have provided a new view of myelinated axons which is considerably more complex. The primary difference between the classical view of myelinated axons and the present one is the realization that there are a multitude of functionally distinct potassium channels. Clearly myelinated axons are really no different than other neuronal structures having potassium channels which regulate their excitability. By comparing the role of potassium

conductances in myelinated axons to those in other neurones, one may draw wider conclusions as to how conductances with similar properties regulate function in neuronal structures, in general. Table 7-1 summarizes the classification of the potassium conductances in myelinated axons into the relevant classes of potassium conductances discussed in the introduction.

TABLE 7-1

Conductance	Class	Blocker(s)	Function	Ref
$G_{Kf1}$	$I_{DTX}$	TEA; 4-AP; DTX	VRA-APR; DRA&VRA-EAcc	1, 2, 3, 13
$G_{Kf2}$	$I_{Cap}$ ?	TEA; 4-AP Capsaicin	DRA-APR; DRA-EAcc VRA-LAcc VRA-Adp	1, 4, 5, 6 13
$G_{Ks}$	$I_K$	TEA; $Ba^{2+}$	DRA&VRA-Adp DRA&VRA-LAcc	4, 9, 5, 6 2
$G_{AR}$	Type2	$Cs^+$ not $Ba^{2+}$	Limits PT-AHP	8, 10
$G_{K(Na)}$	?	TEA	LAcc	7, 11, 12
$G_{leak}$	N/A	none	none ?	

Abbreviations. DRA Dorsal Root Axon, VRF. Ventral Root Axon, APR. Action Potential Repolarization, EAcc Early Accommodation, LAcc Late Accommodation, Adp: Adaptation, PT-AHP Post Tetanic-Afterhyperpolarization

#### References.

1. Dubois 1981, 2. Benoit and Dubois 1986, 3. Poulter et al. 1989, 4. Dubois 1982; 5. Chapter 3, 6. chapter 4, 7. Chapter 2, 8. Chapter 3; 9. Chapter 1; 10. Schwandt et al 1988 11. Dryer et al 1989; 12. Schwandt et al 1989 13. Grissmer 1986 (complete references in Reference section)

*FAST ACTIVATING POTASSIUM CONDUCTANCES**G<sub>Kf1</sub>*

Currents which are selectively blocked by DTX and 4-AP appear to activate quickly ( $\tau < 2\text{-}4\text{ms}$ ) and inactivate very slowly ( $\tau > 1\text{sec}$ ; Gustaffson et al. 1982; Feltz and Stansfeld 1988; Penner et al. 1986; Schauf 1987; Stansfeld et al. 1986; Stansfeld et al. 1987). Block of DTX sensitive currents reduced accommodation (Feltz and Stansfeld 1988; Stansfeld et al. 1986; Stansfeld et al. 1987) and prolonged action potential duration (Penner et al., 1986; Schauf 1987) in a number of preparations. Binding studies have suggested that this conductance is widely distributed throughout the CNS in many species (Dolly et al. 1987). MCDP, a toxin with similar specificity and the same binding site as DTX, had similar pharmacological effects as DTX (Bidard et al. 1987; Stansfeld et al., 1987). Thus it would appear that there is a distinct conductance,  $I_{\text{DTX}}$ , present in many types of neuronal tissues, whose function is to regulate cell firing and action potential repolarization.

The results of this study appear to agree with the above stated conclusion. However, owing to the presence of  $G_{\text{Ks}}$ ,  $G_{\text{Kf1}}$  is only responsible for accommodation of action potential generation in the early part of a continuous stimulus in ventral and dorsal root axons (VRA and DRA, respectively). In addition, it was demonstrated that action potential repolarization is regulated by  $G_{\text{Kf1}}$  in VRA. These conclusions are based primarily on the use of DTX, a specific blocker of  $G_{\text{Kf1}}$  (Benoit and Dubois 1986) and 4-AP which blocks both  $G_{\text{Kf1}}$  and  $G_{\text{Kf2}}$  (Dubois 1981). By comparing the gating characteristics of  $G_{\text{Kf1}}$  to the properties of other potassium conductances sensitive to DTX blockade, it is

evident that  $G_{Kf1}$  fits into the classification for  $I_{DTX}$  suggested by Feltz and Stansfeld (1988). Therefore, myelinated axons might be included in the list of tissues which have an  $I_{DTX}$ .

### $G_{Kf2}$

The primary role of  $G_{Kf2}$  in DRA appears to be the repolarization of the fibre. This conclusion clearly differs from the accepted explanation in which the large "background" leak conductance is responsible for action potential repolarization (Hille 1984; Schmidt and Stämpfli 1964). However, the voltage dependence of  $G_{Kf2}$  is not likely the main determinant of its function, since  $G_{Kf1}$ , which has a different voltage dependence than  $G_{Kf2}$ , is responsible for action potential repolarization in VRA. These conductances repolarize the axon primarily because they represent the majority of the total fast conductance. That is, their action is independent of their voltage dependence and they behave like a large leak conductance. As mentioned in Chapter 4 it is likely that  $G_{Kf2}$  partially contributes to the ability of the axon to accommodate during the early part of the stimulus. This conclusion is based on a comparison of the effects of DTX to 4-AP, since 4-AP reduced accommodation more than DTX application alone.

However, owing to its voltage dependence, (it activates some 30-40 mV above resting membrane potential) it is difficult to compare the role of  $G_{Kf2}$  in axons with a similar current in other tissues. Its pharmacology may place it with other fast activating potassium currents found in mammalian and avian dorsal root ganglia neurones, since they are selectively blocked by the plant toxin

capsaicin (Dubois 1982; Peterson et al. 1987). Capsaicin also had a similar effect to 4-AP, since application prolonged action potentials recorded from cultured chicken and rat DRG (Godfraind et al. 1981). Therefore,  $G_{Kf2}$  ( $I_{Cap}$  ?) might be pharmacologically and functionally grouped with other capsaicin sensitive currents.

### *SLOWLY ACTIVATING POTASSIUM CONDUCTANCES*

#### $G_{Ks}$

The gating characteristics of  $G_{Ks}$  are similar to the gating characteristics of the delayed rectifier ( $I_K$ ), present in vertebrate neurones. In general, the activation kinetics of  $I_K$  are slow (compared to  $I_A$  and  $I_{DTX}$ ). Its voltage dependence is varied, but  $I_K$  threshold seems to correlate with the resting membrane potential of the neurone where it is located. A recent review by Rudy (1988) states that one function of  $I_K$  is action potential repolarization and thus it regulates action potential duration. Based on the pharmacology presented in Chapter 4 this is not true; blockade of  $G_{Ks}$  appeared to have no additional effect on action potential repolarization after  $G_{Kf1}$  and  $G_{Kf2}$  were blocked. In fact, it is difficult to rationalize how  $I_K$ , a current which activates with a time constant of 10-100 ms (Rudy 1988) or longer (cf. Segal et al. 1984), could have a significant effect on action potential repolarization. So, although TEA blocks  $I_K$  and TEA has been shown to affect action potential repolarization in a variety of neurones (Rudy 1988), this probably reflects a lack of TEA selectivity (for example it also blocks the fast  $G_{K(Ca)}$ ) rather than the function of  $I_K$ .

On the other hand, the properties of  $I_K$  make it well suited for regulation of late accommodation and/or spike frequency adaptation. Since it requires a prolonged stimulus to turn it on, its slow development would be expected to alter action potential generation during a prolonged stimulus. Aside from the evidence presented here there are few studies which have addressed this attribute directly. Indirect evidence that  $I_K$  may function in this manner comes from a study by Stansfeld et al. (1987), who found that there is little or no TEA sensitive component in the total cell potassium current found in A cells of the rat nodose ganglia. There is only a fast activating DTX sensitive current ie. there is no  $I_K$ . After application of DTX or MCDP, continuous spiking with no spike frequency adaptation was observed in response to current clamp steps lasting up to 300 ms (Stansfeld et al. 1987). Therefore, the lack of  $I_K$  seems to be linked with an inability of the cell to alter its action potential frequency after blockade of  $I_{DTX}$ . Analogous results were reported using hippocampal cells in culture, which have no  $I_{DTX}$ . Application of TEA blocks a slowly activating potassium conductance with concomitant increase in excitability (Segal and Barker 1984).

### $G_{AR}$

Chapter 3 described the anomalous or inward rectification present in frog large myelinated primary afferent fibres. This rectification is activated slowly ( $\tau > 400$  ms), blocked by cesium ions but not by barium ions, and is reduced by decreasing the external potassium or sodium ion concentration. Inward rectification with these characteristics has been classified by Spain et al. (1987) as being Type 2 inward rectification also reported to exist in other neurones (Halli-

well and Adams 1982; Mayer and Westbrook 1983; Spain et al. 1987).

Our results suggest that  $G_{AR}$  may regulate the length of the post tetanic afterhyperpolarization in myelinated axons. The stimulation protocol used likely activates the electrogenic pump in axons (Barrett and Barrett 1982; Bergman et al. 1980). Therefore, it is believed that  $G_{AR}$  acts by limiting the length of the hyperpolarization produced by such a stimulation. Electrogenic pump activity can last as long as 15 seconds (Bergman et al. 1980) suggesting that  $G_{AR}$  is well suited to regulate this activity as evidenced by the DAP observed after a hyperpolarizing current pulse (as opposed to the DAP following an action potential). This DAP lasts as long as 10 seconds and likely reflects the slow closing of  $G_{AR}$  after activation.

### $G_{K(Na)}$

It is well established that there are no calcium channels in axonal membranes (Stämpfli and Hille, 1976) nor is there any effect of raised internal calcium on any of the identified potassium conductances in myelinated axons (Dubois 1981). Therefore it is interesting to note, in light of the absence of a  $G_{K(Ca)}$  operating in myelinated axons, that the sodium ion "steps in" to play a role left vacant by calcium. The function of this conductance may be similar to the slowly activating  $G_{K(Ca)}$ ,  $I_{AHP}$ , in hippocampal neurones (Madison and Nicoll 1984). Reducing  $I_{AHP}$  by calcium channel blockade (Madison and Nicoll 1984) or  $\beta_1$  receptor stimulation with noradrenaline decreased accommodation (Madison and Nicoll 1986). Similarly, Foehring et al. (1989) reported that norepinephrine (noradrenaline) suppressed both a calcium and sodium



dependent potassium conductance in Betz cells of the cat somatosensory cortex. This raises the possibility that the channel in the CNS activated by sodium or calcium may originate from the same gene. Both clones code for similar proteins (potassium channels modulated by noradrenaline) and alternative splicing or post translational modification has altered the cation site which activates the channel. Similarly, in frog one might speculate that the sodium dependent potassium conductance is a clone of calcium dependent potassium conductances which exist in the dorsal root ganglia.

#### *OTHER FUNCTIONAL ROLES OF POTASSIUM CONDUCTANCES IN MYELINATED AXONS*

Aside from the general conclusions one can draw from the comparison of the potassium conductances in myelinated axons with those in other neurones, these conductances display functions uniquely important to the axon. Functions such as conduction velocity, and neural coding are particularly relevant to myelinated axons and may also be modulated by potassium conductances.

##### *Conduction velocity*

Large myelinated axons are unique owing to the speed they are able to conduct action potentials. As mentioned in the Introduction conduction velocity depends on the capacitance of the internodal membrane, internodal length and fibre diameter. In mammalian fibres blockade of the fast potassium conductance with 4-AP had only a small affect on conduction velocity (Ritchie and Stagg 1982). However, Figure 4.5 in Chapter 4 (Poulter et al. 1989) may indicate

that potassium conductances may affect conduction velocity in frog. Before decreasing the axonal conductance with DTX the conduction velocity is not measurable since the stimulus artifact is too close to the rising phase of the action potential. However, afterwards the stimulus artifact is resolvable indicating that the conduction velocity had slowed without a change in the upstroke  $dV/dt$ . This might be explained by an increase in the time constant in charging (due to the increased resistance). So, while voltage threshold is unchanged by DTX treatment (Poulter et al. 1989) the time required to reach this threshold is increased and the conduction velocity slows.

Also evident in Figure 4.5 is the long depolarizing after potential, which has been attributed to the passive discharge of the large effective internodal capacitance in other vertebrate large myelinated axons (Barrett and Barrett 1982; Blight and Someya 1985). This phenomenon was only rarely seen in our recordings with the potassium conductances unblocked (unpublished observations). However, in the presence of DTX (or 4-AP, TEA) this phenomenon was always observed. This implies that only after the nodal membrane resistance is sufficiently increased does current flow through the myelin sheath. That is, the myelin sheath becomes a relatively low resistance path for current flow only after potassium channel blockade. It has been suggested that the functional significance of a lower resistance myelin sheath may be to minimize the time constant of the internodal region compared to the nodal time constant and therefore increase conduction velocity (Blight 1985). However if this were the case one might expect that conduction velocity would increase after potassium channel blockade .

*Leak conductance: Action potential repolarization and resting membrane potential*

After blockade of anomalous rectification the resulting steady state resistance  $R_{ss}$  likely represents the leak resistance of the membrane (Ohmic or non voltage dependent) in parallel with leak resistance associated with the seal of the membrane around the microelectrode. On average this value was  $\approx 140 \text{ M}\Omega$ . This value is most certainly an underestimate of the true leak resistance since damage caused by penetration of the microelectrode will tend to make this value smaller. Therefore, the effective leak conductance is even less than the  $7 \text{ nS}$  ( $1/140 \text{ M}\Omega$ ) calculated from  $R_{ss}$ . It is unlikely that a conductance of this magnitude is able to significantly contribute to action potential repolarization. Furthermore, it is unlikely that the leak conductance is largely responsible for resting membrane potential. At resting membrane potential, the resistance of the fibre may be estimated to be as small as  $5\text{-}10 \text{ M}\Omega$ . Therefore, the conductance active at resting membrane potential can be 30-15 times greater than the leak conductance. This suggests that other conductances are responsible for governing resting membrane potential ( $G_{Ks}$ ,  $G_{K(Na)}$ ?). It has been suggested by Baker et al. (1987) that the leak resistance is not in parallel but in series with the other membrane resistances. This was suggested to account for a component of the resting membrane potential which was insensitive to variations in the external ionic composition, that is, a component which is non Nernstian in behaviour. While this may be true, it still does not account for our observations, unless one is ready to propose that there is a voltage dependent series (or parallel for that matter) "leak" resistance which inactivates when the membrane is hyperpolarized.

*Excitability and neural coding*

Obviously the excitability of myelinated axons will have a profound effect on how reflexes and nociception are controlled. Perception of the periphery begins by the stimulation of a receptor organ. For example, when a constant tension is applied to a spindle fibre organ it produces a train of action potentials. At first the potential generated by the spindle receptor fires a rapid burst of action potentials after which action potential generation slows to a constant rate (adaptation). If the tension is held constant the frequency of action potential generation remains constant; when the tension is released action potential generation terminates (Ottoson and Shepard 1971). This burst of action potentials now traveling in the myelinated axon is subject to further modulation by axonal conductances.

First the axon will limit the maximum frequency that the action potentials can be transmitted. In the absence of potassium channel block (unpublished observations and in chapter 4, 5 and 6) the maximum rate of action potential generation was  $\approx 150$  Hz, which corresponds to a minimum "lag time" between action potentials of  $\approx 7$  ms. One might first suppose that this rate is primarily set by the recovery from inactivation. However, Aldrich et al. (1983) have argued, based on results obtained from single channel recordings, that the time constant of inactivation is  $\approx 0.5$  ms. Assuming that the recovery occurs at the same rate and sodium channel kinetics were the only factor regulating maximal spike frequency, axons should be able to produce rates of firing greater than 150 Hz. Because this is not the case, it implies that other factors set the upper limit at which spikes can be generated.

Another possible factor will be the time constant ( $\tau_m$ ) of the axonal membrane, which is determined by the membrane capacitance ( $C_m$ ) and the resistance ( $R_m$ ; ie.  $\tau_m = R_m C_m$ ). The larger the  $\tau_m$  the slower the maximal firing rate (Hodgkin and Stämpfli 1949b). Any conductance active at the resting membrane potential will tend to make  $\tau_m$  small. In opposition to this effect any rectification present would shunt the stimulus and limit action potential generation. In the absence of block, it is likely that the large outward rectification limits the spiking frequency, since the time constant of the axonal membrane ( $\tau < 1.0$  ms, Hille 1967) should support a faster rate than 150 Hz. Therefore, potassium conductances limit the frequency of discharge from the spindle fibre, limiting the maximum frequency action potentials can invade primary afferent terminals.

The second attribute which may be affected by the properties of the axon is an alteration in the rate of firing produced by the spindle fibre. Recordings from sensory axons originating in the semicircular canals demonstrated that an increase in action potential discharge rate signaled an increase in the angular velocity of spin of the subject. However, unlike spindle fibres, which do not adapt, a slowing in action potential generation to levels observed at rest signaled the maintenance of angular velocity and not, as one might expect, a slowing in angular velocity (Fernandez and Goldberg 1976). If the neural coding for relaying tension information is the same as that relayed from the semi circular canals, constant action potential discharge from the spindle fibres may be slowed by the axon to signal the maintenance of tension. This mechanism may have the added benefit of preventing neurotransmitter depletion of the primary afferent terminals allowing for the prolonged stimulation of the

ventral root cell body.

To conclude, the speculation provided above suggests that output from a receptor organ can be greatly influenced by the excitability of the axon. Consequently, the release pattern of the neurotransmitter from the primary afferent terminal will be affected and the perception and reaction to peripheral stimuli will be affected. Thus it is evident that the role of myelinated axons may be of fundamental importance to how neural coding signals information from the periphery.

#### *SUMMARY AND CONCLUSION*

Frog myelinated axons are endowed with a number of potassium conductances which have relatively specific functions similar to functions of potassium conductances in other neuronal structures. Fast activating potassium conductances regulate action potential repolarization, early accommodation, adaptation and perhaps action potential conduction velocity. In frog myelinated axon the conductance  $G_{Kf1}$  is pharmacologically and functionally similar to the current  $I_{DTX}$  found in other neurones; whereas,  $G_{Kf2}$  may be related to a family of potassium channels, which regulate action potential repolarization and are selectively blocked by capsaicin. It also may play a role in early accommodation and adaptation. The slowly activating conductances regulate longer lasting phenomena only. The conductance  $G_{Ks}$  or  $I_K$  has no effect on action potential repolarization, but it appears to be responsible for late adaptation and accommodation. The type 2 anomalous rectification limits the AHP resulting from the activation of the electrogenic pump by a long lasting tetanus. The function of

the sodium activated potassium conductance is speculative, but it may play a role in adaptation and accommodation as well. These specific roles of potassium conductances in myelinated axons indicate that they are regulated in an analogous manner to other neuronal structures. Therefore, their regulation and behaviour are considerably more complex than previously believed. Thus it would appear that the axon may be an important regulatory site for neural encoding and "hard wired" reflexes.

## **REFERENCES**



- Adams, P.R. and Galvan, M. Voltage-dependent currents of vertebrate neurons and their role in membrane excitability *Adv. Neurol.* 44:137-170, 1986.
- Adrian, R.H. Rectification in muscle membrane. *Progr. Biophys. Molec. Biol.* 19:340-369, 1969.
- Agnew, W.S., Levinson, S.R., Brabson, J.S. and Raftery, M.A. Purification of the tetrodotoxin-binding component associated with the voltage sensitive sodium channel from *Electrophorus electricus* electroplax membranes *Proc. Natl. Acad. Sci.* 75:2606-2610, 1978.
- Aldrich, R.W., Corey, D.P., and Stevens, C.F. A reinterpretation of mammalian sodium channel gating based on single channel recording. *Nature* 306:436-441, 1983.
- Anderson, C., Mackinnon, C., Smith, C. and Miller, C. Charybdotoxin block of single  $\text{Ca}^{2+}$ -activated  $\text{K}^{+}$  channels *J. Gen. Physiol.* 91:317-333, 1988.
- Anderson, A.J. and Harvey, A.L. Omega-conotoxin does not block the verapamil sensitive calcium channels at the mouse motor nerve terminals. *Neurosci. Lett.* 82:177-180, 1987.
- Andrietti, F. and Bernardini, G. Segmented and "equivalent" representation of the cable equation. *Biophys. J.* 46:615-623, 1984.

- Arbuthnott, E.R., Boyd, I.A. and Kalu, K.U. Ultrastructural dimensions of myelinated peripheral nerve fibres in the cat and their relation to conduction velocity. *J. Physiol. Lond.* 308:125-157, 1980.
- Arhem, P. and Johansson, S. A model for the fast 4-aminopyridine effects on amphibian myelinated nerve fibres. A study based on voltage-clamp experiments. *Acta. Physiol. Scand.* 137:53-61 1989.
- Armstrong, C.M. Interference of injected tetra-*n*-propylammonium with outward sodium current in squid giant axon. *Nature* 211:322-323, 1966.
- Armstrong, C.M. Sodium channels and gating currents *Physiol. Rev.* 61:644-683, 1981.
- Armstrong, C.M. Time course of TEA<sup>+</sup>-induced anomalous rectification in squid giant axons. *J. Gen. Physiol.* 50:491-503, 1966.
- Armstrong, C.M. and Binstock, L. Anomalous rectification in the squid giant axon injected with tetraethylammonium. *J. Gen. Physiol.* 48:859-872, 1965.
- Ashcroft, F. M., Heiny, J. A., and Vergara, J. Inward rectification in the transverse tubular system of frog skeletal muscle studied with potentiometric dyes. *J. Physiol. Lond.* 359: 269-291, 1985.
- Attwell, D., Eisner, D., and Cohen, I. Voltage clamp and tracer flux data : effects of a restricted extra-cellular space. *Q. Rev. Biophys.* 12: 213-261, 1979.

- Auld, V.J., Goldin, Kraft, D.S., Marshall, J., Dunn, J.M., Catterall, W.A., Lester, H.A., Davidson, N. and Dunn, R.J. A rat brain  $\text{Na}^+$  channel  $\alpha$  subunit with novel gating properties. *Neuron* 1:449-461, 1988.
- Bader, C.R., Bernheim, L. and Bertrand, D. Sodium activated potassium conductance in cultured avian neurones. *Nature* 317:540-542, 1985.
- Bader, C.R. and Bertrand, D. Effect of changes in intra- and extracellular sodium on the inward (anomalous) rectification in salamander photoreceptors. *J. Physiol. Lond.* 347: 611-631, 1984.
- Baker, M., Bostock, H., Grafe, P. and Martius, P. Function and distribution of three types of rectifying channels in rat spinal root myelinated axons. *J. Physiol. Lond.* 383:45-67, 1987.
- Baker, P.F. and Robinson, K.A. Chemical modification of crab nerves can make them insensitive to the local anesthetics tetrodotoxin and saxitoxin. *Nature* 257:412-414, 1975.
- Barrett, E.F. and Barrett, J.N. Intracellular recording from vertebrate myelinated axons: mechanism of the depolarizing afterpotential. *J. Physiol. Lond.* 323:117-144, 1982.
- Barrett, E.F., Morita, K. and Scappaticci, K.A. Effects of tetraethylammonium on the depolarizing after-potential and passive properties of lizard myelinated axons. *J. Physiol. Lond.* 402:65-78, 1988.

- Bean, B.P., Sturek, M., Puga, A., and Hermismeyer, K. Calcium channels in muscle cells isolated from rat mesenteric arteries: modulation by dihydropyridine drugs. *Circ. Res.* 59:229-35, 1986.
- Benham C.D., Hess P., and Tsien, R.W. Two types of calcium channels in single smooth cells from rabbit ear artery studied with whole cell and single-channel recordings. *Circ. Res.* 61(Suppl. I):10-16, 1987.
- Benoit, E., and Dubois, J.-M. Toxin I from the snake *Dendroaspis polylepis polylepis*: a highly specific blocker of one type of potassium channel in myelinated nerve fiber. *Brain Res.* 377:374-377, 1986.
- Benzanilla, F. A high capacity data recording device based on a digital audio processor and a video cassette recorder. *J. Biophys. Soc.* 47, 437-441:1985.
- Bergman, C. Increase of sodium concentration near the inner surface of the nodal membrane. *Pflügers Arch.* 317:287-302, 1970.
- Bergman, C., Nonner, W. and Stämpfli, R. Sustained spontaneous activity of Ranvier nodes induced by combined actions of TEA and the lack of calcium. *Pflügers Arch.* 302:24-37, 1968.
- Bergman, C. and Stämpfli, R. Différence de perméabilité des fibres nerveuses myelinisées sensorielles et motrices à l'ion potassium. *Helv. physiol. pharmac. Acta.* 24:247-298, 1966.

- Bergman, J., Dubois J.-M., and Bergman, C. Post tetanic membrane potential in single axon and myelinated nerve trunk *Ann. N.Y. Acad. Sci.* 339:21- 38, 1980.
- Bidard, J.N., Mourre, C. and Lazdunski, M. Two potent central convulsant peptides, a bee venom toxin, the MCD peptide, and a snake venom toxin dendrotoxin I, known to block  $K^+$  channels have interacting receptor sites. *Biochem. Biophys. Res. Commun.* 143:383-389, 1987.
- Binah, O., Mager, S., and Palti, Y. Effect of  $Cs^+$ ,  $Li^+$  and  $Na^+$  on the potassium conductance and gating kinetics in the frog node of Ranvier. *Pflügers Arch.* 411: 312-315, 1988.
- Black, J.A., Freidman, B., Waxman, S.G., Elmer, L.W. and Angelides, K.J. Immuno-ultrastructural localization of sodium channels at nodes of Ranvier and perinodal astrocytes in rat optic nerve. *Proc. R. Soc. Lond. B* 238:29-51, 1989.
- Black, J.A., Kocsis J.D. and Waxman S.G. Ion channel organization of the myelinated fiber. *Trends Neurosci.* 13:48-54, 1990.
- Blatz, A.L. and Magleby, K.L. Single apamin-blocked  $Ca^{2+}$ -activated  $K^+$  channels of small conductance in rat skeletal muscle. *Nature* 323:718-720, 1986.
- Blight, A.R. Computer simulation of action potentials and afterpotentials in mammalian myelinated axons : The case for a lower resistance myelin sheath. *Neurosci.* 15:13-31, 1985.

- Blight, A.R. and Someya, S. Depolarizing afterpotentials in myelinated axons of mammalian spinal cord. *Neurosci* 15: 1-12, 1985 .
- Borque, C.W., Randle, J.C.R. and Renaud L. P. Calcium dependent potassium conductance in the rat supraoptic nucleus neurosecretory neurones. *J. Neurophysiol* 54:1375-1382, 1985.
- Bostock, H. and Sears, T.A. Continuous conduction in demyelinated mammalian nerve fibres. *Nature* 263:786-787, 1976.
- Bostock, H. and Sears, T.A. The internodal axon membrane: Electrical excitability and continuous conduction in segmental demyelination. *J. Physiol. Lond.* 280:273-301, 1978.
- Bostock, H. Conduction changes in mammalian axon following demyelination. (In: *Abnormal Nerves and Muscles as Impulse Generators* ed. Culp, W.J. and Ochoa, J.) Oxford University Press, Oxford, New York p. 236-253, 1982
- Bowe, C.M., Kocsis, J.D. Targ, E. and Waxman, S.G. Physiological effects of 4-aminopyridine on demyelinated mammalian motor and sensory fibers. *Ann Neurol* 22:264-268, 1987.
- Bray, G.M., Rasminsky, M. and Aguayo, A.J. Interactions between axons and their sheath cells. *Ann. Rev Neurosci* 4:127-162, 1981

- Brink, F. The role of calcium ions in neural processes. *Pharmacol. Rev.* 6:243-298, 1954.
- Brismar, T. Potential clamp analysis of the membrane current in rat myelinated nerve fibres. *J. Physiol. Lond.* 298:171-184, 1980.
- Bromm, B. and Frankenhaeuser, B. Repetitive discharge of the excitable membrane computed on the basis of voltage clamp data for the node of Ranvier. *Pflügers Arch.* 332:21-27, 1972.
- Bromm, B. and Rahn U. Repetitive Aktivität des isolierten Schnürrings bei Reizung mit Nullien- Symmetrischen Strömen. *Pflügers Arch.* 306:153-164, 1969.
- Brown, H. and Di Francesco, D. Voltage clamp investigations of membrane currents underlying pace-maker activity in rabbit sino-atrial node. *J. Physiol. Lond.* 308: 331-351, 1980.
- Bush, B.M.H. Non-impulsive stretch receptors in crustaceans. In *Neurones Without Impulses* ( eds Roberts A. and Bush B.M.H. ) pg. 147-176, Cambridge University Press, Cambridge, 1981.
- Campbell, D.T. and Hille, B. Kinetic and pharmacological properties of the sodium channel of frog skeletal muscle. *J. Gen. Physiol.* 67:309-323, 1976.
- Carbone, E. and Lux, H.D. Single low voltage-activated calcium channels in chick and rat sensory neurones. *J. Physiol. Lond.* 386:571-601, 1987.

- Carbone E., Prestipino G., Spadavecchia L., Franciolini F., and Possani, L.D.  
Blocking of the squid axon  $K^+$  channel by noxiustoxin: a toxin from the  
venom of the scorpion *Centruroides noxius*. *Pflügers Arch.* 408:423-431,  
1987.
- Carbone, E., Wanke, E., Prestipino, G., Possani, L.D., and Maelicke, A. Selective  
blockade of voltage- dependent  $K^+$  channels by a novel scorpion toxin.  
*Nature* 296:90-91, 1982.
- Carpenter, D.O. Electrogenic sodium pump and high specific resistance in nerve  
cell bodies of the squid . *Science* 179:1136-1138, 1973.
- Castle, N.A., Haylett, D.G. and Jenkinson, D.H. Toxins in the characterization of  
potassium channels. *Trends Neurosci.* 12:59-65, 1989.
- Castle, N.A. and Strong, P.N. Identification of two forms from scorpion (*Leiurus*  
*quinquestriatus*) venom which block distinct classes of calcium-activated  
potassium channel. *F.E.B.S. Lett.* 209:117-121, 1986.
- Catterall, W.A. Neurotoxins that act on voltage sensitive sodium channels in ex-  
citabile membranes. *Annu. Rev. Pharmacol. Toxicol.* 20:15-43, 1980.
- Catterall, W.A. Common modes of drug action on sodium channels: local anesthet-  
ics, antiarrhythmics and anticonvulsants. *Trends. Pharmacol. Sci.* 8:57-64,  
1987.



- Catterall, W.A. Structure and function of voltage-sensitive ion channels. *Science* 242:50-61, 1989.
- Catton, W.T. Cutaneous mechanoreceptors In: Llinas R, Precht W (ed) *Frog Neurobiology*. chapter 21. Springer-Verlag, Berlin, p 629-642, 1976.
- Chiu S.Y. Changes in excitable membrane properties in Schwann cells of adult rabbit sciatic nerves following nerve transection. *J. Physiol. Lond.* 396:173-188, 1988.
- Chiu, S.Y., Ritchie, J.M. and Stagg, D. A quantitative description of membrane currents in rabbit myelinated nerve. *J. Physiol. Lond.* 292:149-166, 1979.
- Chiu, S.Y. and Ritchie, J.M. Potassium channels in nodal and internodal membrane of mammalian myelinated fibres. *Nature* 284:170-171, 1980.
- Chiu, S.Y. and Ritchie, J.M. Evidence for the presence of potassium channels in the internode of frog myelinated nerve fibres. *J. Physiol. Lond.* 322:485-501, 1982.
- Chiu, S.Y. and Ritchie, J.M. On the physiological role of internodal potassium channels and the security of conduction in myelinated nerve fibres. *Proc. R. Soc. Lond.* B220:415-422, 1984.
- Chiu, S.Y., Shrager, P. and Ritchie, J.M. Neuronal-type  $\text{Na}^+$  and  $\text{K}^+$  channels in rabbit cultured Schwann cells. *Nature* 311:156-157, 1984.

- Collier, B. and Exley K.A. Mechanism of the antagonism by tetraethylammonium of neuromuscular block due to *d*-tubocurarine or calcium deficiency. *Nature* 199;702-703, 1963.
- Collier, B., Padjen, A.L., Quik, M. and Smith, P.A. Convulsant and possible anticholinergic actions of dendrotoxin in the amphibian spinal cord. *Brit. J. Pharmacol.* 73:525-533, 1982.
- Conner, J.A. and Stevens C.F. Voltage clamp studies of a transient outward membrane current in gastropod neural somata. *J. Physiol.* 213:21-30, 1971.
- Constanti, A. and Galvan, M. Fast inward-rectifying current accounts for anomalous rectification in olfactory cortex neurones. *J. Physiol. Lond.* 335: 153-178, 1983.
- Conti, F., Hille, B. and Nonner, W. Non-stationary fluctuations of the potassium conductance at the node of Ranvier of the frog. *J. Physiol. Lond.* 353:199-230, 1984.
- Conti, F. and Neher, E. Single channel recordings of  $K^+$  currents in squid axons. *Nature* 285:140-143, 1980.
- Cooke I.M. Inhibition of impulse activity in a sensory neuron by an electrogenic pump. *J. Gen Physiol.* 57:125-163, 1971.

- Cooper, E. and Shrier, A. Single channel analysis of the fast transient potassium currents from rat nodose neurones. *J. Physiol. Lond.* 369:199-208, 1985.
- Cota, G. and Stefani, E. A fast activated inward calcium current in twitch muscle of the frog (*Rana montezuma*). *J. Physiol. Lond.* 370:151-163, 1986.
- Courtney, K.R. Mechanism of frequency dependent inhibition of sodium channels in frog myelinated nerve by the lidocaine derivative GEA 968. *J. Pharmacol. Exp. Ther.* 195:225-236, 1975.
- Crepel, F. and Penit-Soria, J. Inward rectification and low threshold calcium conductance in rat cerebellar Purkinje cells. An *in vitro* study. *J. Physiol. Lond.* 372: 1-23, 1986.
- Curtis, B.M. and Catterall, W.A. Purification of the calcium antagonist receptor of the voltage-sensitive calcium channel from skeletal muscle transverse tubules. *Biochemistry* 23:2113-2117, 1986.
- Curtis, H.J. and Cole, K.S. Transverse electric impedance of the squid giant axon. *J. Physiol. Lond.* 145:529-546, 1938.
- Daut, J. Modulation of excitatory synaptic response by fast transient  $K^+$  current in snail neurones. *Nature (New Biology)* 246:193-196, 1973.
- Di Francesco, D. A study of the ionic nature of the pacemaker in calf Purkinje fibres. *J. Physiol. Lond.* 314: 377-393, 1981.

Dodge, F. A., Jr. *A Study of Permeability Changes Underlying Excitation in Myelinated Nerve Fibers of the Frog*. The Rockefeller Institute, Ph.D. Thesis. University Microfilms, Inc., Ann Arbor, MI, 1963.

Dolly, J.O., Halliwell, J.V., Black, J.D., Williams, R.S., Pelchen-Matthews, A., Breeze, A.L., Mehraban, F., Othman, I.B. and Black, A.R. Botulinum neurotoxin and dendrotoxin as probes for studies on transmitter release. *J. Physiol. Paris* 79:280-303, 1984.

Dolly, O.J., Stansfeld, C.E., Breeze, A., Pelchan-Matthews, A., Marsh, S.J. and Brown, D.A. Dendrotoxin and its homologues as probes for voltage dependent potassium channels. In: *Neurotoxins and their pharmacological implications* edited by Peter Jenner, New York: Raven Press, 1987, p.81-114.

Dubois, J.M. Evidence for the existence of three types of potassium channels in the frog Ranvier node membrane. *J. Physiol. Lond.* 318:297-316, 1981.

Dubois, J.M. Capsaicin blocks one class of  $K^{+}$  channels in the frog node of Ranvier. *Brain Res.* 245:372-375, 1982.

Dubois, J.M. and Bergman, C. Late sodium current in the Node of Ranvier. *Pflügers Arch.* 357:361-364, 1975.

- Dubois J.M. and Schneider, M.F. Kinetics of intramembrane charge movement and sodium current in frog node of Ranvier. *J. Gen. Physiol.* 79:571-602 1982.
- Dryer S.E., Fuji J.T. and Martin A.R. A  $\text{Na}^+$ -activated  $\text{K}^+$  current in cultured brain stem neurones from chicks. *J. Physiol. Lond.* 410, 283-296 1989.
- Eng, D.L., Gordon, T.R., Kocsis, J.D. and Waxman, S.G. Development of 4-AP and TEA sensitivities in mammalian myelinated nerve fibers. *J. Neurophysiol.* 60:2168-2179, 1988.
- Ellisman, M.H., Lindsey, J.D., Wiley-Livingston, C. and Levinson, S.R. Differentiation of axonal membrane systems, the axolemma, and the axoplasmic matrix. In *Structure and Function in Excitable Cells* (D.C. Chang et al. eds.) New York: Plenum Press, pp. 3-23, 1983.
- Erlanger, J. and Blair, E. A. Manifestations of segmentation in myelinated axons. *Amer. J. Physiol.* 110:287-311, 1934.
- Erlanger, J. and Blair, E. A. Salt free isotonic solutions and nerve conduction. *Amer. J. Physiol.* 124:341-359, 1938a.
- Erlanger, J. and Blair, E. A. Comparative observations on motor and sensory fibers with special reference to repetitiousness. *Am. J. Physiol.* 121:431-453, 1938b.
- Feltz, A. and Stansfeld, C.E. Dendrotoxin- sensitive small conductance  $\text{K}^+$  channels in isolated rat sensory neurones. *J. Physiol. Lond.* 406:208p, 1988.

- Fernandez, C and Goldberg, J.M. Physiology of peripheral neurons innervating otolith organs of the squirrel monkey. III. Response Dynamics. *J. Neurophysiol.* 36:179-204, 1976.
- Flockerzi, V., Oeken, H.-J., Hofmann, F., Pelzer, D., Cavalie, A. and Trautwein, W. Purified dihydropyridine site from skeletal muscle t-tubules is a functional calcium channel. *Nature* 323:66-68, 1986.
- Foehring, R.C., Schwandt, P.C. and Crill, W.E. Norepinephrine selectively reduces slow  $\text{Ca}^{2+}$ - and  $\text{Na}^{+}$ - mediated  $\text{K}^{+}$  currents in cat neurocortical neurons. *J. Neurophysiol.* 61:245-256, 1989.
- Foster, R.E., Connors, B. and Waxman, S.G. Rat optic nerve: electrophysiological, pharmacological and anatomical studies during development. *Dev. Brain Res.* 3:361-376, 1982.
- Fox, A.P., Nowycky, M.C. and Tsien, R. Kinetic and pharmacological properties distinguishing three types of calcium currents in chick sensory neurones. *J. Physiol. Lond.* 394:149-172, 1987a.
- Fox, A.P., Nowycky, M.C. and Tsien, R. Single channel recordings of three types of calcium channels in chick sensory neurones. *J. Physiol. Lond.* 394:173-200, 1987b.

Frankenhaeuser, B. and Huxley, A.F. The action potential in the myelinated nerve fiber of *Xenopus Laevis* as computed on the basis of voltage clamp data. *J. Physiol. Lond.* 171:302-315, 1964.

Frazier, D.T., Narahashi, T. and Yamada, M. The site of action and active form of local anesthetics. Experiments with quaternary compounds. *J. Pharmacol. Exp. Ther.* 171:45-51, 1970.

Gallin, E.K. and McKinney, L.C. Identification of inward and outward rectifying K conductances in cultured human macrophages. *Soc. Neurosci. Abstr.* 12:1341, 1986.

Gainer, H., Tasaki, I. and Lasek, R.J. Evidence for the glia-neuron protein transfer hypothesis from intracellular perfusion studies of squid axons. *J. Cell. Biol.* 74:524-530, 1977.

Godfraind, J.M., Jessel, T.M., Kelly, J.S., McBurney, R.N., Mudge, A.W. and Yamamoto, M. Capsaicin prolongs action potential duration in cultured sensory neurones. *J. Physiol. Lond.* 312:32P-33P, 1981.

Gonzalez, M., Quinonez, M., and Argibay, J. A. Inward rectification in muscle fibres of the toad *Bufo Marinus*. *Comp. Biochem. Physiol. [A]*. 81: 619-625, 1985.

Gordon, D., Merrick, D., Wollner, D.A. and Catterall, W.A. Biochemical properties of sodium channels in a wide range of excitable tissues studied with site-directed antibodies. *Biochemistry* 27:7032-7038, 1988.

- Gorman, A.L.F. and Mirolli, M. The passive properties of the membrane of a molluscan neurone. *J. Physiol. Lond.* 227:35-49, 1972.
- Gray, P.T.A. and Ritchie J.M. Ion channels in schwann and glia cells. *Trends Neurosci.* 8:411-415, 1985
- Grissmer, S. Properties of potassium and sodium channels in frog internode. *J. Physiol. Lond.* 381:119-134, 1986.
- Guggino, S.E., Guggino, W.B., Greef, N., and Sacktor, B. Blocking agents of  $\text{Ca}^{2+}$ -activated  $\text{K}^{+}$  channels in cultured medullary thick ascending limb cells. *Am. J. Physiol.* 21:C128-C137, 1987.
- Gustaffson, B., Galvan, M., Grafe, P. and Wigstrom, H. Transient outward current in mammalian neurones blocked by 4-aminopyridine. *Nature* 299:252-254, 1982.
- Haberman, E. Apamin. *Pharmacol. Ther.* 25:255-270, 1984.
- Hagiwara, S. *Membrane Potential-Dependent Ion Channels in Cell Membrane. Phylogenetic and Developmental Approaches.* Raven Press, N.Y. 118 pp. 1983.
- Hagiwara, S. and Jaffe, L. A. Electrical properties of egg cell membranes. *Ann. Rev. Biophys. Bioeng.* 8: 385-416, 1979.



- Hagiwara, S., Kusano, K. and Saito, N. Membrane changes of *Onchidium* nerve cell in potassium rich media. *J. Physiol. Lond.* 155:470-489, 1961.
- Hagiwara, S. and Takahashi, K. The anomalous rectification and cation selectivity of the membrane of a starfish egg. *J. Membr. Biol.* 18: 61-80, 1974.
- Haimann, C and Bader, C.R. Sodium-activated potassium channel in avian sensory neurons. *C. Biol. Intr. Rep.* 13:1113-1139, 1989.
- Halliwel, J. V. and Adams, P. R. Voltage clamp analysis of muscarinic excitation in hippocampal neurons. *Brain Res.* 250: 71-92, 1982.
- Halliwel, J.V., Othman, I.B., Pelchen-Matthews, A. and Dolly, J.O. Central action of dendrotoxin: selective reduction of a transient K conductance in hippocampus and binding to localized acceptors. *Proc. Natl. Acad. Sci. U.S.A.* 83:493-497, 1986.
- Harvey, A.L. and Anderson, A.J. Dendrotoxins: snake toxins that block potassium channels and facilitate neurotransmitter release. *Pharm. Ther.* 31:33-55, 1985.
- Harvey, A.L. and Gage, P.W. Increase of evoked release of acetylcholine at the neuromuscular junction by a fraction from the venom of the eastern green mamba snake (*Dendroaspis angusticeps*). *Toxicon* 19:373-381, 1981.

- Hartshorne, R.P., and Catterall, W.A. Purification of the saxitoxin receptor of the sodium channel from rat brain. *Proc.Natl. Acad. Sci.* 78:4620-4624, 1981.
- Hartshorne, R.P., Keeler, B.U., Talvenheimo, J.C., Catterall, W.A. and Montal, M. Functional reconstitution of the purified brain sodium channel in planar lipid bilayers. *Proc.Natl. Acad. Sci.* 82:240-244, 1985.
- Hashiguchi, T. and Padjen, A.L. Membrane properties of primary afferent axons: a study by intracellular recording. *Abs. Soc. Neurosci.* 9:511, 1983.
- Hermann, A. and Gorman, A.L.F. Effects of 4-aminopyridine on potassium currents in a molluscan neurone. *J.Gen. Physiol.* 78:63-86, 1981.
- Hestrin, S. The interaction of potassium with the activation of anomalous rectification in frog muscle membrane. *J. Physiol. Lond.* 317: 497-508, 1981.
- Hille, B. The selective inhibition of delayed potassium currents in nerve by tetraethylammonium. *J. Gen. Physiol.* 50:1287-1302, 1967.
- Hille, B. Ionic channels in nerve membranes. *Progr. Biophys. Molec. Biol.* 21:1-32, 1970.
- Hille, B. Voltage clamp studies on myelinated nerve fibres. In *Biophysics and Physiology of Excitable Membranes*. Ed. by W.J.Adelman, Jr., Van Nostrand Reinhold Co., N.Y. p.230-246, 1971.

- Hille, B. The pH dependent rate of action of local anesthetics on the node of Ranvier. *J. Gen Physiol* 69:475-496, 1977a.
- Hille, B. Local anesthetics: Hydrophilic and hydrophobic pathways for drug receptor reaction. *J. Gen Physiol* 69:497-515, 1977b.
- Hille, B. *Ionic Channels of Excitable Membranes*. Sinauer Associates, Sunderland, MA. pp 426, 1984.
- Hirning, L.D., Fox, A.P., McClesky, E. W., Olivera, B.M., Thayer, S.A., Miller, R.J. and Tsien, R.W. Dominant role of N-type  $\text{Ca}^{2+}$  channels in evoked release of norepinephrine from sympathetic neurons. *Science* 239:57-61, 1988.
- Hodgkin, A.L. *The Conduction of the Nervous Impulse* University Press, Liverpool, 1971.
- Hodgkin, A.L. and Huxley, A.F. Measurement of the current-voltage relations in the membrane of the giant axon of *Loligo*. *J. Physiol. Lond.* 116:424-448. 1952a.
- Hodgkin, A.L. and Huxley, A.F. A quantitative description of membrane current and its application to conduction and excitation in nerve. *J. Physiol. Lond.* 117:500-544, 1952.
- Hodgkin, A.L. and Katz, B. The effect of sodium ions on the electrical activity of the giant axon of the squid. *J. Physiol. Lond.* 108:27-77, 1949.

- Hodgkin, A.L. and Rushton, W.A.H. The electrical constants of a crustacean nerve fibre. *Proc. Roy. Soc. Lond. Ser. B* 133:444-479, 1946.
- Hondeghem, L.M. and Katzung, Time- and voltage-dependent interactions of antiarrhythmic drugs with cardiac sodium channels. *Biochim. Biophys. Acta* 472:373-398, 1977.
- Horackova, M., Nonner, W. and Stämpfli, R. Action potentials and voltage clamp currents of single rat Ranvier nodes. *Proc. int. Union Physiol. Sci.* 7:198, 1968.
- Hoshi, T. and Aldrich, R.W. Voltage-dependent  $K^+$  currents and underlying single channel in pheochromocytoma cells. *J. Gen. Physiol.* 91:73-106. 1988a.
- Hoshi, T. and Aldrich, R.W. Gating kinetics of four classes of voltage-dependent  $K^+$  channels in pheochromocytoma cells. *J. Gen. Physiol.* 91:107-131, 1988b.
- Hursh, J.B. Conduction velocity and diameter of nerve fibres. *Am. J. Physiol.* 127:131-139, 1939.
- Huxley, A.F. and Stämpfli, R. Evidence for saltatory conduction in peripheral myelinated nerve fibres. *J. Physiol. Lond.* 108:315-339, 1949a.

- Huxley, A.F. and Stämpfli, R. Saltatory Transmission of the nervous impulse. *Arch. Sci. Physiol.* 3:435-448, 1949b.
- Huxley, A.F. and Stämpfli, R. Direct determination of membrane resting potential and action potential in single myelinated nerve fibres. *J. Physiol. Lond.* 112:476-495, 1951a.
- Huxley, A.F. and Stämpfli, R. Effect of potassium and sodium on resting and action potential of single myelinated nerve fibres. *J. Physiol. Lond.* 112:496-508, 1951b.
- Ilyn, V.I., Katina, I.E., Lonskii, A.V., Makovsky, V.S. and Polishchuk, E.V. The Cole-Moore effect in nodal membrane *Rana ridibunda*: Evidence for fast and slow potassium channels. *J. Mem. Biol.* 57:179-193, 1980.
- Jack, J. J., Noble, D., and Tsien, R. W. *Electrical current flow in excitable cells*. Oxford: Clarendon Press, 1975.
- Jahnsen, H. and Llinas, R. Ionic basis for the electroresponsiveness and oscillatory behaviour of guinea-pig thalamic neurones *in vitro*. *J. Physiol. Lond.* 349:227-247, 1984.
- Jonas, P., Braü, M.E., Hermsteiner, M. and Vogel, W. Single channel recording in myelinated nerve fibers reveals one type of Na channel but different K channels. *Proc. Natl. Acad. Sci. U.S.A.* 86:7238-7242, 1989.

- Jones, R.E., Heron, J.R., Foster, D.H., Snolgar, R.S. and Mason, R.J. Effects of 4-aminopyridine in patients with Multiple Sclerosis. *J. Neurological. Sci.* 60:353-362, 1983.
- Kaczmarek L.K. and Levitan I.B. *Neuromodulation: The biochemical control of neuronal excitability*. New York. New York, Oxford University Press. 1987.
- Kandel, E. R. and Tauc, L. Anomalous rectification in the metacerebral giant cells and its consequences for synaptic transmission. *J. Physiol. Lond.* 183: 287-304, 1966.
- Kasai, H., Aosaki, T., and Fukuda, J. Presynaptic Ca-agonist w-conotoxin irreversibly blocks N-type Ca-channels in chick sensory neurons. *Neurosci. Res.* 4:228-235, 1987.
- Kasai, H., Kameyama, K., Yamaguchi, K. and Fukuda, J. Single transient K channels in mammalian sensory neurons. *Biophys. J.* 49:1243-1247, 1986.
- Katz, B. Multiple responses to constant current in frog's medullated nerve. *J. Physiol. Lond.* 88:239-255 1936.
- Katz, B. *Electrical Excitation of Nerve.*, Oxford: University Press, 1939, p.8.
- Katz, B. Les constantes électriques de la membrane du muscle. *Arch. Sci. Physiol.* 3:285-299, 1949.

- Kenyon, J.L. and Gibbons, W.R. 4-aminopyridine and the early outward current in sheep cardiac Purkinje fibers. *J. Gen Physiol.* 73:139-157, 1979.
- Kerr, L.M., and Yoshikami, D. A venom peptide with a novel presynaptic blocking action. *Nature* 308:282-284, 1984.
- Kocsis, J.D., Eng, D.L., Gordon, T.R. and Waxman, S.G. Functional differences between 4-aminopyridine and tetraethylammonium-sensitive potassium channels in myelinated axons. *Neurosci. Lett.* 75:193-198, 1987.
- Kocsis, J.D., Eng, D.L., and Waxman, S.G. Mammalian optic nerve fibers display two pharmacologically distinct potassium channels. *Brain Res.* 383:357-361, 1985.
- Kocsis, J.D., Waxman, S.G., Hildebrand, C. and Ruit, J.A. Regenerating mammalian nerve fibres: changes in action potential waveform and firing characteristics following blockage of potassium conductance. *Proc. R. Soc. Lond. B*, 217:277-287, 1982.
- Kocsis, J.D. and Waxman, S.G. *Hand Book of Clinical Neurology* (Vol 3: The Demyelinating Diseases) (Koetsier, J.C. ed.) pg. 29-47, 1985.
- Koketsu, K. Action of tetraethylammonium chloride on neuromuscular transmission in frogs. *Am. J. Physiol.* 193:213-218, 1958.
- Koketsu, K. The electrogenic sodium pump. *Advan. in Biophys.* 2: 77-112, 1971.

- Kreigler, J.S., Krishman, N. and Singer, M. Trophic interactions of neurons and glia. *Adv. Neurol.* 31:479-504, 1981.
- Krylov, B.V. Model of adaptation of the nerve fiber ranvier node membrane to the action of a steady current as the result of sodium channel inactivation. *Neirofiziologiya* 15:390-394, 1984.
- Krylov, B.V. and Makovsky, V.S. Spike frequency adaptation in amphibia sensory fibers is probably due to slow K channels. *Nature* 275:549-551, 1978.
- Lancaster, B. and Nicoll, R.A. Properties of two calcium-activated hyperpolarizations in rat hippocampal neurones. *J. Physiol. Lond.* 389:187-203, 1987.
- Landon, D.N. The structure of the nerve fibre. In *Abnormal Nerves and Muscles as Impulse Generators* (eds. Culp W.J. and Ochoa J.), pg. 27-53, Oxford University Press, New York, Oxford, 1982.
- Leech, C. A. and Stanfeld, P. R. Inward rectification in frog skeletal muscle fibres and its dependence on membrane potential and external potassium. *J. Physiol. Lond.* 319: 195-209, 1981.
- Lillie, R.S.J. Factors affecting transmission and recovery in the passive iron nerve model. *J. Gen. Physiol.* 7:473-507, 1925.



- MacKinnon, R. and Miller, C. Mutant potassium channels with altered binding of charybdotoxin, a pore blocking peptide inhibitor. *Science* 245:1382-1385, 1989.
- Madison, D.V. and Nicoll, R.A. Control of repetitive discharge of rat pyramidal neurones *in vitro*. *J. Physiol. Lond.* 354:319-331, 1984.
- Madison, D.V. and Nicoll, R.A. Cyclic adenosine 3', 5' mono-phosphate mediates Beta-receptor actions of pyramidal neurones *in vitro*. *J. Physiol. Lond.* 372:245-259, 1986.
- Mayer, M. L. and Westbrook, G. L. A voltage-clamp analysis of inward (anomalous) rectification in mouse spinal sensory ganglion neurones. *J. Physiol. Lond.* 340: 19-45, 1983.
- Maylie, J. and Morad, M. Ionic currents responsible for the generation of pacemaker currents in the rabbit sinoatrial node. *J. Physiol. Lond.* 355:215-235, 1984.
- McCleskey, E.W., Fox, A.P., Feldman, D.H., Cruz, L.J. Olivera, B.M. and Tsien, R.W. Omega-conotoxin: Direct and persistent blockade of specific types of calcium channels in neurons but not muscle. *Proc. Natl. Acad. Sci. U.S.A.* 84:4327-4331, 1987.
- Meech, R.W. Calcium dependent potassium activation in nervous tissue. *Ann. Rev. Biophys. Bioeng.* 7:1-18. 1978.

- Meeves, H. and Pichon, Y. The effect of internal and external 4- aminopyridine on the potassium currents in intracellularly perfused squid axons. *J. Physiol. Lond.* 286:511-532, 1977.
- Messner, D.J., Feller, D.J., Scheuer, T. and Catterall, W.A. Functional properties of rat brain sodium channels lacking the  $\beta_1$  and  $\beta_2$  subunit. *J. Biol. Chem.* 261:14882-14890, 1986.
- Miller, C. Genetic manipulation of ion channels: A new approach to structure and mechanism. *Neuron* 2:1195-1205, 1989.
- Miller, C., Moczydlowski, E., Latorre, R. and Phillips, M. Charybdotoxin, a protein inhibitor of  $\text{Ca}^{2+}$ -activated  $\text{K}^+$  channels in mammalian skeletal muscle. *Nature* 313:316-318, 1985.
- Moore, J.W., Joyner, R.W., Brill, M.H., Waxman, S.D., and Najar-Joa, M. Simulation of conduction in uniform myelinated fibers. Relative changes in nodal and internodal parameters. *Biophys. J.* 21:147-160, 1978.
- Narahashi, T., Shapiro, B.I., Deguchi, T., Scuka, M. and Wang, C.M. Effects of scorpion venom on squid axon membranes. *Am. J. Physiol.* 222:850-857, 1972.
- Neher, E. Two fast transient current components during voltage clamp on snail neurones. *J. Gen. Physiol.* 58:36-53, 1971.

- Neumcke, B., Schwarz, W. and Stämpfli, R. Differences between K channels in motor and sensory nerve fibers of the frog as revealed by fluctuation analysis. *Pflügers Arch.* 387:9-16, 1980.
- Nilius, B., Hess, P., Lansman, J.B., and Tsien, R.W. A novel type of cardiac calcium channel in ventricular cells. *Nature* 316:443-446, 1985.
- Noda, M., Shimizu, S., Tanabe, T., Takai, T., Kayano, T., Ikeda, T., Takahashi, H., Nakayama, M., Kanaoka, Y., Minamino, N., Kanagawa, K., Matsuo, H., Raftery, M., Hirose, T., Inayama, S., Hayahasida, H., Miyata, T. and Numa, S. Primary structure of *Electrophorus electricus* sodium channel deduced from cDNA. *Nature* 312:121-127, 1984.
- Nowicky, M.C., Fox, A.P. and Tsien, R.W. Three types of neuronal calcium channels with different calcium sensitivity. *Nature* 316:440-443, 1985a.
- Nowicky, M.C., Fox, A.P. and Tsien, R.W. Long opening mode of gating of neuronal calcium channels and its promotion by the dihydropyridine calcium agonist Bay K 8644. *Proc. Natl. Acad. Sci. U.S.A.* 82:2178-2182, 1985b.
- O'Neil, R. G. Voltage-dependent interaction of barium and cesium with the potassium conductance of the cortical collecting duct apical cell membrane. *J. Membr. Biol.* 74: 165-73, 1983.

- Ottoson, D., and Shepard, G.M. Transducer properties and integrative mechanisms in the frog's muscle spindle. In *Handbook of sensory Physiology, Sec 1: The nervous System, Vol 1; Principles of Receptor Physiology* (W.R. Lowenstein, ed.) New York: Springer-Verlag, pg.443-499, 1971.
- Padjen, A.L. and Hashiguchi, T. Primary afferent depolarization in frog spinal cord is associated with an increase in membrane conductance. *Can. J. Physiol. Pharmacol.* 61:626-631, 1983.
- Padjen, A.L. and Poulter, M.O. A study of anomalous (inward) rectification in frog myelinated axon. *Soc. Neurosci. Abs.* 15:75, 1989.
- Papazian, D.M., Schwarz, T.L., Tempel, B.L., Jan, Y.N., Jan, L.Y. Cloning of genomic and complementary DNA from Shaker, a putative potassium channel gene from *Drosophila*. *Science* 237:749-753, 1987.
- Pappone, P.A. and Cahalan, M.D. *Pandius imperator* scorpion venom blocks voltage-gated potassium channels in nerve fibers. *J. Neurosci* 7:3300-3305, 1987.
- Pennefather, P., and Goh, J. Relationship between calcium load and the decay rate of  $I_{AHP}$  in bullfrog ganglion neurons. *Soc. Neurosci. Abs.* 14:1089, 1988.
- Pennefather, P., Lancaster, B., Adams, P.K. and Nicoll, R.A. Two distinct Ca dependent K currents in bullfrog sympathetic ganglion cells. *Proc. Natl. Acad. U.S.A.* 82:3040-3044, 1985.

- Penner, R., Petersen, M., Pierau, F.K. & Dreyer, F. Dendrotoxin: a selective blocker of a non-inactivating potassium current in guinea-pig dorsal root ganglion neurones. *Pflügers Arch.* 407:365-369, 1986.
- Perney, T.M., Hirning, L.D., Leeman, S.E. and Miller, R.J. Multiple calcium channels mediate neurotransmitter release from peripheral neurones. *Proc. Natl. Acad. Sci. U.S.A.* 83:6656-6659, 1986.
- Peterson, M., Pierau, Fr.-K. and Weyrich, M. The influence of capsaicin on membrane currents in dorsal root ganglion neurones of guinea-pig and chicken. *Pflügers Arch.* 409:403-410, 1987.
- Poulter, M.O. Hashiguchi, T. and Padjen, A.L. Dendrotoxin blocks action potential accommodation in frog myelinated axon. *J. Neurophysiol.* 62:174-184, 1989.
- Poulter, M. O. and Padjen, A.L. Extracellular cesium blocks anomalous rectification in frog myelinated axon. *Proc. Can. Fed. Biol. Sci.* 31: 138, 1988a.
- Poulter, M.O. and Padjen, A.L. Intracellular application of TEA and 4-AP blocks action potential accommodation in frog myelinated axon. *Soc. Neurosci. Abs.* 14:299, 1988b.
- Poulter, M.O. and Padjen, A.L. Sodium dependent action potentials elicit a potassium dependent afterhyperpolarization in frog myelinated axon. *Soc. Neurosci. Abs.* 15:77, 1989.

Purves R.D. *Microelectrode Methods for Intracellular Recording and Ionophoresis*. Academic Press: London U.K., 1981.

Rall, W. Core conductor theory and cable properties of neurons. *Handbook of Physiology* 1:39-97, 1977.

Ranvier L.A. *Leçons sur L'histologie du system nerveuse*. Savy, Paris, 1878.

Rasminsky, M. Ectopic excitation, ephaptic transmission and autoexcitation in peripheral nerve fibres of mutant mice. (In: *Abnormal Nerves and Muscles as Impulse Generators* ed. Culp, W.J. and Ochoa, J.) Oxford University Press, Oxford, New York p. 344-362, 1982

Rasminsky, M. and Sears, T.A. Internodal conduction in undissected demyelinated nerve fibres. *J. Physiol. Lond.* 227:323- 350, 1972.

Redman, J.R. Junctional mechanisms at group Ia synapses. *Prog. Neurobiol.* 12:33-83, 1979.

Reed, J.K. and Raferty, M.A. Properties of the tetrodotoxin binding component in plasma membranes isolated from *Electrophorus electricus*. *Biochemistry* 15:944-953, 1976.

Reynolds, I.J., Wagner, J.A., Synder, S.H., Thayer, S.A, Olivera, B.M., and Miller, R.J. Brain voltage sensitive calcium channel subtypes differentiated by w-conotoxin GVIA. *Proc. Natl. Acad. Sci. U.S.A.* 83:8804-8807, 1986.

Ritchie, J.M. Electrogenic ion pumping in nervous tissue. In: *Current topics in Bioenergetics* (D. Rao Sanadi ed.) 4:327-356, 1970.

Ritchie, J.M., On the relation between fibre diameter and conduction velocity in myelinated nerve fibres. *Proc. R. Soc. Lond.* B217:29-35, 1982a.

Ritchie, J.M., Sodium and potassium channels in regenerating and developing mammalian myelinated nerves. *Proc. R. Soc. Lond.* B215:273-283, 1982b.

Ritchie, J.M. and Stagg, D. A note on the effects of potassium conductance ( $g_K$ ) on conduction velocity in myelinated fibres. *J. Physiol. Lond.* 328:33-33P, 1982.

Ritchie, J.M. and Rogart, R.B. Density of sodium channels in mammalian nerve fibers and nature of the axonal membrane under the myelin sheath. *Proc. Natl. Sci. Acad.* 74:211-215, 1977.

Roberts, W.M. and Hudspeth, J.A. Co-localization of Ca channels with Ca-activated K channels in hair cells of the bullfrog sacculus. *Soc. Neurosci. Abs.* 13:177, 1987.

Robinson, R.A. and Stokes, R.H. *Electrolyte solutions*. 2<sup>nd</sup> revised edition, Butter-

- Rogawski, M.A. The A-Current: how ubiquitous a feature of excitable cells is it? *Trends Neurosci.* 8:214-219, 1985.
- Romey, G., Chicheportiche, R. and Lazdunski, M. Scorpion neurotoxin- A presynaptic toxin which affects both  $\text{Na}^+$  and  $\text{K}^+$  channels in axons. *Biochem. Biophys. Res. Commun.* 64:115-121, 1975.
- Romey, G. and Lazdunski, M. The coexistence in rat muscle cells of two distinct classes of  $\text{Ca}^{2+}$ - dependent  $\text{K}^+$  channels with different pharmacological properties and physiological functions. *Biochem. Biophys. Res. Commun.* 118:669-674, 1984.
- Rudy, B. Diversity and ubiquity of K channels. *Neurosci.* 25:729-749, 1988.
- Rushton, W.A.H. A theory of the effects of fibre size in medullated nerve. *J. Physiol. Lond.* 115:101-122.
- Sanders, F.K. and Whitteridge, D. Conduction velocity and myelin thickness in regenerating nerve fibres. *J. Physiol. Lond.* 105:152-174, 1946.
- Sanguinetti, M.C. and Kass, R.S. Voltage-dependent block of calcium current by dihydropyridine calcium channel antagonists. *Circ. Res.* 55:336-348, 1984.
- Schauf, C.L. Dendrotoxin blocks potassium channels and slows sodium inactivation in Myxicola giant axons. *J. Pharmacol. Exp Ther.* 241:793-796, 1987.



Schmidt, H. and Stämpfli, R. Nachweis unterschiedlicher elektrophysiologischer Eigenschaften motorischer und sensibler Nervenfasern des Frosches. *Helv. physiol. pharmac. Acta.* 22:C143-145, 1964.

Schmidt, H. and Stämpfli, R. Die Wirkung von Tetraäthylammonium auf den einzelnen Ranvierschen Schnürring. *Pflügers Arch.* 287:311-325, 1966.

Schneider, M.J., Rowgowski, R.S., Krueger, B.K. and Blaustein M.P. Charybdotoxin blocks both Ca activated K channels and Ca independent voltage gated K channels in rat brain synaptosomes. *F.E.B.S. Lett.* 250:433-436, 1989.

Schwarz, J.R., Bromm, B., Spielmann, R.P. & Weytjens, J.L.F. Development of Na inactivation in motor and sensory myelinated nerve fibers of *Rana esculenta*. *Pflügers Arch.* 398:126-129, 1983.

Schwarz, T.L., Tempel, B.L., Papazian, D.M., Jan, Y.N. & Jan, L.Y. Multiple potassium channel components are produced by alternate splicing at *Shaker* locus in *Drosophila*. *Nature* 331:137-142, 1988.

Schweitz, H., Stansfeld, C.E. Bidard, J.-N., Fagni, L., Maes, P., and Lazdunski, M. Charybdotoxin blocks dendrotoxin-sensitive voltage activated K<sup>+</sup> channels. *F.E.B.S. Lett.* 250:519-522, 1989.

- Schwindt, P. C., Spain, W. J., and Crill, W. E. Influence of anomalous rectifier activation on afterhyperpolarizations of neurons from cat sensorimotor cortex in vitro *J. Neurophysiol.* 59:468-481, 1988.
- Schwindt P.C., Spain W.J. And Crill W.E. Long lasting reduction of excitability by a sodium dependent potassium conductance in cat neocortical neurons *J. Neurophysiol.* 61:233-244, 1989.
- Segal, M. and Barker, J.L. Rat hippocampal neurons in culture : Potassium conductances. *J. Neurophysiol.* 51:1409-1433, 1984.
- Segal, M., Rogowski, M.A. and Barker J.L. A transient potassium conductance regulates the excitability of cultured hippocampal and spinal neurons. *J. Neurosci.* 4:604-609, 1984.
- Shapovalov, A.I. and Shiriaev, B.I. Spontaneous miniature potentials in primary afferent fibres. *Experientia. Basel* 35:348-349, 1979.
- Sherret R.M.H., Bostock, H. and Sears, T.A. Effects of 4-aminopyridine on normal and demyelinated mammalian nerve. *Nature* 283:570-572, 1980.
- Shrager, P. Ionic channels and signal conduction in single remyelinating frog nerve fibre. *J. Physiol.* 404:695-712, 1988.
- Shrager, P. and Profera, C. Inhibition of the receptor for Tetrodotoxin in nerve membranes by reagents modifying carboxyl groups. *Biochim. Biophys. Acta.* 318:141-146, 1973.

- Sitges, M., Possani, L.D., and Bayon, D. Noxiustoxin, a short- chain toxin from the mexican scorpion *Centruroides noxius*, induces transmitter release by blocking  $K^+$  permeability. *J. Neurosci.* 6:1570-1574, 1986.
- Sokolove P.G. Computer simulation of after inhibition in the crayfish slowly adapting stretch receptor neuron. *Biophys. J.* 12:1429-1451, 1972.
- Spain, W. J., Schwindt, P. C., and Crill, W. E. Anomalous rectification in neurons from cat sensorimotor cortex in vitro. *J. Neurophysiol.* 57:1555-1576, 1987.
- Stämpfli, R. and Hille, B. Electrophysiology of the peripheral myelinated nerve. In *Frog Neurobiology*, (Ed. R.Llinas and W.Precht), Springer Verlag, New York, pp. 1-32, 1976.
- Stafstrom, C.E., Schwindt P.C., Chubb, M.C. and Crill W.E. Properties of the persistent sodium conductance and calcium conductance in layer V neurons from cat sensorimotor cortex in vitro. *J. Neurophysiol.* 53:153-170, 1985.
- Stanfeld, P.R. The effect of tetraethylammonium ion on the delayed currents of frog skeletal muscle *J. Physiol. Lond.* 209:209-231, 1970.
- Stansfeld, C.E., Marsh, S.J., Halliwell, J.V. and Brown, D.A. 4-Aminopyridine and dendrotoxin induce repetitive firing in rat visceral sensory neurones by blocking a slowly inactivating outward current. *Neurosci. Lett.* 64:299-304, 1986.

- Stansfeld, C.E., Marsh, S.J., Parcej, D.N., Dolly J.O. and Brown D.A. Mast cell degranulating peptide and dendrotoxin inhibit a fast activating potassium current and bind to common neuronal proteins. *Neuroscience* 23:893-902, 1987.
- Stefoski, D., Davis, F.A., Faut, M. and Schauf, C.L. 4-aminopyridine improves clinical signs in multiple sclerosis *Ann. Neurol.* 21:71-77, 1987.
- Storm, J.F. Action potential repolarization and a fast hyperpolarization in rat hippocampal pyramidal neurones. *J. Physiol.* 365:733-759, 1987.
- Strichartz, G. Molecular mechanisms of nerve block by local anesthetics. *Anesthesiology* 45:421-441, 1976.
- Strühmer, W., Ruppersberg, J.P. Schröter, K.H., Sakmann, B., Stocker, M., Giese, K.P., Perschke, A., Baumann, A., and Pongs, O. Molecular basis of functional diversity of voltage-gated potassium channels in mammalian brain. *EMBO J.* 8:3235-3244, 1989.
- Szete, M.B., Baranyi, A. and Woody C.D. Intracellular injection of apamin reduces the slow potassium current mediating the afterhyperpolarizations and IPSPs in neocortical neurons of cats. *Brain Res.* 461:64-74, 1988.
- Takumi, T., Ohkubo, H., and Nakanishi, S. Cloning of a membrane protein that induces a slow voltage-gated potassium current. *Science* 242:1042-1045, 1988.

- Tanabe, T., Takeshima, H., Mikami, A., Flockerzi, V., Takahashi, H., Kenji, K., Masayasa, K., Matsuo, H., Hirose, T. and Numa S. Primary structure of the receptor for calcium channel blockers from skeletal muscle. *Nature* 328:313-318, 1987.
- Targ E.F. And Kocsis J.D. 4-aminopyridine leads to restoration of conduction in demyelinated nerve fibres. *Brain Res.* 328:358-361, 1985.
- Tasaki, I Mikrophysiologische Untersuchung über die Grundlage der Erregungsleitung in der markhaltigen Nerven Faser. *Pflüg. Arch. ges. Physiol.* 244:125-144, 1940.
- Tasaki, I. Properties of myelinated fibres in frog sciatic nerve and spinal cord as examined with micro-electrodes. *Jap. J. Physiol.* 3:73-94, 1951.
- Tasaki, I. *Nervous Transmission*. Springfield, Thomas, 1953.
- Tasaki, I. and Hagiwara, S. Demonstration of two stable states in squid giant axon under tetraethylammonium chloride. *J. Gen. Physiol* 40:859-885, 1957.
- Tasaki, I. and Takeuchi, T. Der am Ranverschen Knoten entstehende Aktionsstrom and seine Bedeutung für die Erregungsleitung. *Pflüg. Arch. ges. Physiol.* 244:696-711, 1941.
- Tempel, B.L., Papazian, D.M., Jan, Y.N. & Jan, L.Y. Expression of functional potassium channels in *Xenopus* oocytes. *Nature Lond.* 331:143-145, 1988.

- Thompson, S.H. Three types of pharmacologically distinct potassium channels in molluscan neurons. *J. Physiol. Lond.* 265:465-488, 1977.
- Timpe, L., Schwarz, T.L. Tempel, B.L., Papazian, D.M. Jan, Y.N, and Jan, L.Y. Expression of functional potassium channels from *Shaker* cDNA in *xenopus* oocytes. *Nature* 331:143-145, 1988.
- Ulbricht, W. and Wagner, H.H. The influence of pH on equilibrium effects of tetrodotoxin on myelinated nerve fibres of *Rana esculenta*. *J. Physiol. Lond.* 252:159-184, 1975.
- Ulbricht, W. and Wagner, H.H. Block of potassium channels of the nodal membrane by 4-aminopyridine and its partial removal on depolarization. *Pflügers Arch.* 367:77-87, 1976.
- Valbo, A.B. Accommodation related to inactivation of the sodium permeability in single myelinated nerve fibers from *Xenopus laevis*. *Acta Physiol. Scand.* 61:429-444, 1964.
- Vassilev, P.M., Scheuer, T. and Catterall W.A. Identification of an intracellular peptide segment involved in sodium channel inactivation. *Science* 241:1658-1661, 1988.
- Waxman, S.G. Demyelination in spinal cord injury. *J. Neurol. Sci.* 91:1-14, 1989.

Weller, U., Bernhardt, U., Siemen, D., Dreyer, F., Vogel, W. & Habermann, E.  
Electrophysiological and neurobiochemical evidence for the blockade  
of a potassium channel by dendrotoxin. *Naunyn Schmiedebergs Arch.  
Pharmacol.* 330:77-83, 1985.

Werman, R. An electrophysiological approach to drug receptor mechanisms. *Comp.  
Biochem. Physiol.* 30:997-1017, 1969.

Wong, B.S. and Binstock, D.C. Inhibition of potassium conductance with external  
tetraethylammonium ion. *Biophys. J.* 32:1037-1042, 1980.

Woodbury, J.W. Direct membrane resting and action potentials from single myeli-  
nated nerve fibres. *J. Cell. Comp. Physiol.* 39:323-339, 1952.

Yeh, J.Z. Oxford, G.S. Wu, C.H. and Narahashi, T. Dynamics of aminopyridine  
block of potassium channels in squid axon membrane. *J. Gen. Physiol.*  
68:519-535, 1976.

Zbicz, K.L. and Weight, F.F. Transient voltage and calcium dependent outward  
currents in hippocampal CA3 pyramidal neurones. *J. Neurophysiol.*  
53:1038-1058, 1985.